



International Agreement Report

RELAP5 Assessment on Direct-Contact Condensation in Horizontal Cocurrent Stratified Flow

Prepared by
S. Lee, H. J. Kim

Korea Institute of Nuclear Safety
P.O. Box 16, Daeduk-Danji
Taejon, Korea

Office of Nuclear Regulatory Research
U.S. Nuclear Regulatory Commission
Washington, DC 20555

April 1992

Prepared as part of
The Agreement on Research Participation and Technical Exchange
under the International Thermal-Hydraulic Code Assessment
and Application Program (ICAP)

Published by
U.S. Nuclear Regulatory Commission

NOTICE

This report was prepared under an international cooperative agreement for the exchange of technical information.* Neither the United States Government nor any agency thereof, or any of their employees makes any warranty, expressed or implied, or assumes any legal liability or responsibility for any third party's use, or the results of such use, of any information, apparatus product or process disclosed in this report, or represents that its use by such third party would not infringe privately owned rights.

Available from

Superintendent of Documents
U.S. Government Printing Office
P.O. Box 37082
Washington, D.C. 20013-7082

and

National Technical Information Service
Springfield, VA 22161



International Agreement Report

RELAP5 Assessment on Direct-Contact Condensation in Horizontal Cocurrent Stratified Flow

Prepared by
S. Lee, H. J. Kim

Korea Institute of Nuclear Safety
P.O. Box 16, Daeduk-Danji
Taejeon, Korea

Office of Nuclear Regulatory Research
U.S. Nuclear Regulatory Commission
Washington, DC 20555

April 1992

Prepared as part of
The Agreement on Research Participation and Technical Exchange
under the International Thermal-Hydraulic Code Assessment
and Application Program (ICAP)

Published by
U.S. Nuclear Regulatory Commission

NOTICE

This report is based on work performed under the sponsorship of The Korea Advanced Energy Institute of Korea. The information in this report has been provided to the USNRC under the terms of an information exchange agreement between the United States and Korea (Agreement on Thermal-Hydraulic Research between the United States Nuclear Regulatory Commission and The Korea Advanced Energy Research Institute, May 1, 1986). Korea has consented to the publication of this report as a USNRC document in order that it may receive the widest possible circulation among the reactor safety community. Neither the United States Government nor Korea or any agency thereof, or any of their employees, makes any warranty, expressed or implied, or assumes any legal liability of responsibility for any third party's use, or the results of such use, or any information, apparatus, product or process disclosed in this report or represents that its use by such third party would not infringe privately owned rights.

ICAP

RELAP5 ASSESSMENT ON DIRECT-CONTACT CONDENSATION

IN HORIZONTAL COCURRENT STRATIFIED FLOW

Abstract

Assessment on the direct-contact condensation model was carried out using the RELAP5/MOD2 Cycle 36.04 and the RELAP5/MOD3 Version 5m5 codes. The test data were obtained from the experiments at Northwestern University, which involved the horizontal cocurrent stratified steam/water flow in a rectangular channel.

A nodalization sensitivity study and a simulation with a fixed interfacial area, same as test section, were also carried out to examine the effect of the interfacial heat and mass transfer.

The results showed that the RELAP5 code model under the horizontal stratified flow regime predicted the condensation rate well, though the interfacial heat transfer area was underpredicted. However, some discrepancies with experimental results were found in water layer thickness and local heat transfer coefficient especially when there was a wavy interface. The interfacial wave structure was found to play an important role in describing the interfacial heat and mass transfer, as obtained in the experiment.

List of Contents

| | |
|---|------|
| Abstract..... | iii |
| List of Tables..... | vii |
| List of Figures..... | viii |
| Executive Summary..... | xi |
| Acknowledgment..... | xiii |
| | |
| 1. Introduction | 1 |
| 2. Facility and Test Description | 4 |
| 2.1 Facility Description | 4 |
| 2.2 Test Description | 5 |
| 2.3 Measurement Uncertainty | 6 |
| 3. Code and Modelling Description | 8 |
| 3.1 Code Description | 8 |
| 3.2 Modelling Descriptions | 9 |
| 3.3 Nodalization | 11 |
| 4. Base Case Calculations | 13 |
| 4.1 Base Calculation With RELAP5/MOD3 | 13 |
| 4.2 Base Calculation With RELAP5/MOD2 | 16 |
| 5. Sensitivity and Nodalization Studies | 18 |
| 5.1 Calculation With a Fixed Interfacial Area | 18 |
| 5.2 Nodalization Sensitivity Study | 19 |

| | |
|-------------------------|----|
| 6. Run Statistics | 20 |
| 7. Conclusions | 21 |
| References | 22 |
| Appendix | 88 |

List of Tables

| | | |
|---------|--|----|
| Table 1 | RELAP5/MOD3 Model Improvements | 24 |
| Table 2 | Inlet conditions of the Calculations | 25 |
| Table 3 | Run Statistics Data in Base Cases | 26 |

List of Figures

| | | |
|---------|---|----|
| Fig. 1 | Schematic Diagram of the System [5]..... | 27 |
| Fig. 2 | Channel View of the System [5]..... | 28 |
| Fig. 3 | Experimental Data Matrix [5]..... | 29 |
| Fig. 4 | Nodalization(A) of Cocurrent Condensation Test | 30 |
| Fig. 5 | Nodalization(B) of Cocurrent Condensation Test | 31 |
| Fig. 6 | Vapor Mass Flow (No. 253) | 32 |
| Fig. 7 | Pressure Difference (No. 253) | 33 |
| Fig. 8 | Water Layer Thickness (No. 253) | 34 |
| Fig. 9 | Axial Condensation Rate (No. 253) | 35 |
| Fig. 10 | Vapor Temperature (No. 253) | 36 |
| Fig. 11 | Liquid Temperature (No. 253) | 37 |
| Fig. 12 | Liquid Wall Friction Drag Coefficient (No. 253) | 38 |
| Fig. 13 | Interphase Friction (No. 253) | 39 |
| Fig. 14 | Vapor Mass Flow (No. 259) | 40 |
| Fig. 15 | Pressure Difference (No. 259) | 41 |
| Fig. 16 | Water Layer Thickness (No. 259) | 42 |
| Fig. 17 | Axial Condensation Rate (No. 259) | 43 |
| Fig. 18 | Vapor Temperature (No. 259) | 44 |
| Fig. 19 | Liquid Temperature (No. 259) | 45 |
| Fig. 20 | Liquid Wall Friction Drag Coefficient (No. 259) | 46 |
| Fig. 21 | Interphase Friction (No. 259) | 47 |
| Fig. 22 | Vapor Mass Flow (No. 279) | 48 |
| Fig. 23 | Pressure Difference (No. 279) | 49 |

| | | |
|---------|---|----|
| Fig. 24 | Water Layer Thickness (No. 279) | 50 |
| Fig. 25 | Axial Condensation Rate (No. 279) | 51 |
| Fig. 26 | Vapor Temperature (No. 279) | 52 |
| Fig. 27 | Liquid Temperature (No. 279) | 53 |
| Fig. 28 | Liquid Wall Friction Drag Coefficient (No. 279) | 54 |
| Fig. 29 | Interphase Friction (No. 279) | 55 |
| Fig. 30 | Vapor Mass Flow (No. 293) | 56 |
| Fig. 31 | Pressure Difference (No. 293) | 57 |
| Fig. 32 | Water Layer Thickness (No. 293) | 58 |
| Fig. 33 | Axial Condensation Rate (No. 293) | 59 |
| Fig. 34 | Vapor Temperature (No. 293) | 60 |
| Fig. 35 | Liquid Temperature (No. 293) | 61 |
| Fig. 36 | Liquid Wall Friction Drag Coefficient (No. 293) | 62 |
| Fig. 37 | Interphase Friction (No. 293) | 63 |
| Fig. 38 | Vapor Mass Flow (RELAP5/MOD2) | 64 |
| Fig. 39 | Liquid Mass Flow (RELAP5/MOD2) | 65 |
| Fig. 40 | Pressure Difference (RELAP5/MOD2) | 66 |
| Fig. 41 | Water Layer Thickness (RELAP5/MOD2) | 67 |
| Fig. 42 | Vapor Temperature (RELAP5/MOD2) | 68 |
| Fig. 43 | Liquid Temperature (RELAP5/MOD2) | 69 |
| Fig. 44 | Liquid Wall Friction Drag Coefficient (RELAP5/MOD2) | 70 |
| Fig. 45 | Interphase Friction (RELAP5/MOD2) | 71 |
| Fig. 46 | Vapor Mass Flow (RELAP5/MOD3) | 72 |
| Fig. 47 | Liquid Mass Flow (RELAP5/MOD3) | 73 |
| Fig. 48 | Pressure Difference (RELAP5/MOD3) | 74 |
| Fig. 49 | Water Layer Thickness (RELAP5/MOD3) | 75 |

| | | |
|---------|---|----|
| Fig. 50 | Vapor Temperature (RELAP5/MOD3) | 76 |
| Fig. 51 | Liquid Temperature (RELAP5/MOD3) | 77 |
| Fig. 52 | Liquid Wall Friction Drag Coefficient (RELAP5/MOD3) | 78 |
| Fig. 53 | Interphase Friction (RELAP5/MOD3) | 79 |
| Fig. 54 | Axial Local Heat Transfer Coefficient (RELAP5/MOD3) | 80 |
| Fig. 55 | Prediction of Local Condensation Rate | 81 |
| Fig. 56 | Comparison of Local Condensation Rates | 82 |
| Fig. 57 | Vapor Mass Flow (No. 253 : Mod) | 83 |
| Fig. 58 | Pressure Difference (No. 253 : Mod) | 84 |
| Fig. 59 | Water Layer Thickness (No. 253 : Mod) | 85 |
| Fig. 60 | Axial Condensation Rate (No. 253 : Mod) | 86 |
| Fig. 61 | CPU Time in Base Calculations (No. 253) | 87 |

Executive Summary

The modelling of direct condensation phenomena between liquid and steam interface can play an important role in the analysis of hypothetical Loss of Coolant Accidents. In order to further understand this phenomenon, the steady, cocurrent stratified flow of water vapor and liquid in a horizontal, rectangular channel was studied in a number of experiments performed at Northwestern University. The data from these experiments were selected for the assessments of condensation model in the RELAP5/MOD2 and MOD3 codes, as a part of the independent code assessment plan.

For the nodalization of the experimental apparatus, a model which is very similar to the experiment was first applied. However it was found to be difficult to obtain steady state conditions and to prescribe proper outlet conditions even though the calculation reached steady state condition. Therefore, a simple nodalization was introduced to describe the experimental outlet conditions for the present calculations.

A series of calculations was performed using the RELAP5/MOD2 and MOD3 to compare with the experimental results. The RELAP5 prediction of the condensation rates was in good agreement with the experiments, and no major differences were observed between two base calculations. However, some discrepancies with experimental results were found in water layer thickness and local heat transfer coefficient especially when there was a wavy interface.

A nodalization study for the test component was also carried out by

increasing the number of the volumes from 10 to 20. Comparison shows no difference in the principal variables.

The RERAP5 may not give highly accurate quantitative results in comparison with the experimental data, mainly because of the difference in the pipe geometry used in the code and the experiments. The geometrical restriction has the obvious consequence that the liquid level and interfacial area are coupled in the calculations. In order to examine the effect of the interfacial area, another calculation with a fixed interfacial area, which is the same as the experiment, was performed by implementing that into the PHAINT subroutine in the RELAP5/MOD2. However, the results did not give any improvement on reflecting the effect of the wavy interface accurately.

Therefore, an effort to develop models including the effect of the wavy interface might be taken into consideration to enhance the capability of the RELAP5 by considering the interfacial shear as well as the interfacial heat transfer.

Acknowledgement

This report was completed under the sponsorship of the Korean Ministry of Science and Technology. Dr. Sang Hoon Lee, President of the Korea Institute of Nuclear Safety, contributed significantly to the project administration.

Authors expressed a great appreciation to professor K. C. Park in Seoul National University, professors M. H. Chun, H. C. No in Korea Advanced Institute of Science and Technology, and S. J. Cho in R&D Center of KEPCO for their in-depth technical reviews in Korea.

Final thank goes to Miss E. K. Kim for preparing data.

1. Introduction

The International Code Assessment and Application Program (ICAP) has been conducted by fourteen nations and multinational organizations under the auspices of the USNRC[1]. For the pressurized water reactor analysis, the USNRC selected two Best Estimate (BE) codes: RELAP5/MOD2 and TRAC/PF1/MOD1[2]. The goal of the program is to assess the prediction capabilities of the current BE thermal hydraulic codes utilizing the available facility test and plant data. At present the ICAP activities in Korea are aimed to help quantifying uncertainties in the codes so that the codes may be used for regulatory purposes.

This report is a part of the Korean contribution to the ICAP. The RELAP5/MOD2[3] Cycle 36.04 and the RELAP5/MOD3[4] Version 5m5 were used in the present assessment for the simulation of the condensation experiment in horizontal cocurrent stratified flow conducted by the work of Lim and Bankoff [5].

The condensation phenomena in stratified two-phase flows are of great interest to the refrigeration industries, in secondary oil recovery processes, in steam-jet propulsion systems, and in nuclear reactor programs. The direct-contact condensation effects on heat and mass transfer between liquid and vapor interface become one of the safety issues in nuclear reactor transients[6]. Especially, when the cold emergency core cooling water comes into contact with steam, the interfacial heat and mass transfer dominates the transients. The

condensation phenomena under various flow regimes can be characterized by the interfacial heat transfer coefficient and the interfacial heat transfer area. It is therefore important to predict them exactly, so there have been intensive studies in these areas through experiments as well as model developments.

The test facility[5] was designed and constructed to measure the condensation rate of steam along the channel in cocurrent, horizontal flow of steam and water. The channel cross-section is rectangular in shape with a height of 6.35 cm, a width of 30.48 cm, and a length of 160.1 cm. Since the RELAP5 is one-dimensional transient thermo-hydraulic system analysis computer code, the rectangular channel in the experiment can only be specified as a PIPE component which has one azimuthal segment. Then, the interfacial heat transfer area is calculated from the equivalent hydraulic diameter.

Calculations, performed with both the RELAP5/MOD2 and MOD3, were compared with the experimental results. In order to examine the effect of the interfacial area, another calculation with a fixed interfacial area, which is the same as the experiment, was performed by implementing that into the PHAINT subroutine in the RELAP5/MOD2. A nodalization study was also carried out by increasing the number of volumes of the test PIPE from 10 to 20.

Section 2 contains a description of the equipment and procedure used in the tests, and of the reported data. Section 3 describes the code features of the RELAP5, the two cases of nodalizations for the test section and the input models. The interfacial heat and mass transfer

model and particularly, the model change of the interphase drag in the RELAP5 JD3 are also described in section 3. The results and the discussions on the variations in the inlet steam and water flow rates are treated in Section 4. The motivations for the sensitivity and nodalization studies and their results are included in Section 5. The code efficiency is evaluated in Section 6 through run statistics. Conclusions drawn from this study and the possible implications for further assessment are presented in Section 7.

2. Facility and Test Description

2.1 Facility Description

Measurements[5] of local steam condensation rates of cocurrent stratified flow of steam and subcooled water were carried out at atmospheric pressure in a horizontal rectangular channel. Fig. 1 shows a schematic diagram of the system. The channel was constructed of 6.4 mm thick stainless steel with pyrex glass windows, and its dimensions are about 1.6 m long, 0.3 m wide, and 0.06 m high as shown in Fig. 2. The channel was insulated on the upper and lower surfaces with 50 mm layers of fiberglass to minimize possible heat loss through the surface of the channel.

Steam and water inlet plenums are designed to provide uniform flow at the entrance of the channel. The exit plenum separates the exit steam and water flows in a uniform manner such that the channel flow is not disturbed.

Steam is obtained from the building supply line. The steam passes through a gate valve and a steam-water separator to remove any liquid droplets that might be present. After being throttled by a globe valve, the steam flow rate is metered with 2 inch venturi and enters the plenum chamber. Water used in the experiment is stored in a 450 gallon steel tank. Water is pumped by centrifugal pump from the water tank to test section. The water flow rate is measured by 1 and 1/4 inch venturi.

Water and condensate leave the channel through the exit plenum and are pumped to a heat exchanger and returned to the water tank. The water line forms a closed loop; whereas the steam line is an open loop.

A pitot tube is inserted for the measurement of local mean steam velocity, a tiny hole of 0.8 mm is drilled at wall for static pressure measurements, a conductivity probe is inserted for water height measurements and a thermocouple is inserted for the measurements of temperatures.

2.2 Test Description

Condensation rate measurements have been made under different conditions by varying the system parameters: 1) the inlet steam flow rate, 2) the inlet water flow rate, 3) the initial water layer thickness, and 4) the degree of water subcooling.

A data matrix for this experiment is shown in Fig. 3. The steam flow rate varied from 0.04 kg/sec to 0.16 kg/sec. The water flow rate varied from 0.2 kg/sec to 1.45 kg/sec. The maximum ranges of water and steam flow rates were restricted by either the initiation of bridging phenomena or the occurrence of a hydraulic jump near the entrance region.

Data for water layer thickness, vapor flow rate, and the differential pressure were tabulated at the 5 locations along the flow path, together with flow rates, water temperatures at the inlet and outlet and inlet vapor temperatures.

The steam flow was established at a constant value for at least 10

minutes before beginning the water flow, and all data were taken in steady-state conditions. Vapor velocities were measured at vertical increments of about 4 mm from the liquid surface, and the integrated to provide mass flow rates at each axial station. The vapor was slightly superheated, and variations were performed on inlet flow rates, water level, and the amount of subcooling of the water.

To observe the effect of velocity on condensation, the water height at entrance was varied. Thus for the same flow rate, the velocities of steam and water will change at the entrance section. Water inlet temperature of 25 C and 50 C were used. By adjusting the amount of cooling water at the heat exchanger, the inlet water temperature is controlled and kept constant.

2.3 Measurement Uncertainty

The accuracy of inlet steam mass flux and each pitot tube measurement were checked by two methods: 1) the energy balance and 2) the comparison of venturi reading with the integrated pitot tube measurements[5]. In the first method, the energy balance was obtained by measuring the water flow rate, the water inlet and outlet temperatures when all the steam is condensed. To ensure that all the steam condenses, three full jet spray nozzles were installed at the exit plenum. The second method is the comparison between venturi and pitot tube measurement which were made without condensation. In this case, steam flowed through the test section in the usual manner without water present or with the presence of water.

The mass flow rate obtained from the venturi reading, pitot tubes traverses and the energy balance are all agreed within + 3 %.

3. Code and Modelling Description

3.1 Code Description

The RELAP5/MOD2 code has been developed for best-estimate transient simulation of PWRs and associated systems. The code is based on a non-homogeneous and non-equilibrium model for one dimensional, two-phase system that is solved by a fast, partially implicit numerical scheme to permit economical evaluation of system transients. Recently, the RELAP5/MOD3 code development program has been initiated to develop a code version suitable for the analysis of all transients and postulated accidents in PWR systems including both large and small break LOCAs as well as the full range of operational transients. Although the emphasis of the RELAP5/MOD3 development is on large break LOCA, improvements to existing code models, based on the results of assessments against small break LOCA and operational transient test data, are also being made. Table 1 is a list of the phenomena and code models, improved from the RELAP5/MOD2, that are being addressed by the RELAP5/MOD3 code development program.

The RELAP5/MOD2 Cycle 36.04 and the RELAP5/MOD3 Version 5m5 were used in this assessment.

3.2 Modelling Description

In RELAP5/MOD2 and MOD3, the interfacial mass transfer is modelled according to the thermodynamic process, interphase heat transfer regime and flow regime. After the thermodynamic process is decided, the flow regime map is used to determine the phasic interfacial area and to select the interphase heat transfer correlation.

The interfacial heat transfer between the gas and liquid phase actually involves both heat and mass transfer. Temperature gradient-driven interfacial heat transfer is computed between each phase and the interface. The temperature at the interface is assigned the saturation value for the local pressure. Heat transfer correlation for each side of the interface are provided in the code. The form used in defining the heat transfer correlations for superheated liquid, subcooled liquid, superheated gas, and subcooled gas is that for a volumetric heat transfer coefficient. Since heat transfer coefficients are given in the form of a dimensionless parameter (usually Nusselt number, Nu), the volumetric heat transfer coefficients are coded as follow.[7]:

$$h_i = (k / L) \text{Nu}_{agf}$$

where h_i = volumetric interfacial heat transfer coefficient

k = thermal conductivity

L = characteristic length

agf = interfacial area per unit volume

The volumetric interfacial area, agf , is based on simple geometric considerations.

For smooth interface,

$$agf = 4 \sin \theta / (\pi D)$$

For wavy interface,

$$agf = (4 \sin \theta / (\pi D)) F27$$

where θ = angle between the vertical and the stratified liquid level

D = pipe diameter

$F27 = 1 + \sqrt{|v_g/v_{crit}|}$ is a multiplicative parameter is applied to agf in the code to attempt to account for an increase in agf due to a wavy surface. This parameter $F27$ appropriately increases as v_g increases. An evaluation of the validity of function $F27$ requires comparison with experiment.

Independent assessment of the RELAP5/MOD2 code through the ICAP has identified a number of deficiencies in the code [8]. For the interphase drag calculation, it has been reported [9] that the RELAP5/MOD2 overpredicted the void fraction profile in the simulation of the ROSA-IV Two Phase Test Facility (TPTF) and overpredicted the hot leg void fraction in the simulation of ROSA-IV Large Scale Test Facility (LSTF). The junction-based interphase drag, which were incorporated into RELAP5/MOD3, uses the donor void fraction to evaluate the interphase drag rather than

using the MOD2 method of averaging the interphase drag from the two volumes on either side of the junction. The JAERI TPTF void fraction calculations were significantly improved with this modification, although it was just done for specific junctions[10]. However, it may be expected that this improvement is only for the case where the flow experiences a significant change (e.g., a change in direction, from horizontal to vertical) across the junction.

3.3 Nodalization

In RELAP5, the only apparent means of modelling a rectangular channel is by specifying a PIPE component which has one azimuthal segment. Thus it appears that the RELAP5 can model condensing flow parallel to a horizontal vapor-liquid interface only in PIPE component. The flow area of the test section is given equal to the actual flow area and the equivalent diameters of the test section is calculated using the relation between flow area and wetted perimeter.

The test section as shown in Fig. 1 is one-dimensionally nodalized into four TIME DEPENDENT VOLUMES, four SINGLE VOLUMES, two TIME DEPENDENT JUNCTIONS, five SINGLE JUNCTIONS, and one PIPE. This nodalization of the test section is shown in Fig. 4, and the input deck is described in Appendix. The PIPE, representing the main test section, consists of 10 nodes. The size of the time step was chosen to be 10E-6 and 10E-1 seconds as the minimum and the maximum time step, respectively. The steady state option was selected for the calculation.

It was found difficult to obtain steady state conditions due to oscillation of the principal parameters and to prescribe proper outlet conditions even though the calculation reached steady state condition. Therefore, a simple nodalization was introduced to describe the experimental outlet conditions. The test section is one-dimensionally nodalized into two TIME DEPENDENT VOLUMES, one TIME DEPENDENT JUNCTION, one SINGLE JUNCTION, and one PIPE. This nodalization of the test section is shown in Fig. 5, and the input deck is described in Appendix. The PIPE, representing the main test section, consists of 10 nodes. The size of the time step was chosen to be $10E-6$ and $10E-1$ seconds as the minimum and the maximum time step, respectively. The steady state option was selected for the assessment.

3. Base Case Calculation

Four calculations among the experimental data (test no. 253, 259, 279, and 293) were done using the RELAP5/MOD3 Version 5m5 and the RELAP5/MOD2 Cycle 36.04 codes. The initial conditions of the experiments are summarized by the test matrix in Fig.3, and the corresponding inlet conditions of the four tests are represented in Table 2.

4.1 Base Calculation With RELAP5/MOD3

For various inlet conditions, the calculated and experimental variables as a function of axial position are shown in Figs. 6 to 37 and Figs. 46 to 56.

i) Steam Flow Rate

Fig. 46 shows the effect of the inlet steam flow rate on interfacial heat and mass transfer at constant inlet water flow rate and water temperature. The decrease in steam flow rate is a measure of the mass exchanged through condensation. By increasing the steam flow rate the condensation rates increase and heat transfer coefficients increase as shown in the experiment[5].

The effect of momentum exchange is to retard the steam and accelerate the water. Most of the exchange occurs between the inlet and the first measuring stations, as indicated by the rapid adjustment in water layer

thickness. The steam flow rate drops monotonically from their initial value at the inlet; the magnitude of the drop increases with the inlet steam flow rate. The calculated and experimental steam flow rates are in good agreement.

ii) Water Flow Rate

Fig. 47 shows the effect of the inlet water flow rate on interfacial heat and mass transfer at constant inlet steam flow rate and water temperature. The calculations and the experiments show approximately the same increase in water flow rate.

An increase in the water flow rate leads to an increase in the condensation rate and therefore to a more rapid decrease in the steam flow rate downstream from the inlet. The condensation rate is higher at high water flow rate because the residence time of the water in the channel is less in that case. Thus less heat is transferred to a given volume of water as it flows through the channel, so the subcooling remains high and a large mass exchange rate persists downstream from the inlet.

iii) Local Condensation Rate

The calculated and experimental axial local condensation rates for each test are shown in Figs. 9, 17, 25, and 33. It was found that all the calculated results are in good agreement with the experiment.

The experiment[11] indicated that the thermal resistance in the gas side is negligible compared to the thermal resistance in the liquid side. The condensation rate therefore depends on the ability of the liquid

motion to transport thermal energy away from the interface into the liquid main stream. In this case, it is the interfacial wave agitation which enhances the convection. This explains the increase of condensation rates with higher steam flow rates. On the other hand, the increase in condensation rate with water flow rate can be explained as follows: at the higher water flow rates, water temperature slowly increases due to the larger thermal capacity of the liquid, and therefore the temperature difference remains relatively larger. Because the steam velocity is much larger than water velocity, an increase in water velocity does not increase the interfacial wave agitation rather than the steam velocity. However, an increase in water flow rate may increase the liquid side turbulence intensity in the water and therefore increase the heat transfer coefficient.

Comparisons of the calculated condensation rates with the experiment are shown in Figs. 55 and 56. A relatively large deviation from the experiment was occurred at very lower condensation rate; however, the order of the magnitude was quite small and this deviation became smaller for higher condensation rates. And little differences in the local condensation rate between calculation and experiment are easily seen. It was also observed that the absolute difference between these results were nearly constant along the channel.

iv) Pressure Difference

Figs. 7, 15, 23, and 31 show the change in static pressure along the channel and the entrance to test section is chosen as reference. Due to

large steam condensation, the pressure increases with axial distance.

v) Steam and Water Temperatures

The axial variation of the steam and water temperatures is shown in Figs. 50 and 51. As is to be expected, the steam temperature decreases faster and the water temperature increases faster for higher inlet steam flow rate or for higher inlet water flow rate.

vi) Water Layer Thickness

The principal effects of increasing the inlet steam flow rate are an increase in the level of turbulence creation in the water and an increase in momentum exchange through shear, resulting in a rapid decrease in the water height. This abrupt change in water height leads to a decrease in the thermal boundary layer thickness and consequent increase in heat flux through the water near the interface.

The water layer thickness as a function of axial position is shown in Figs. 8, 16, 24, and 32. Since it may not be possible to evaluate the water layer thickness with one-dimensional model of the code, there are some discrepancies with experimental results, but are satisfied only within the limited range.

vii) Local Heat Transfer Coefficient

Similar discrepancies described as above were found in the local heat transfer coefficient as shown in Fig. 54. It was observed in the experiments^[5] that if the interface is smooth or wavy throughout, the

heat transfer coefficient decreases monotonically, whereas, the interface is smooth from the entrance to a certain point in downstream, and is wavy from there to the exit, the heat transfer coefficient decreases from the entrance to that point and sharply increases in the vicinity of that point and then decreases monotonically. The RELAP5 calculations show that the interfacial heat transfer model did not predict well, especially when there exists a wavy interface, but is satisfied with experimental results only within the limited range.

4.2 Base Case Calculation With RELAP5/MOD2

For various inlet conditions, the calculated and experimental variables as a function of axial position are shown in Figs. 6 to 44. The calculations show approximately the same trend as the RELAP5/MOD3 calculation in steam flow rate, water flow rate, pressure difference, water layer thickness, etc.. Since it may be expected that the RELAP5/MOD3 model in calculating the interphase drag may result in better prediction, only for the case when the flow experiences a significant change (e.g., a change in direction, from horizontal to vertical) across the junction, little difference in comparison with the RELAP5/MOD3 was found in the horizontal, stratified flow.

5. Sensitivity and Nodalization Studies

5.1 Calculation Without a fixed interfacial area

Under stratified flow condition, the interfacial heat transfer area is calculated from the hydraulic diameter and the void fraction. In this experiment, the cross section of the test section is 0.30 m x 0.063 m, resulting in the hydraulic diameter of about 0.105 m. It implies that the maximum width of the flow is not 0.30 m but 0.105 m in the code calculation. The interfacial heat transfer area calculated by RELAP5 is thus about 3 times smaller than actual interfacial area.

The RELAP5 may not give highly accurate quantitative results compared to the experimental data, principally because a pipe has a circular cross section. The geometrical restriction has the obvious consequence that the liquid level and interfacial area are coupled in the calculations. Calculated interphase transfer of mass, momentum, and energy at a point in the flow path are thus more strongly affected by upstream condensation rate than would be the case with a constant interfacial area. The interfacial area, therefore, was fixed to be the same as the area of the test section by implementing that into the PHAINT Subroutine in the RELAP5/MOD2.

The results, represented by the "FIA" in the figures, are shown in Figs. 6 to 21 for various inlet conditions, and compared with the base calculations. Water temperature is higher and steam temperature is lower

than the base calculations due to higher condensation rate. This may have occurred by using larger interfacial heat transfer area in calculating the local condensation rate. It is also shown in the Figs. 12 and 13 that the liquid wall friction drag coefficient is smaller and the interphase friction is larger than the base calculations. The interphase drag per unit volume due to the difference in velocities of the two phases is proportional to the product of the square of the velocity difference, drag coefficient and the interfacial area per unit volume. The interfacial area in this case was implemented larger than the base cases, and then the interphase friction became relatively larger.

5.2 Nodalization Sensitivity Study

The base calculations predict the local condensation rate well, however some discrepancies were found in the water layer thickness and local heat transfer coefficient. Thus calculation with nodalization change in the number of volumes of the test component for test number 253 was carried out by increasing 10 to 20. Comparison shows no difference in the principal parameters as shown in Figs. 57 to 60.

6. Run Statistics

CDC 170-875 Series with NOS Version 2.6.1 and CRAY2S/4-128 were used for the calculations with the RELAP5/MOD2 and the RELAP5/MOD3 Codes, respectively.

Fig. 61 shows the required CPU time vs the real time in the base calculations. The computational efficiency is summarized in Table 3 obtained from the base calculations and can be calculated as follows.

| Calculation | Computer Time (CPU),sec | Number of Time Step (DT) | Number of Volume (N) | Grind Time, CPU/(N*DT) |
|-------------|-------------------------|--------------------------|----------------------|------------------------|
| RELAP5/MOD2 | 102.83 | 5289 | 12 | 0.001620 |
| RELAP5/MOD3 | 28.64 | 5200 | 12 | 0.000451 |

7. Conclusion

The local condensation rate in horizontal cocurrent stratified flow was calculated using the RELAP5/MOD2 and MOD3. It appears that the RELAP5 can model condensing flow parallel to a horizontal vapor-liquid interface only with PIPE component. Therefore, the only apparent means of modelling a rectangular channel is by specifying a PIPE component which has one azimuthal segment.

The RELAP5 prediction of the condensation rates is in good agreement with the experimental data. However, some discrepancies with experimental results were found in water layer thickness and local heat transfer coefficient especially when there was a wavy interface. The interfacial wave structure was found to play an important role in describing interfacial heat and mass transfer, as obtained in the experiment.

A nodalization study at the test section for test number 253 was also carried out by changing the number of the volumes from 10 to 20. Comparison shows no difference in the principal variables. In order to examine the effect of the interfacial area, another calculation with a fixed interfacial area, which is the same as the experiment, was performed by implementing that into the PHAINT subroutine in the RELAP5/MOD2. However, the results did not give any improvement on predicting the wavy interface accurately. Therefore an effort to develop models including the effect of the wavy interface might be taken to enhance the capability of the RELAP5 by considering the interfacial shear as well as the interfacial heat transfer.

References

1. "Guidelines and Procedures for the International Code Assessment and Applications Program," NUREG-1271, April 1987.
2. "Compendium of ECCS Research for Realistic LOCA Analysis," U.S. NRC, NUREG-1230, May 1987.
3. Ransom, V.H. et al., "RELAP5/MOD2 Code Manual, Volume 1: System Models and Numerical Methods, Volume 2: User Guides and Input Requirements," NUREG/CR-4312, EGG 2390, 1987.
4. "Appendix A : RELAP5 Input Data Requirements," EG&G Idaho Inc., 1990.
5. Lim, I.S. et al., "Co-current Steam/Water Flow in a Horizontal Channel," NUREG/CR-2289, Northwestern University, 1981.
6. Kircher, W. and Bankoff, S.G., "Condensation Effects in Reactor Transient," Nucl. Sci. and Eng., Vol. 89, pp. 310-321, 1985.
7. Dimenna, R.A. et al., "RELAP5/MOD2 Models and Correlations," NUREG/CR-5194, EGG-2531, 1988.
8. Ting, P. et al., "International Code Assessment and Applications Program" NUREG-1270, Volume 1, March 1987.
9. Kukida, Y. et al., "Assessment and Improvement of RELAP5/MOD2 Code's Interphase Drag Models," 24th ASME/AIChE National Heat Transfer Conference, Pittsburgh, PA, August 9-12, 1987.
10. Riemke, R.A., "Junction-Based Interphase Drag and Vertical Stratification Modifications For RELAP5/MOD3," EGG-EAST-3580, 1989.

11. Lim, I.S., Tankin, R.S., and Yuen, M.C., "Condensation Measurement of Horizontal Cocurrent Steam/Water Flow," Journal of Heat Transfer, Trans. ASME, Vol. 106, pp. 425-432, 1984.

Table 1. RELAP5/MOD3 Model Improvements

-
- Counter Current And Flow Limiting
 - Interfacial Friction in Bubbly/Slug Flow Regime
 - Vapor Pullthrough, Liquid Entrainment in Horizontal Pipes
 - Critical Heat Flux
 - Interfacial Condensation on Subcooled ECCS Liquid in Horizontal Pipes
 - Horizontal Stratification Inception Criterion
 - Reflood Heat Transfer
 - Vertical Stratification
 - Metal-Water Reaction
 - Fuel Rod Ballooning and Rupture Model
 - Radiation Heat Transfer Model
 - Non-Condensable Gas Modelling
 - Downcomer Penetration and ECCS Bypass
 - Upper Plenum De-entrainment
-

Table 2. Inlet Conditions of the Calculations

| Test No. | Wg (kg/s) | Wl (kg/s) | Tg (C) | Tl (C) | wlt (cm) |
|----------|-----------|-----------|--------|--------|----------|
| 253 | 0.0651 | 0.657 | 138.1 | 21.6 | 1.583 |
| 259 | 0.1593 | 0.765 | 142.3 | 24.2 | 1.583 |
| 279 | 0.1600 | 1.043 | 142.3 | 25.0 | 1.583 |
| 293 | 0.0652 | 1.439 | 137.0 | 24.9 | 1.583 |

where Wg : steam mass flow rate
 Wl : water mass flow rate
 Tg : steam temperature
 Tl : water temperature
 wlt : water layer thickness
 and inlet pressure is 1 atm.

Table 3. Run Statistics Data in Base Case

| Real Time (sec) | CPU Time (sec) | | Attempted ADV | | Mass Error (kg) | |
|--------------------|----------------|-------|---------------|------|-----------------|---------|
| | R5M2* | R5M3* | R5M2 | R5M3 | R5M2 | R5M3 |
| 0 | 0.3 | 0.3 | 0 | 0 | 0 | 0 |
| 10 | 9.7 | 2.5 | 489 | 400 | 4.99E-5 | 2.37E-4 |
| 20 | 17.4 | 4.6 | 889 | 800 | 5.01E-5 | 2.50E-4 |
| 30 | 25.1 | 6.8 | 1289 | 1200 | 5.00E-5 | 2.51E-4 |
| 40 | 32.8 | 8.9 | 1689 | 1600 | | |
| 50 | 40.8 | 11.3 | 2089 | 2000 | | |
| 60 | 48.5 | 13.4 | 2489 | 2400 | | |
| 70 | 56.2 | 15.5 | 2889 | 2800 | | |
| 80 | 63.9 | 17.7 | 3289 | 3200 | " | " |
| 90 | 71.7 | 19.8 | 3689 | 3600 | | |
| 100 | 79.7 | 22.2 | 4089 | 4000 | | |
| 110 | 87.4 | 24.3 | 4489 | 4400 | | |
| 120 | 95.1 | 26.4 | 4889 | 4800 | | |
| 130 | 102.8 | 28.6 | 5289 | 5200 | | |

* R5M2 : RELAP5/MOD2
 R5M3 : RELAP5/MOD3

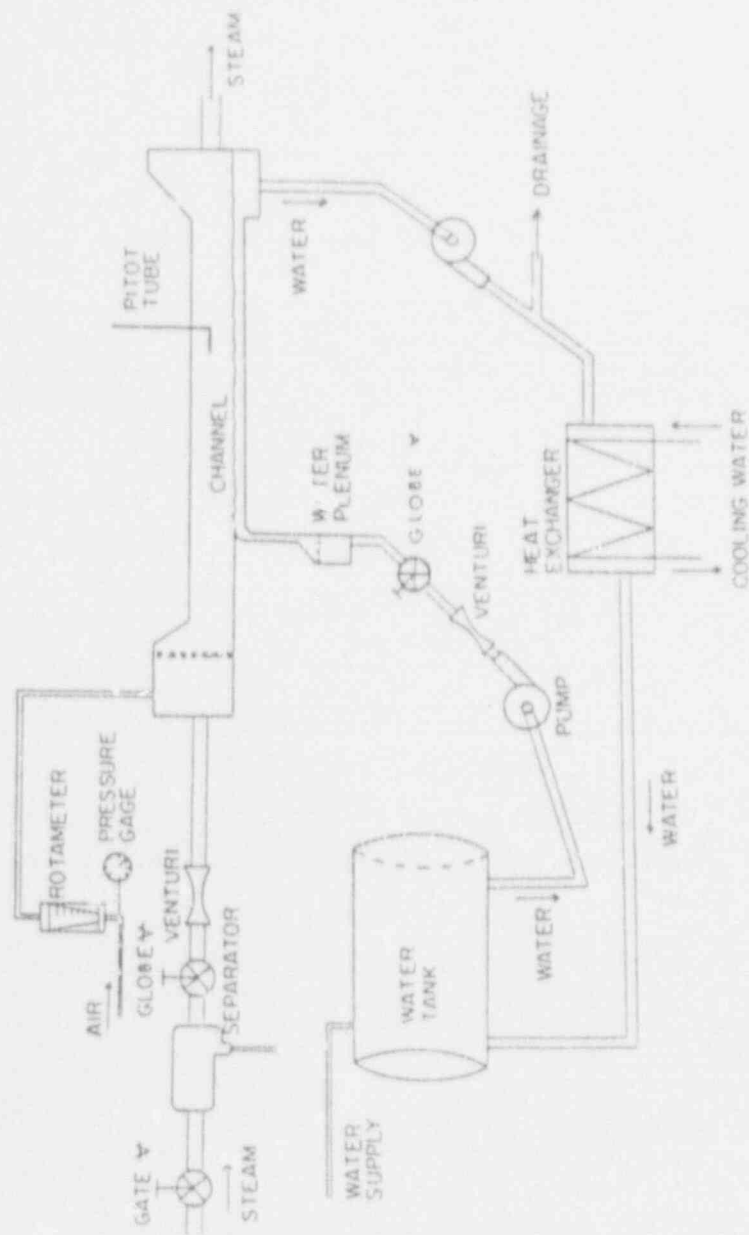


Fig. 1 Schematic Diagram of the System [5]

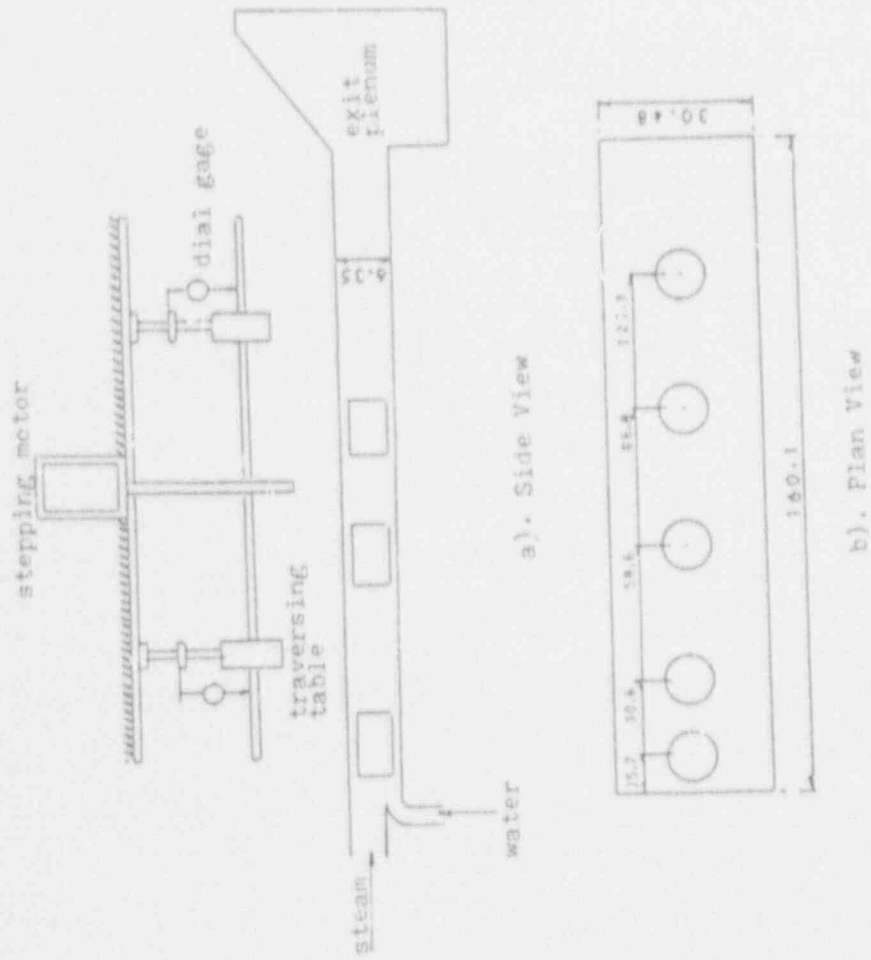


Fig. 2 Channel View of the System (5)

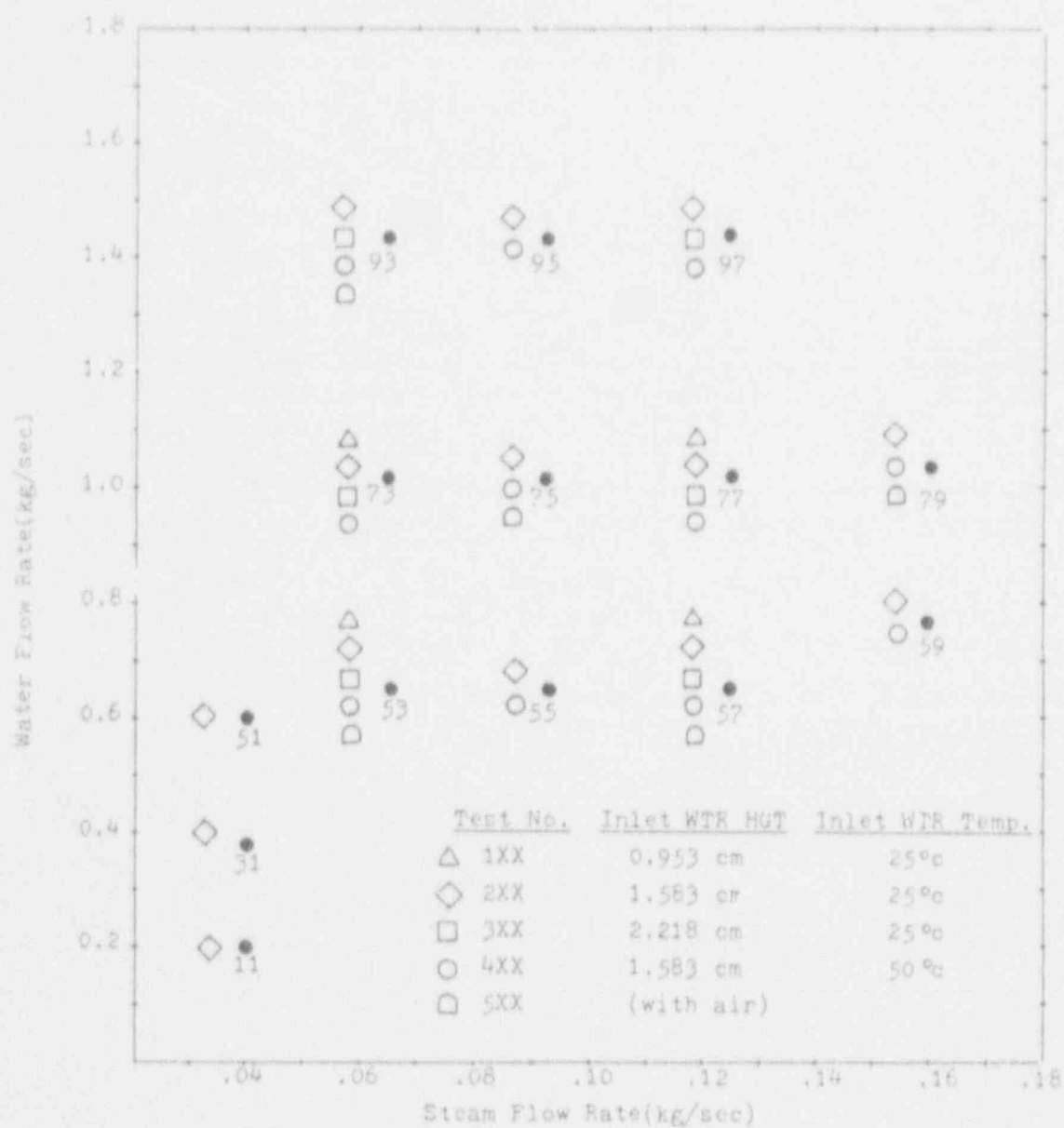


Fig. 3 Experimental Data Matrix [5]

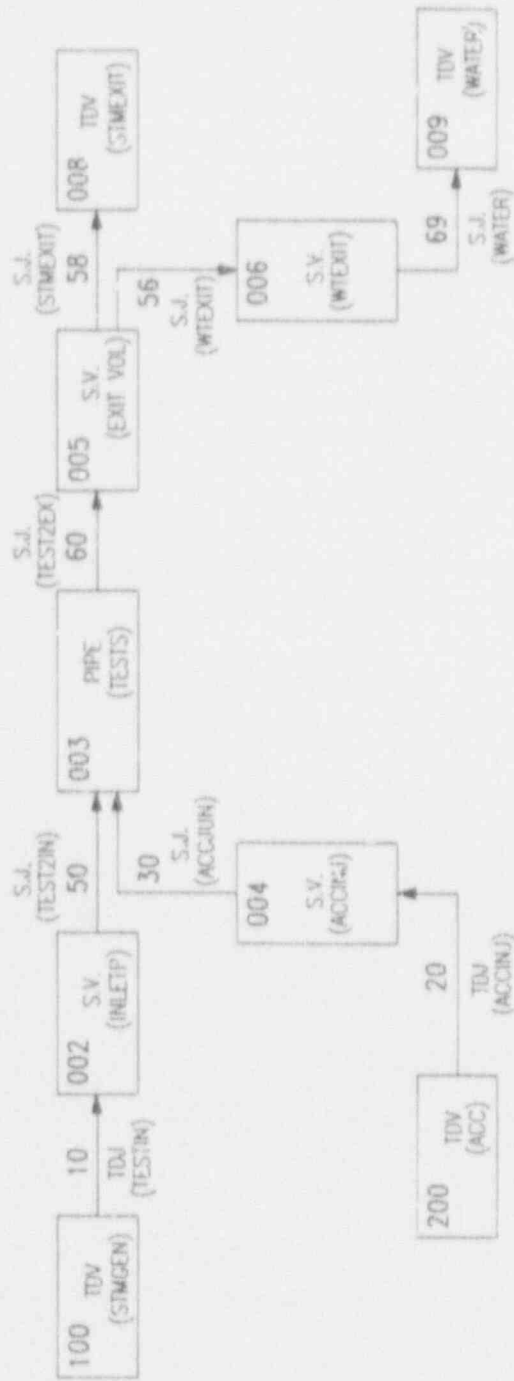


Fig. 4 Nodalization (A) of Concurrent Condensation Test

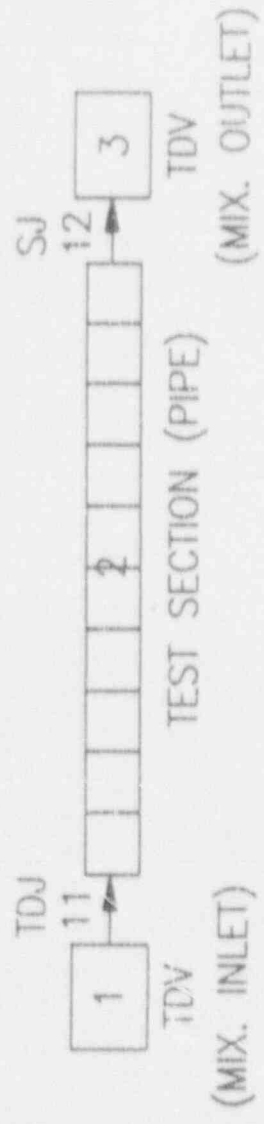


Fig. 5 Notalization (B) of Concurrent Condensation Test.

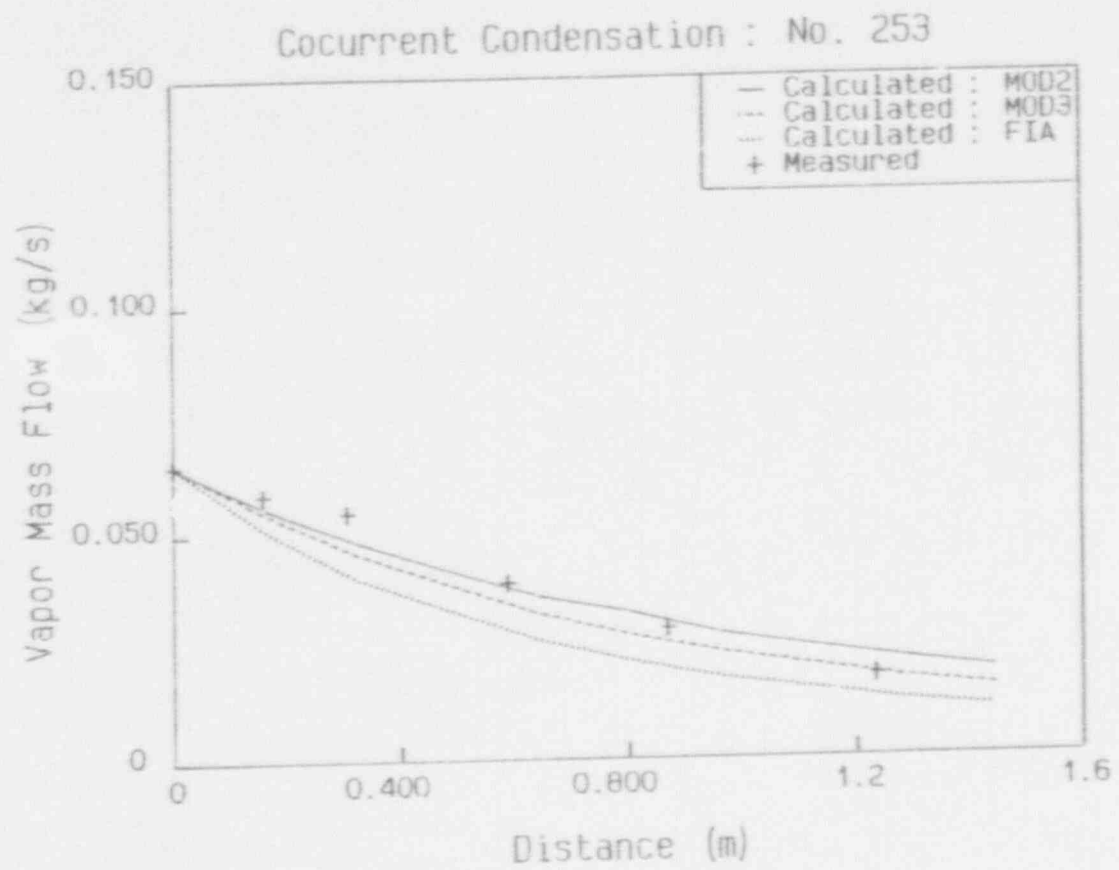


Fig. 6 Vapor Mass Flow (No. 253)

Cocurrent Condensation : No. 253

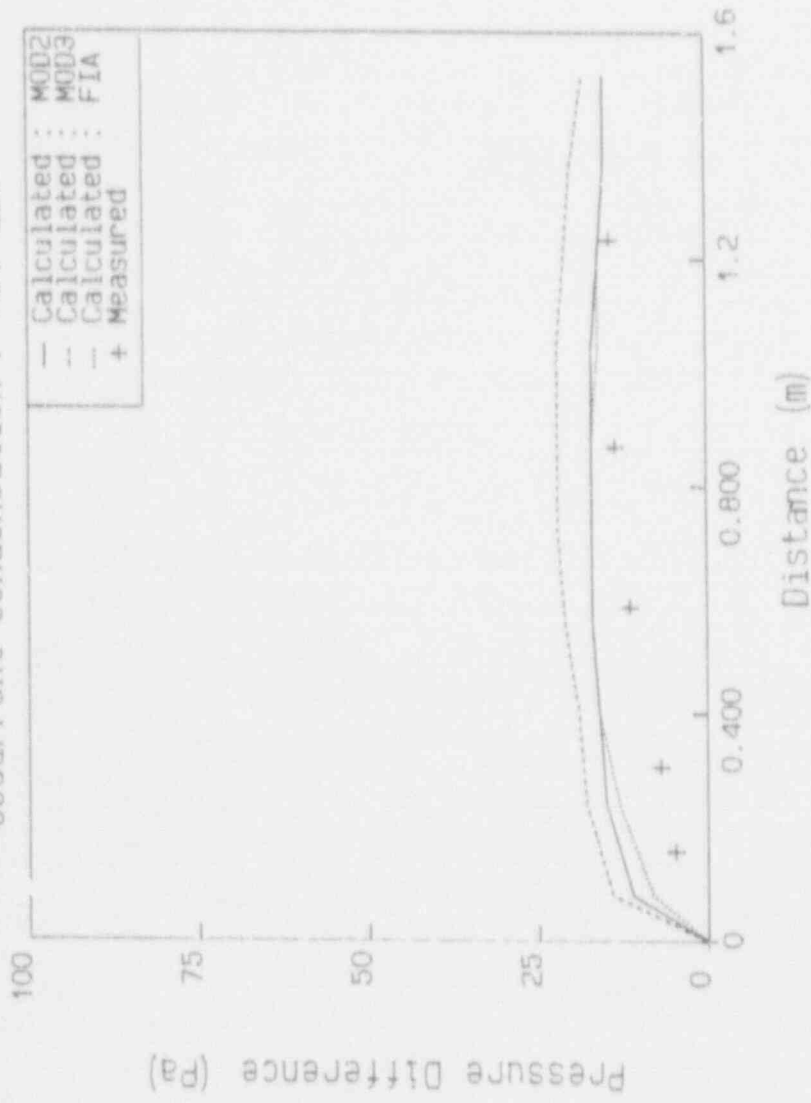


Fig. 7 Pressure Difference (No. 253)

Cocurrent Condensation : No. 253

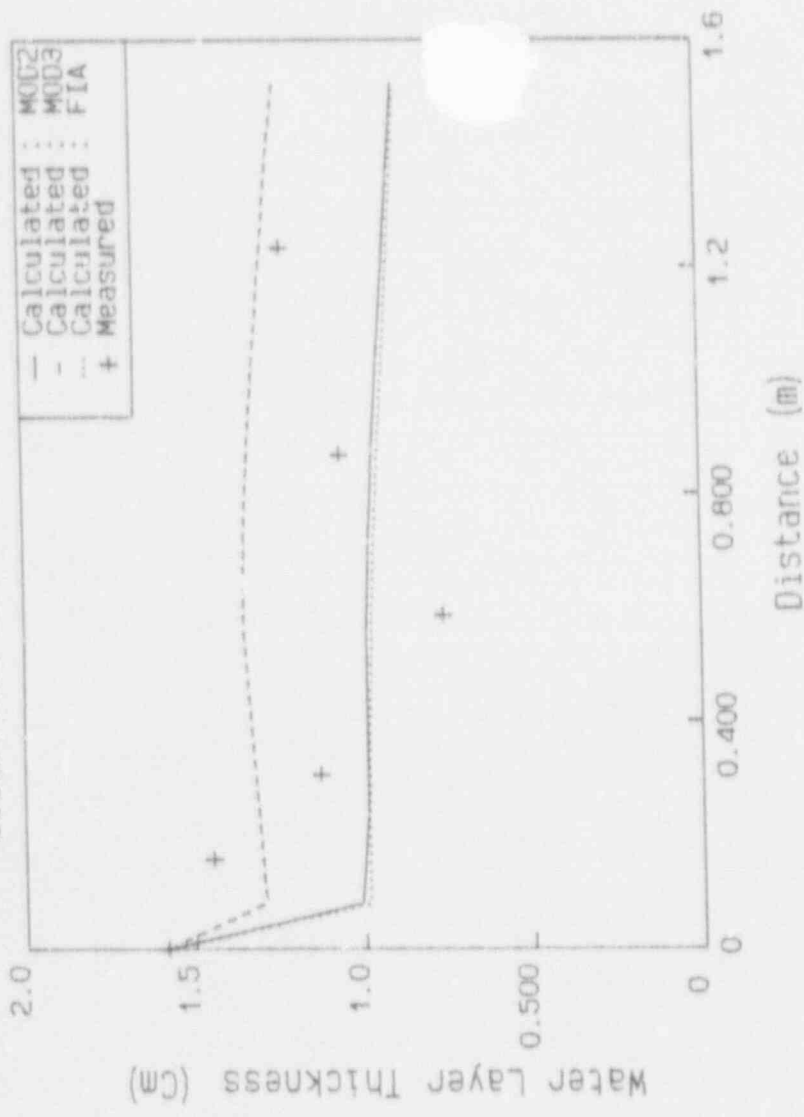


Fig. 8 Water Layer Thickness (No. 253)

Cocurrent Condensation : No. 253

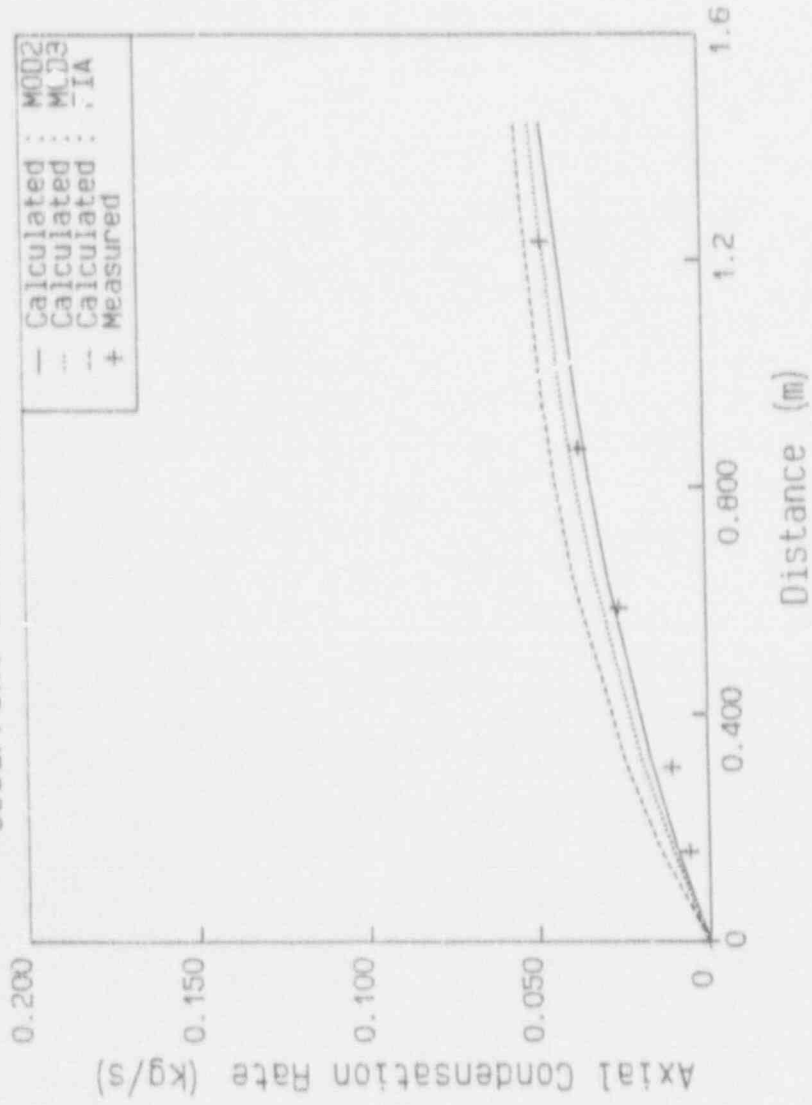


Fig. 9 Axial Condensation Rate (No. 253)

Cocurrent Condensat n : No. 253

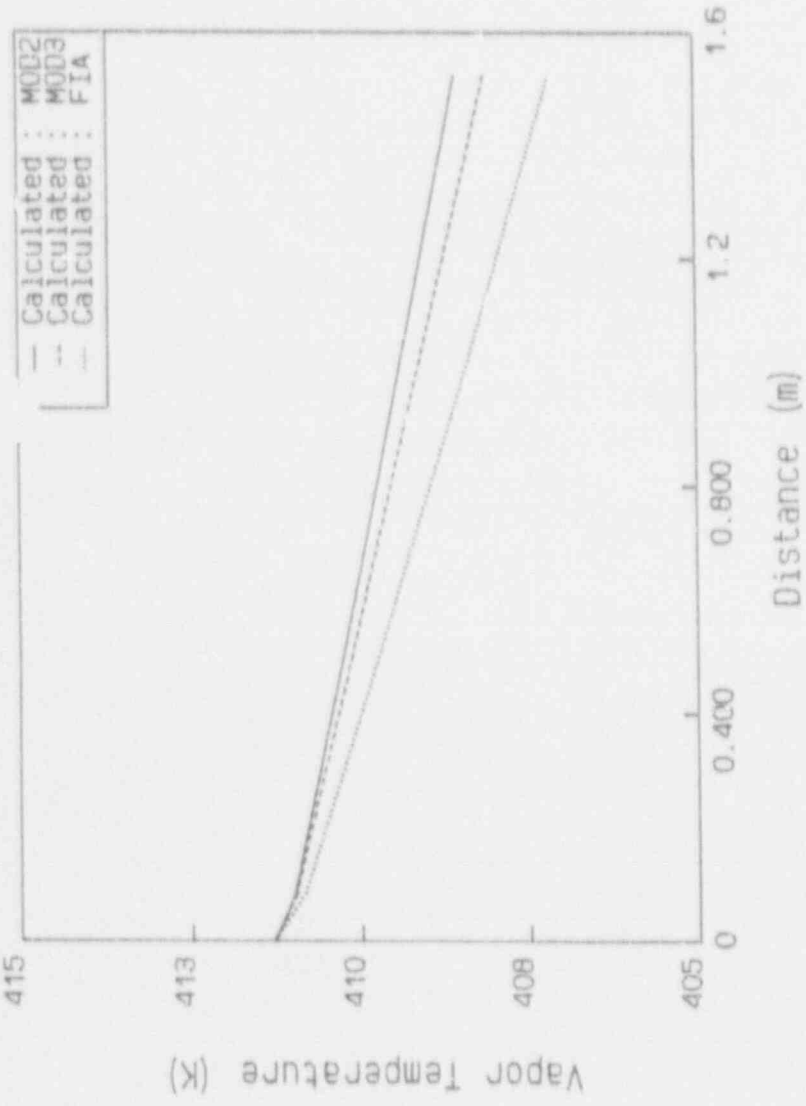


Fig. 10 Vapor Temperature (No. 253)

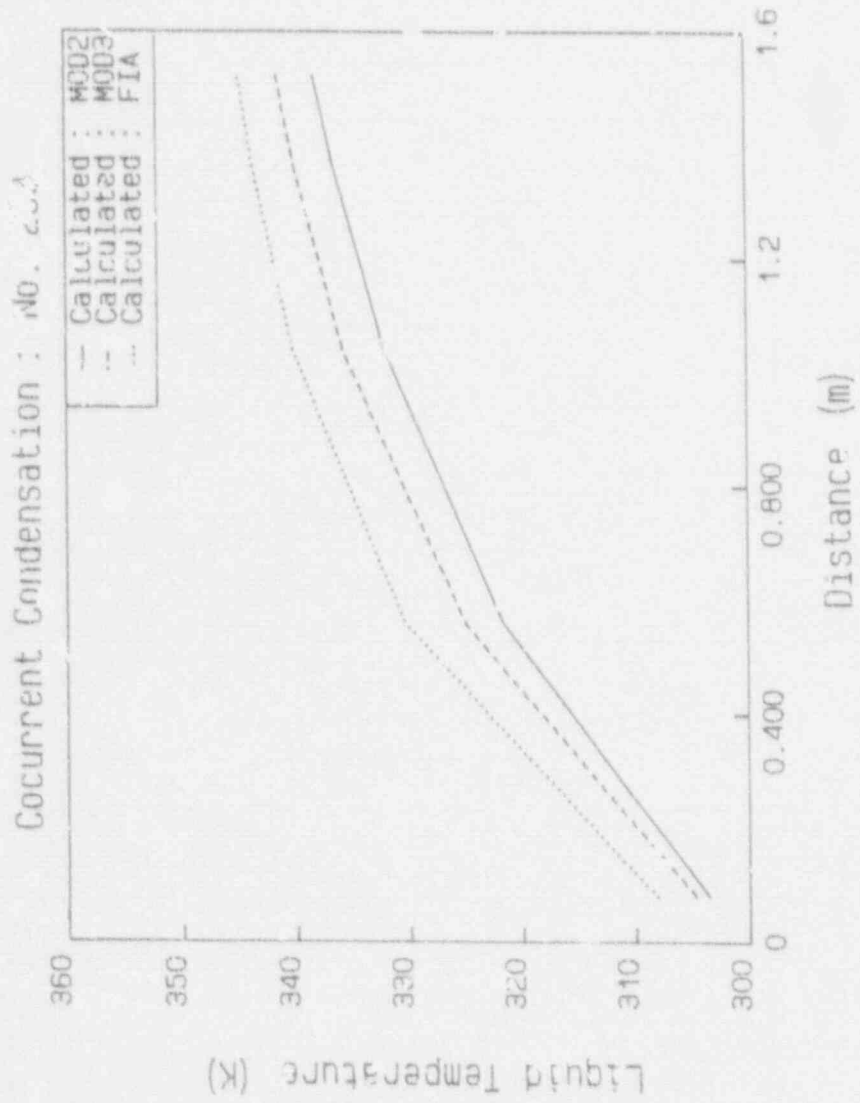


Fig. 11 Liquid Temperature (No. 253)

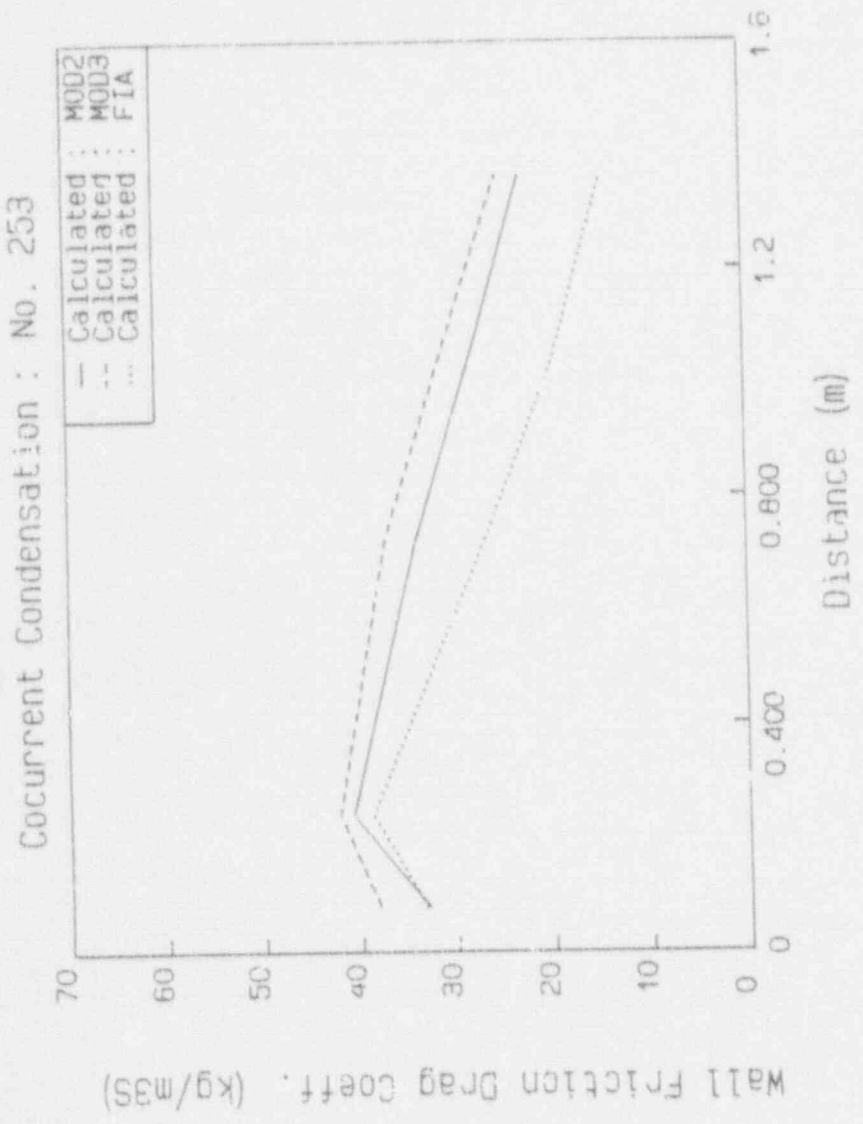


Fig. 12 Liquid Wall Friction Drag Coefficient (No. 253)

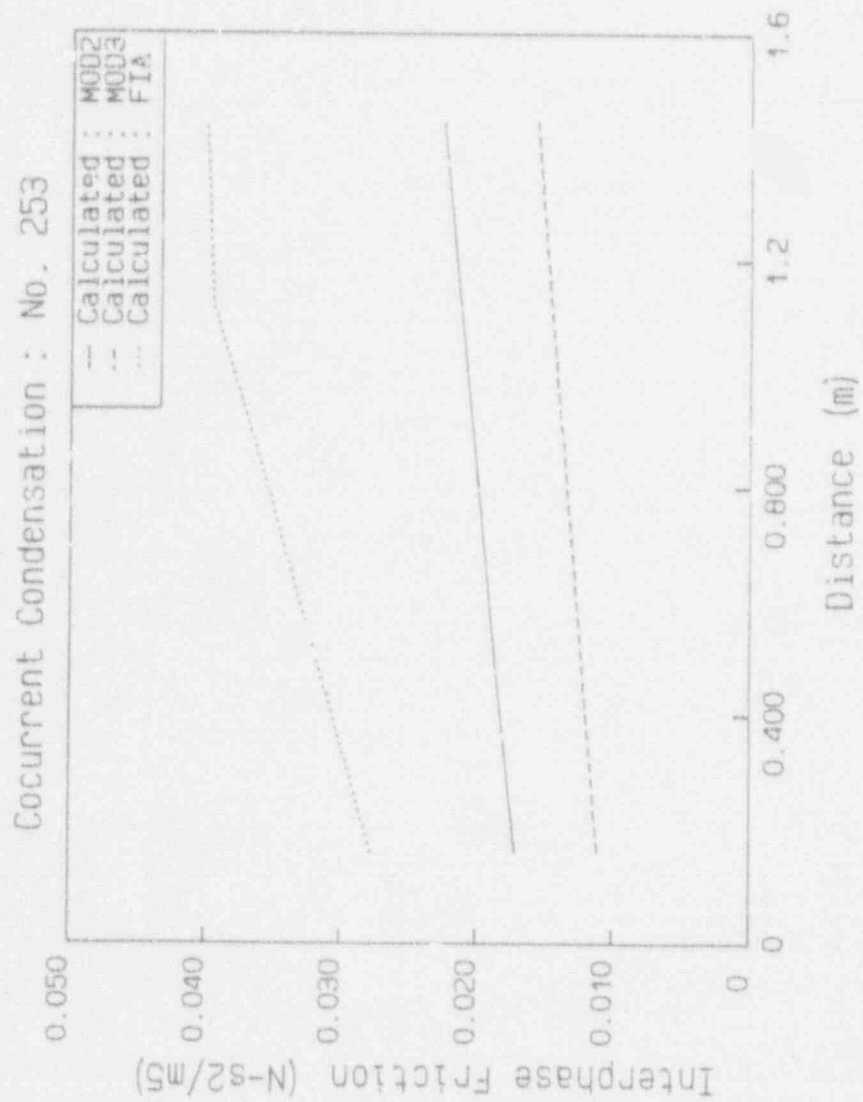


Fig. 13 Interphase Friction (No. 253)

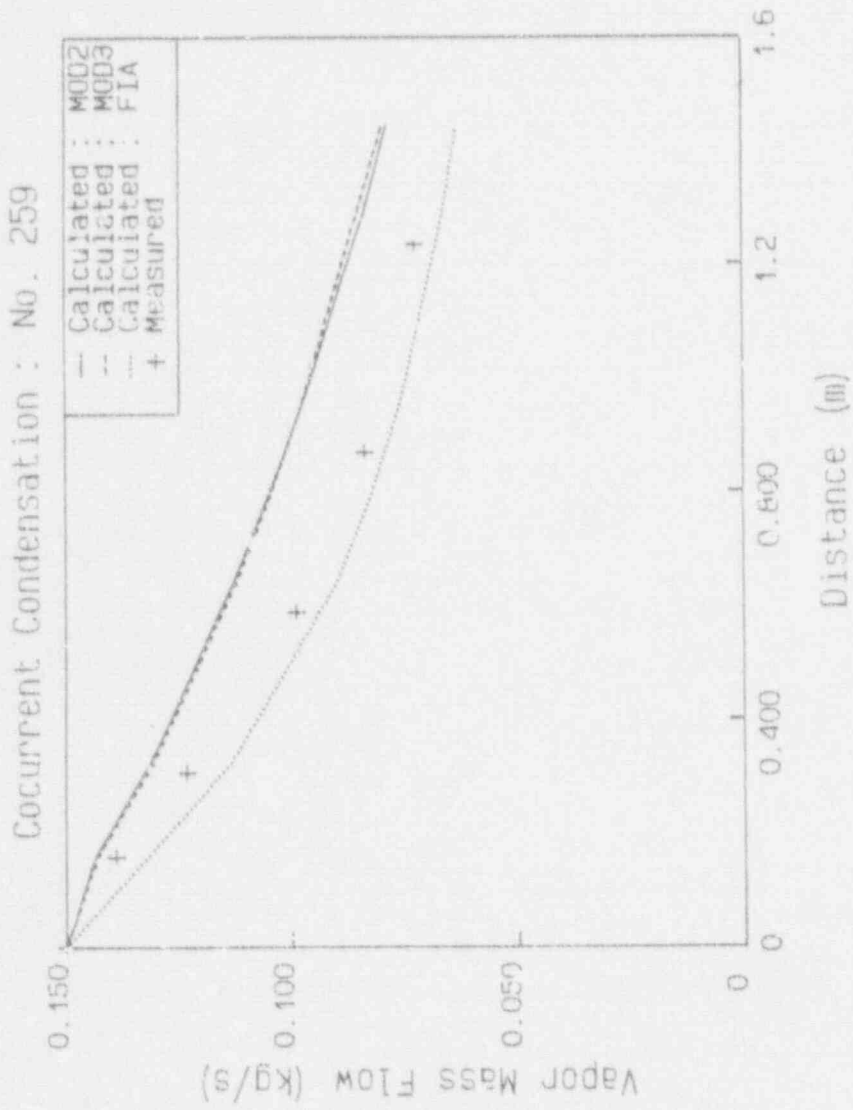


Fig. 14 Vapor Mass Flow (No. 259)

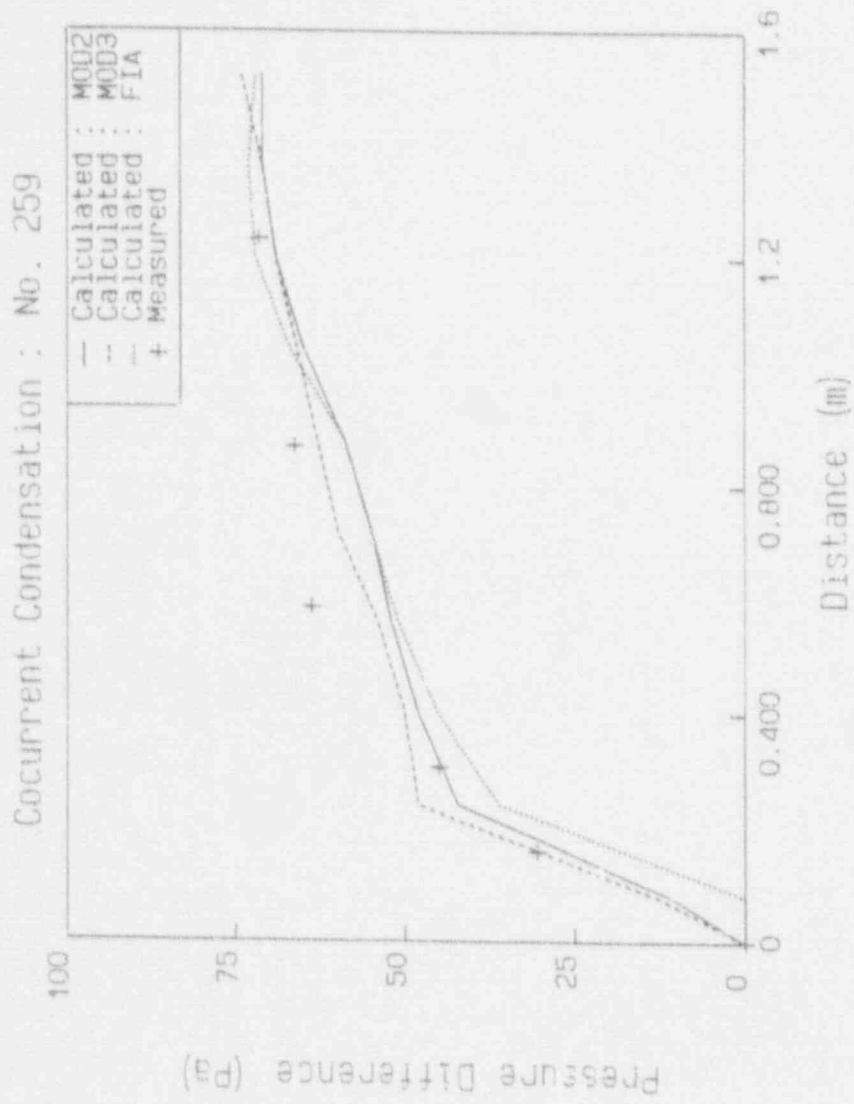


Fig. 15 Pressure Difference (No. 259)

Cocurrent Condensation : No. 259

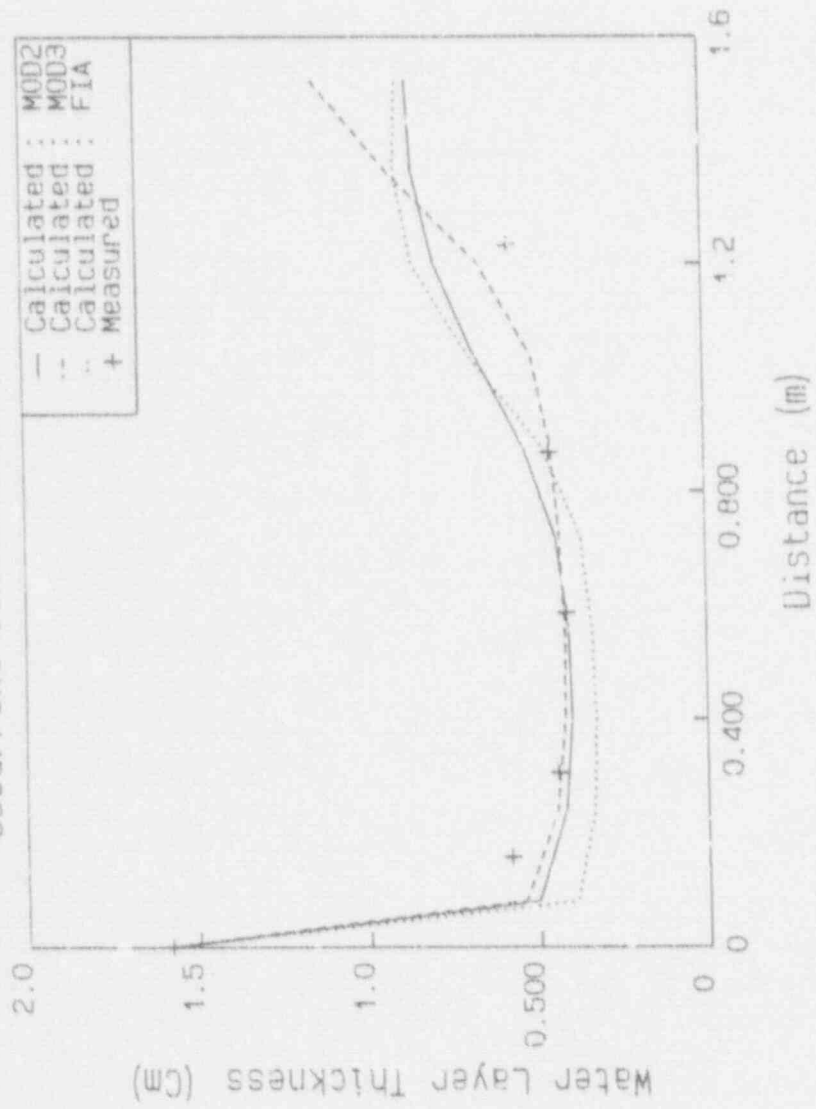


Fig. 16 Water Layer Thickness (No. 259)

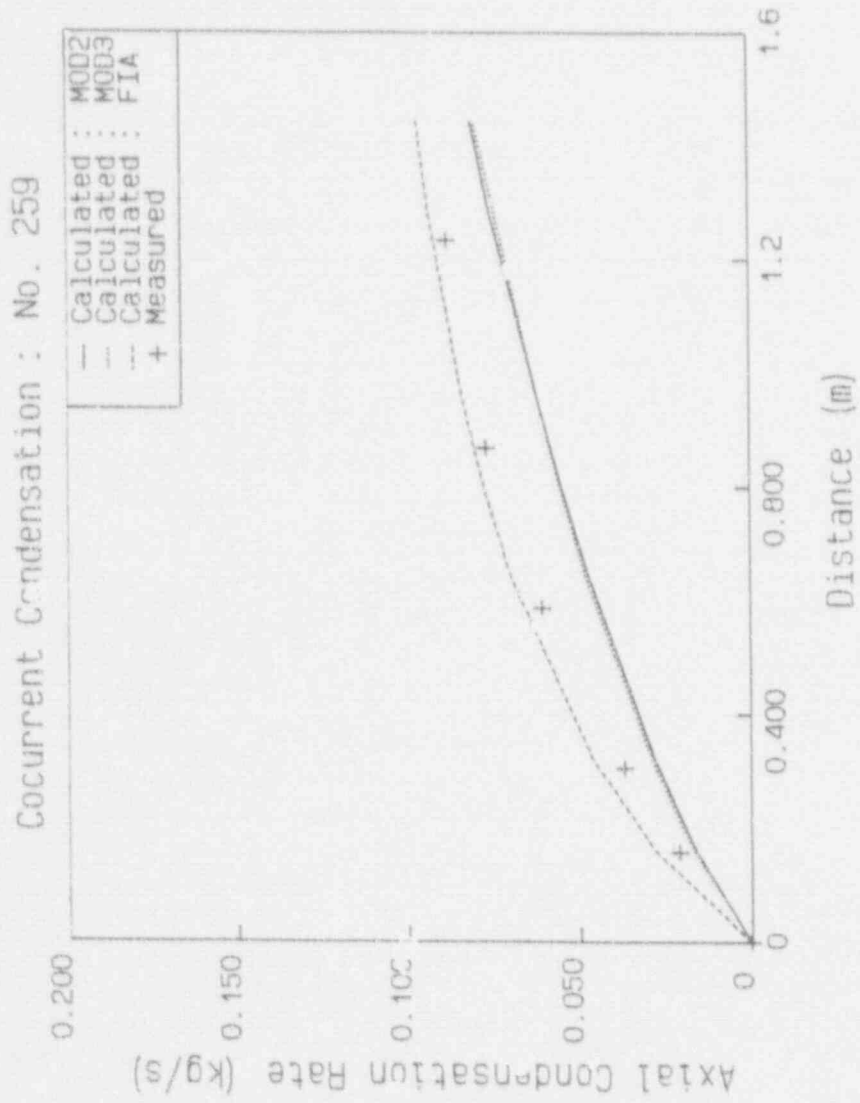


Fig. 17 Axial Condensation Rate (No. 259)

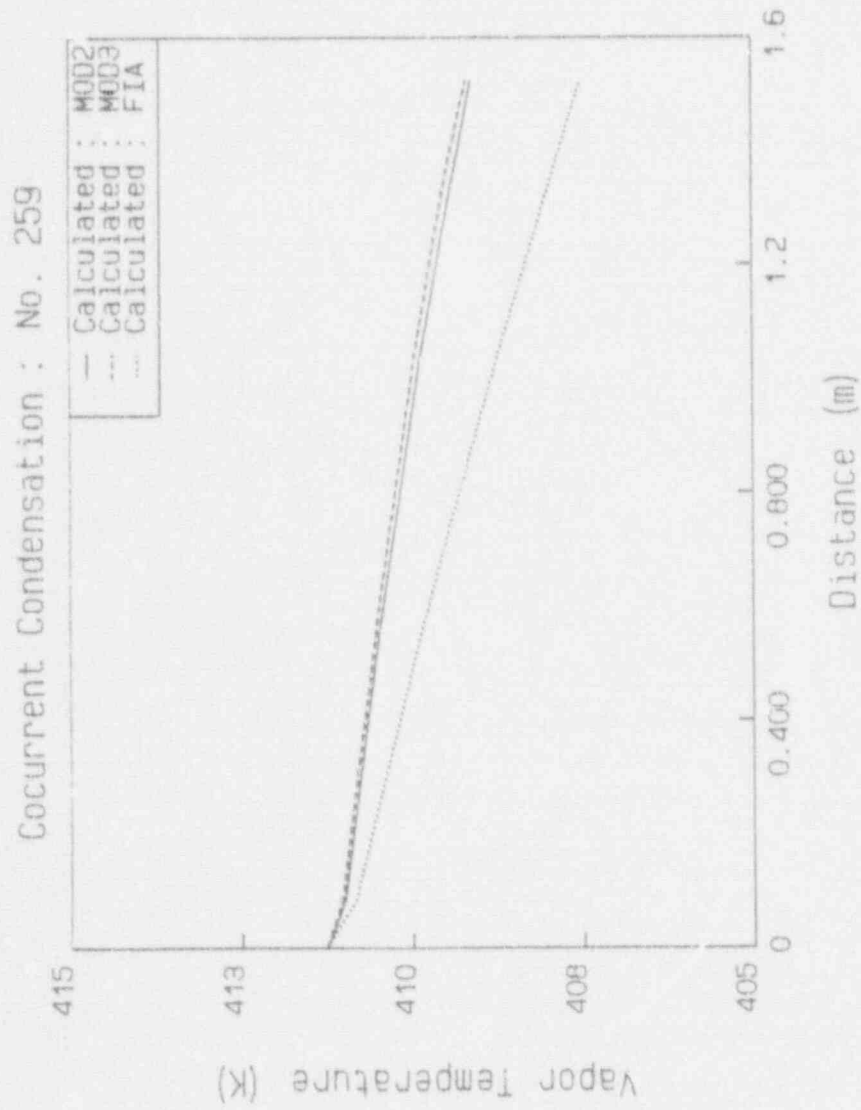


Fig. 18 Vapor Temperature (No. 259)

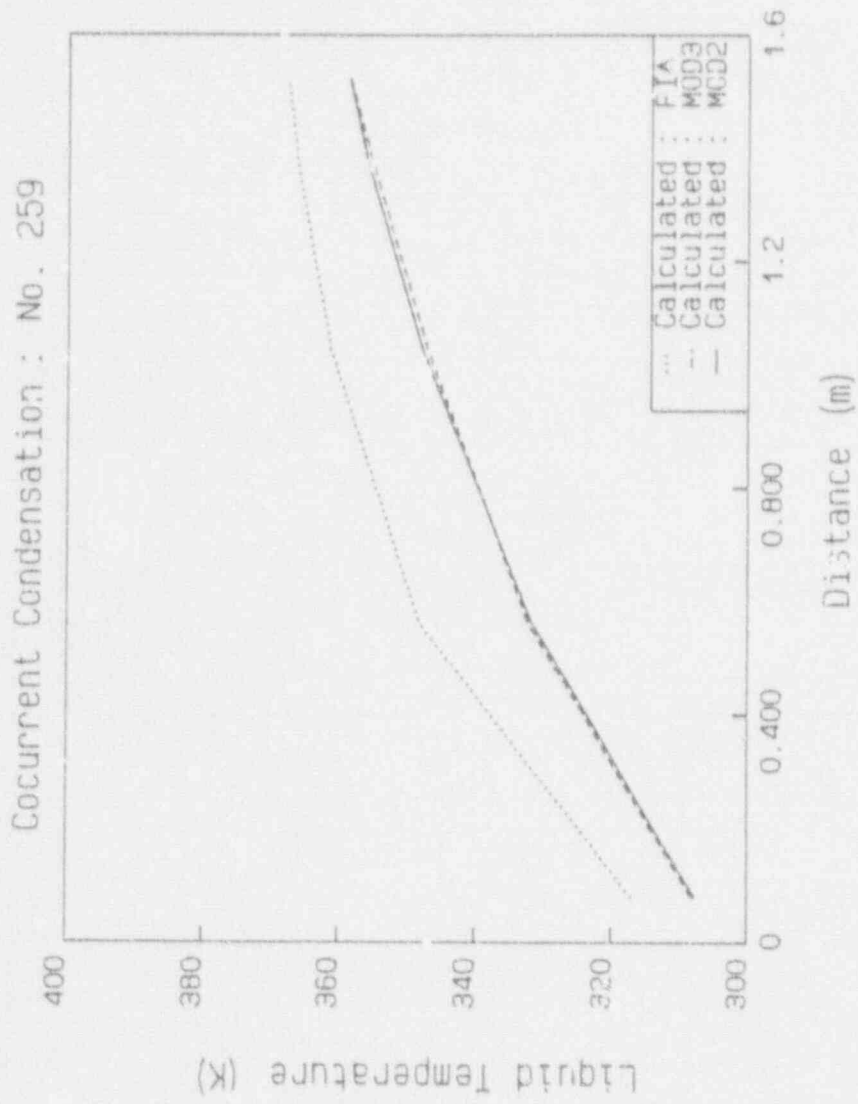
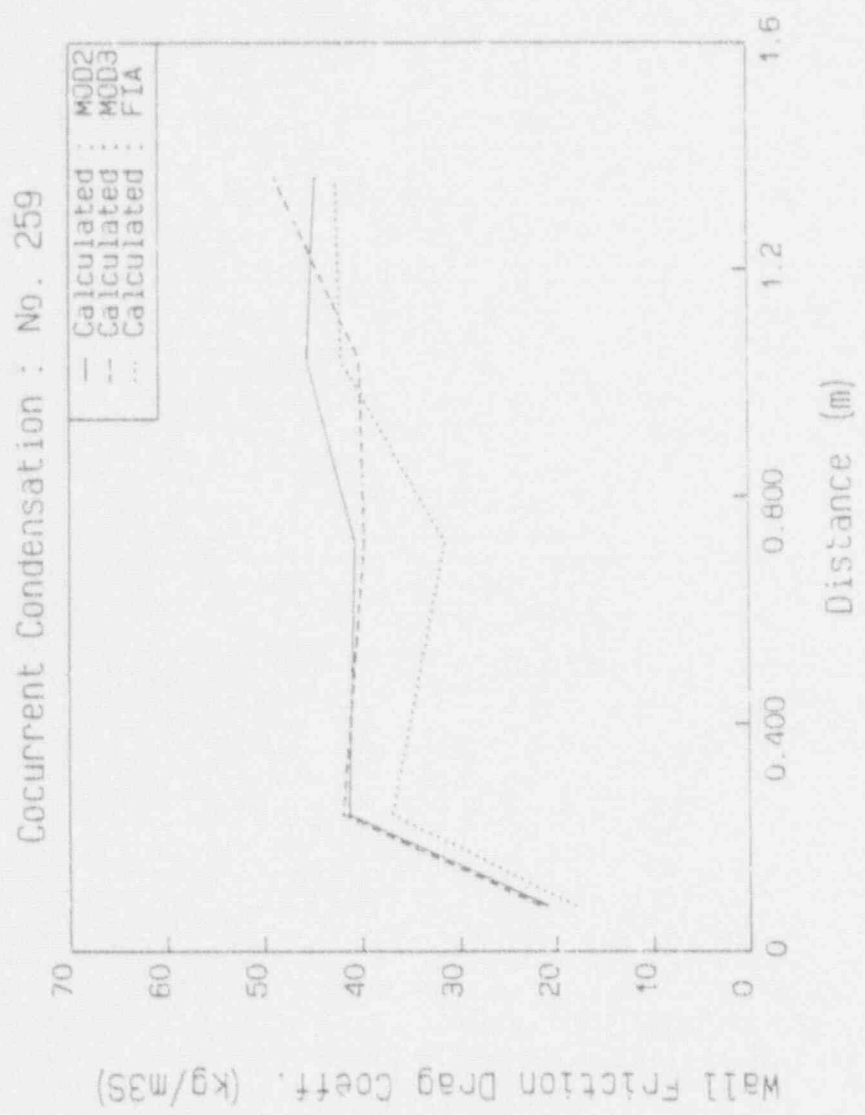


Fig. 19 Liquid Temperature (No. 259)



Wall Friction Drag Coeff. (kg/m³s)

--- Calculated : MJD2
 - - - Calculated : MJD3
 ... Calculated : FIA

Fig. 20 Liquid Wall Friction Drag Coefficient (No. 259)

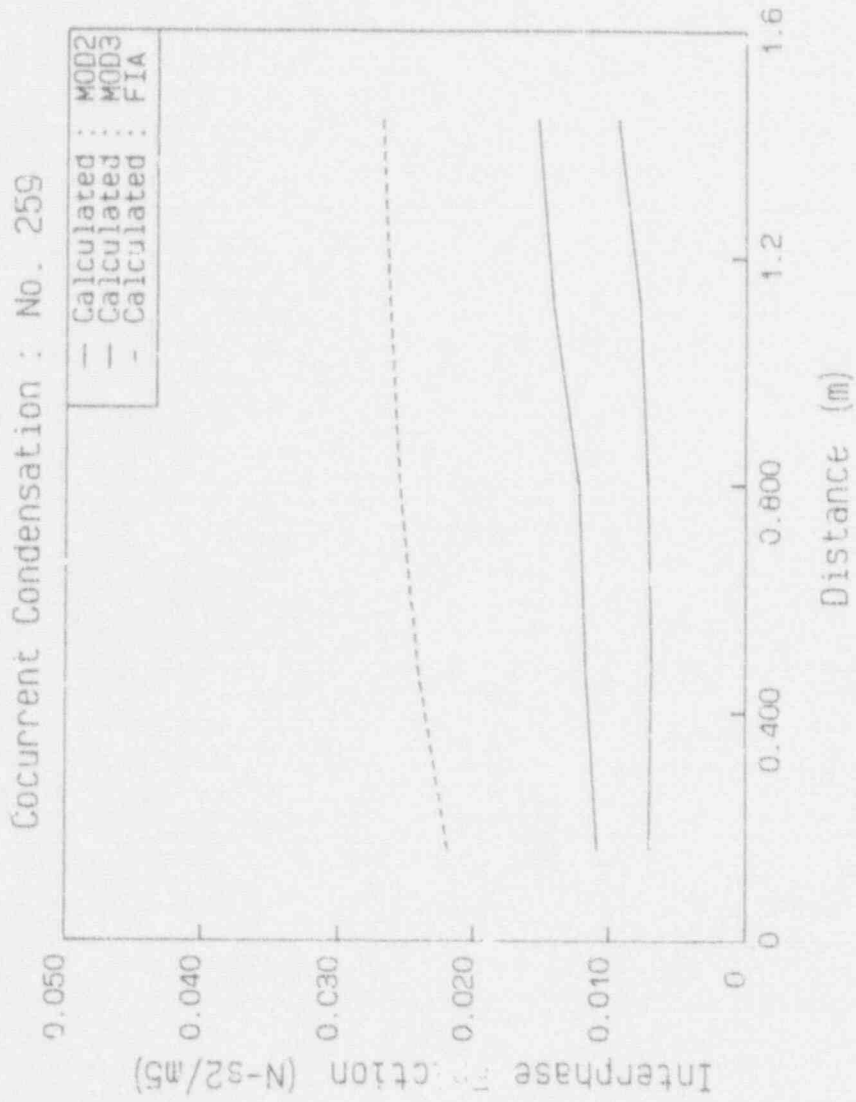


Fig. 21 Interphase Friction (No. 259)

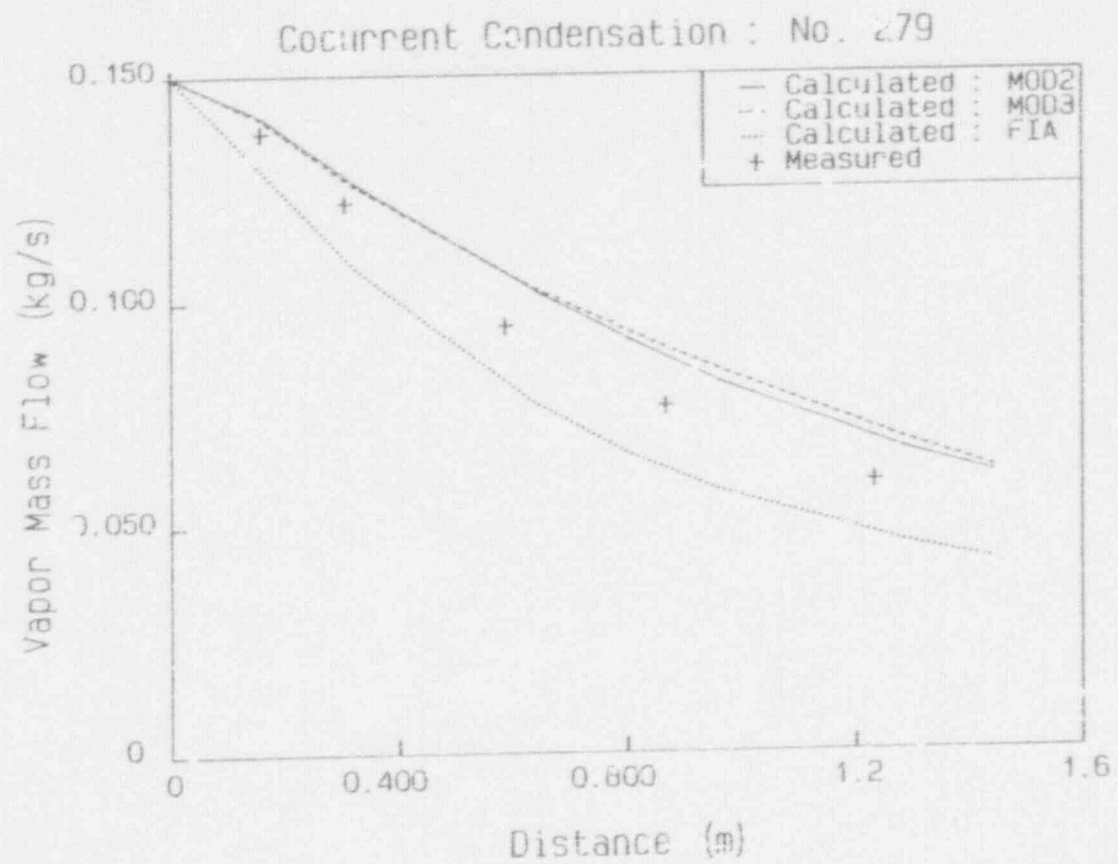


Fig. 22 Vapor Mass Flow (No. 279)

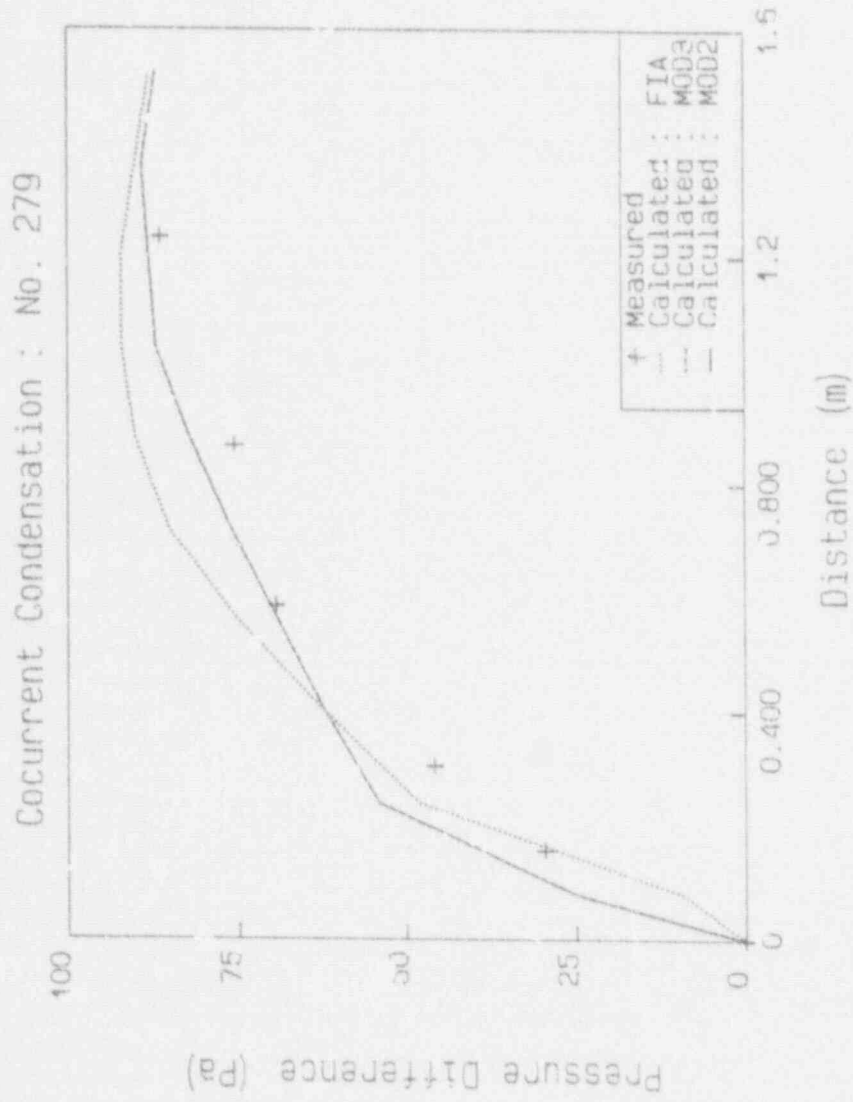


Fig. 23 Pressure Difference (No. 279)

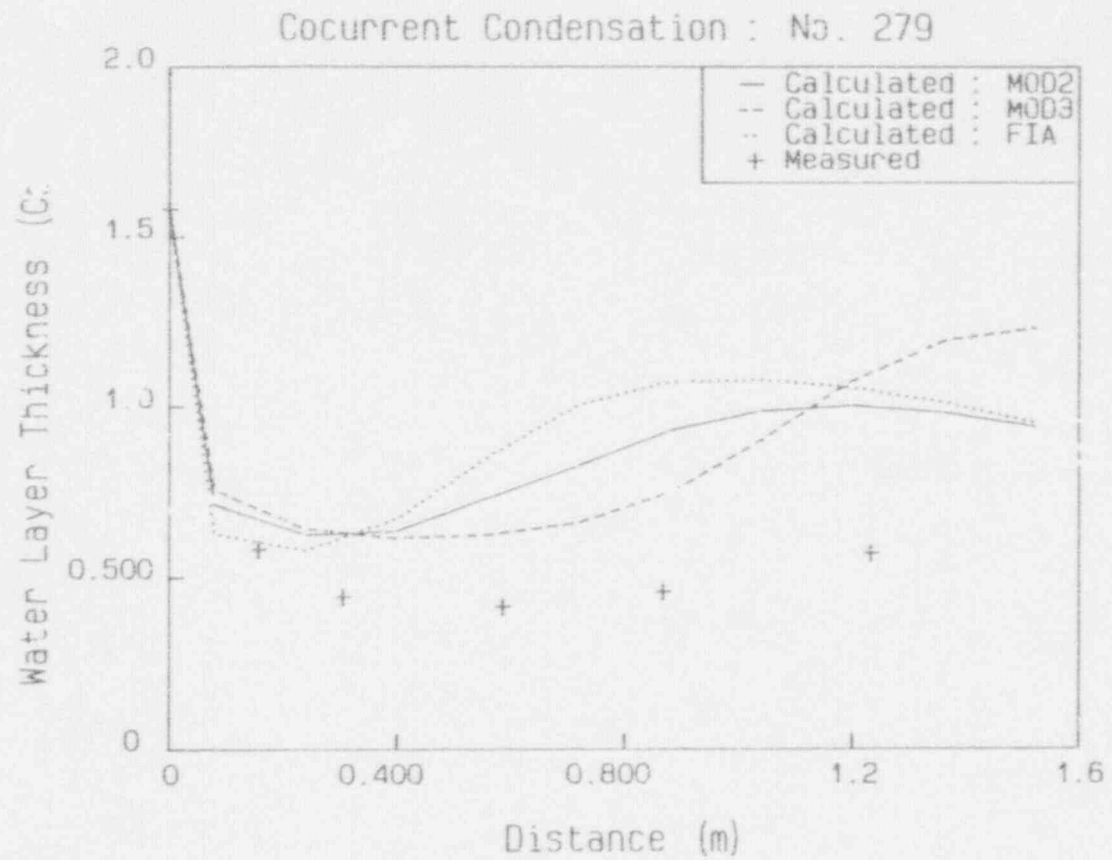


Fig. 24 Water Layer Thickness* (No. 279)

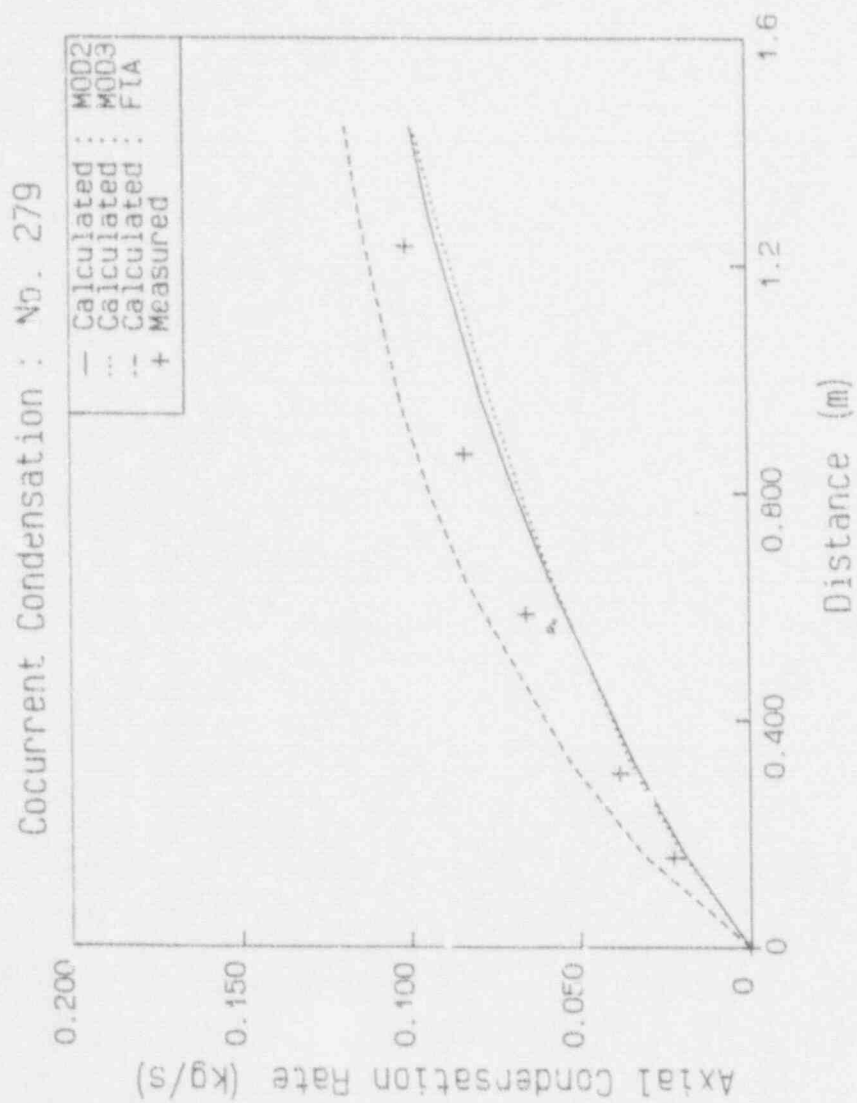


Fig. 25 Axial Condensation Rate (No. 279)

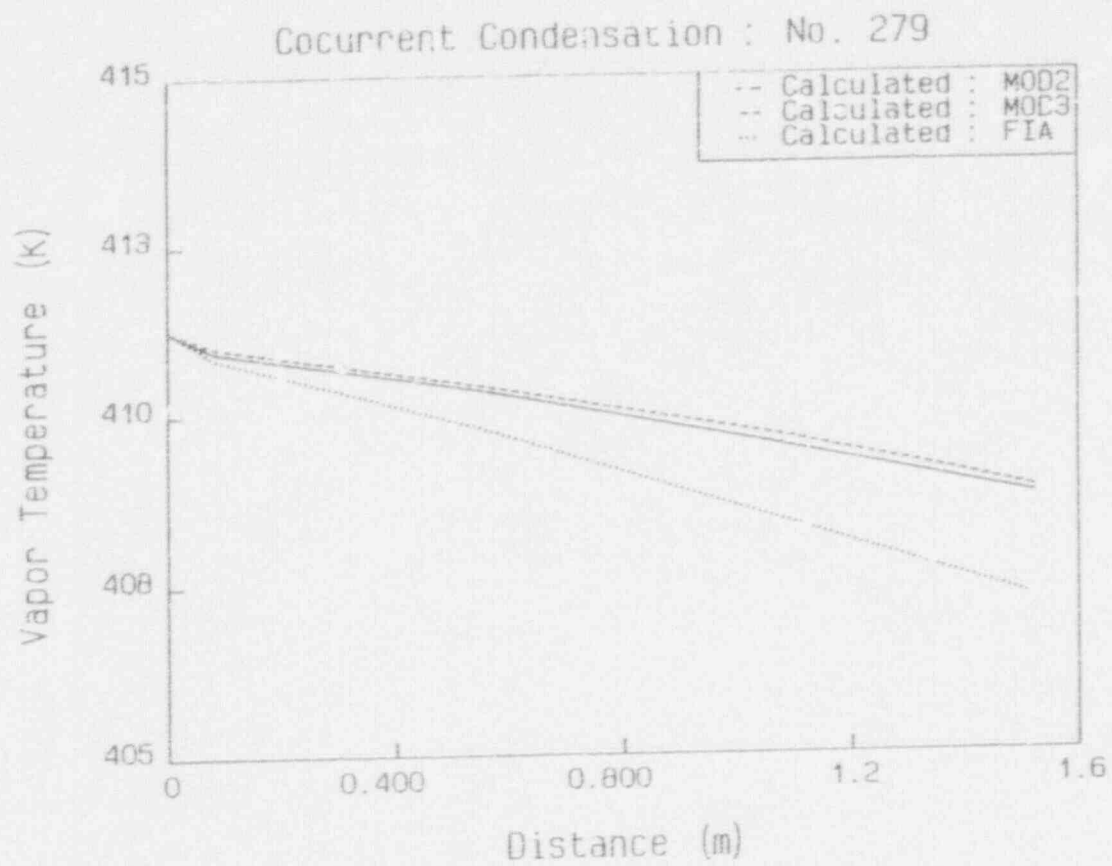


Fig. 26 Vapor Temperature (No. 279)

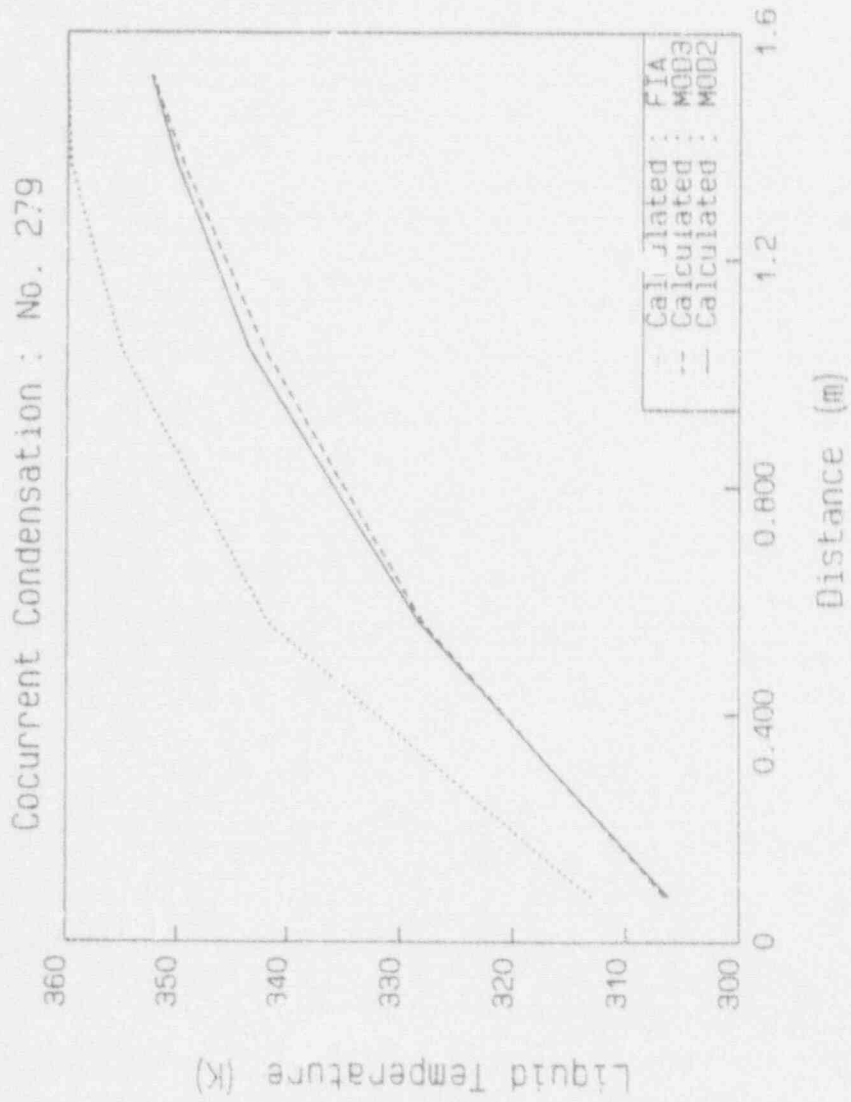


Fig. 27 Liquid Temperature : (No. 279)

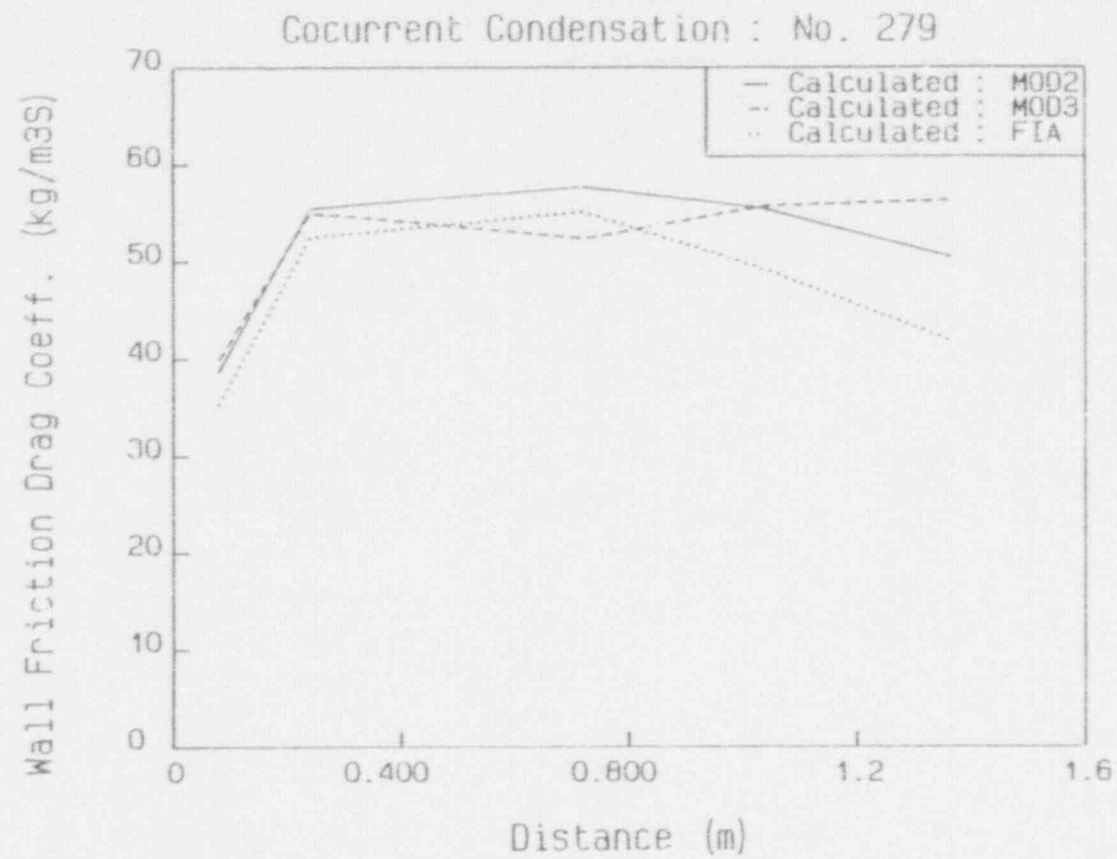


Fig. 28 Liquid Wall Friction Drag Coefficient (No. 279)

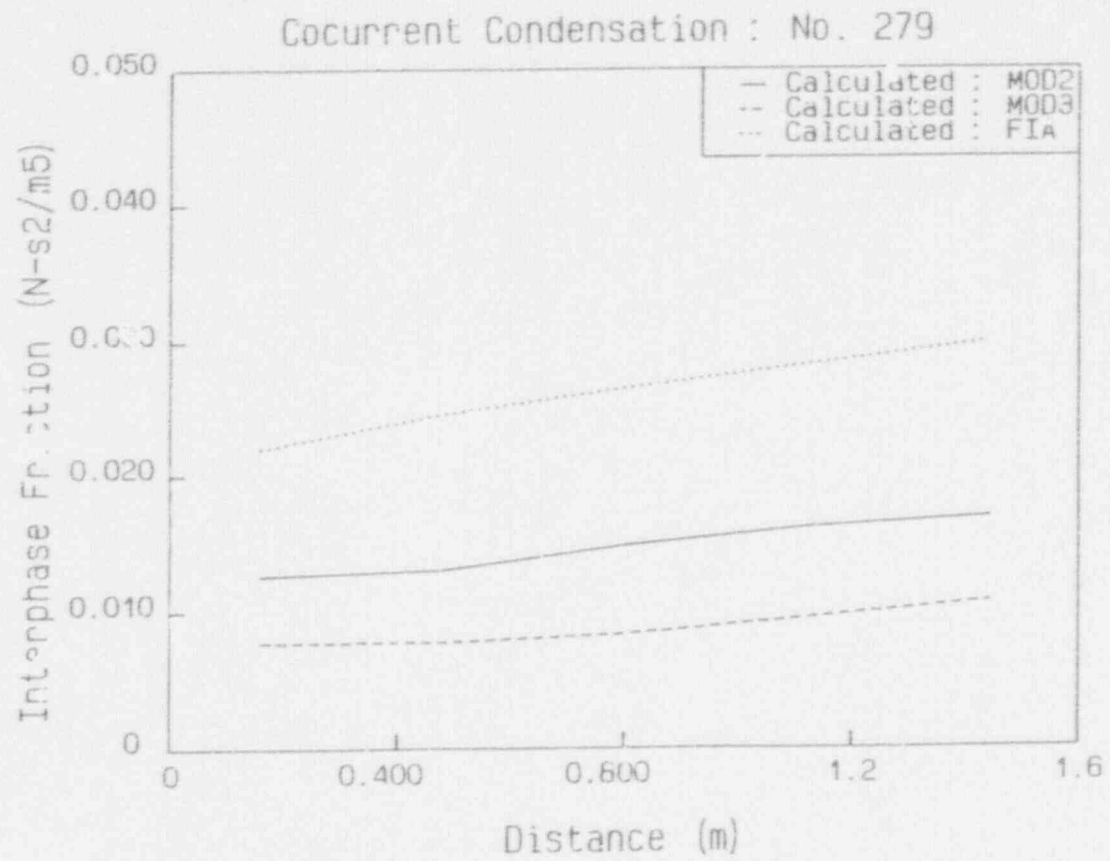


Fig. 29 Interphase Friction (No. 279)

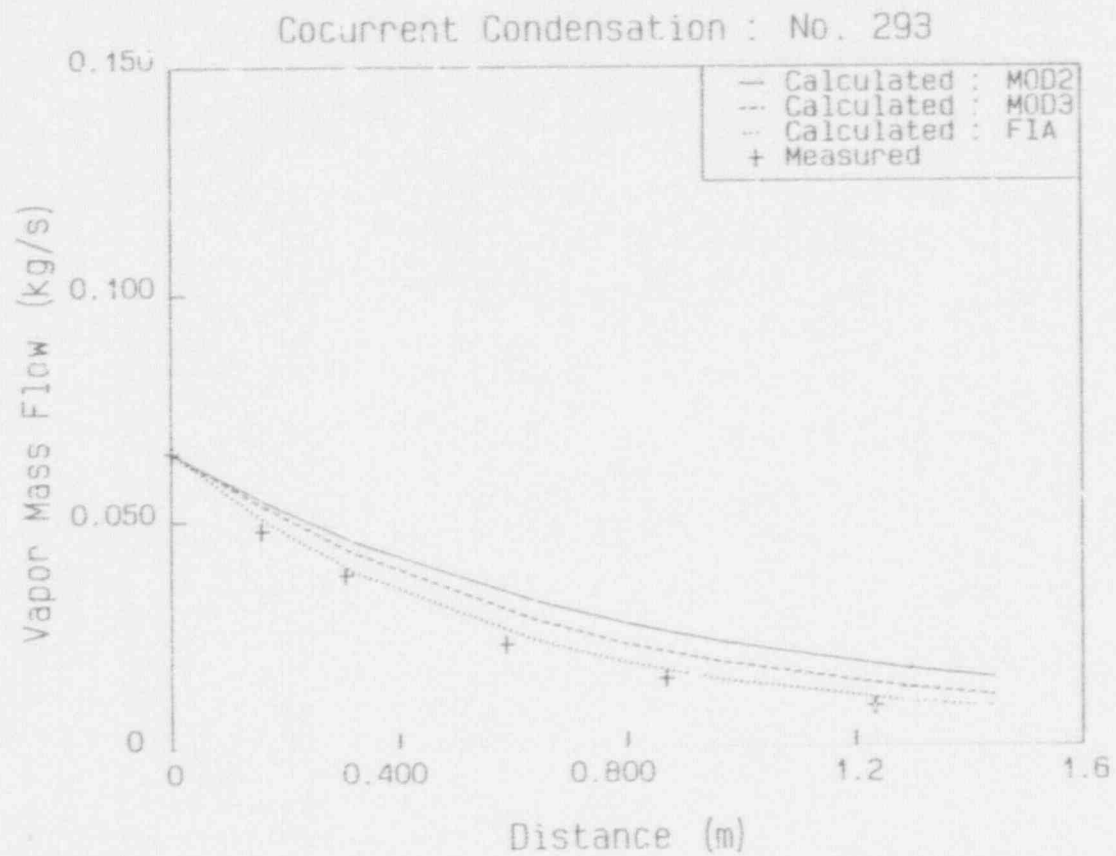


Fig. 30 Vapor Mass Flow (No. 293)

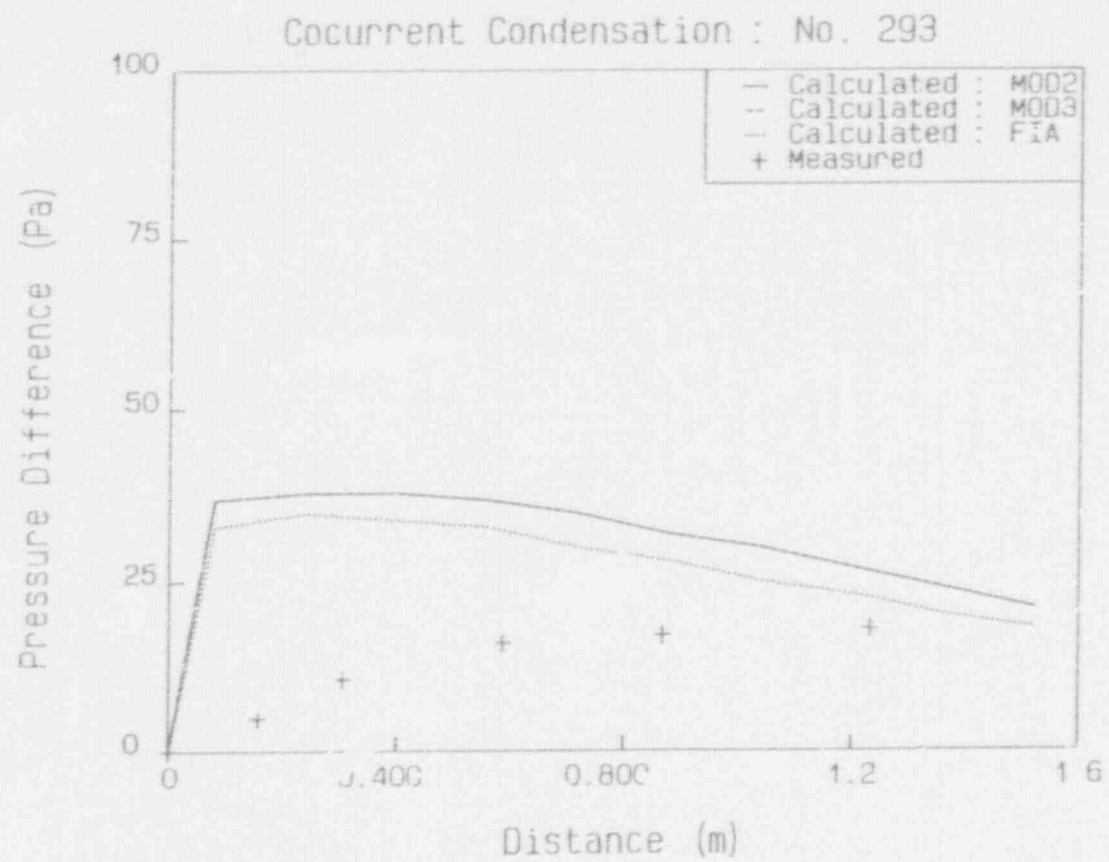


Fig. 31 Pressure Difference (No. 293)

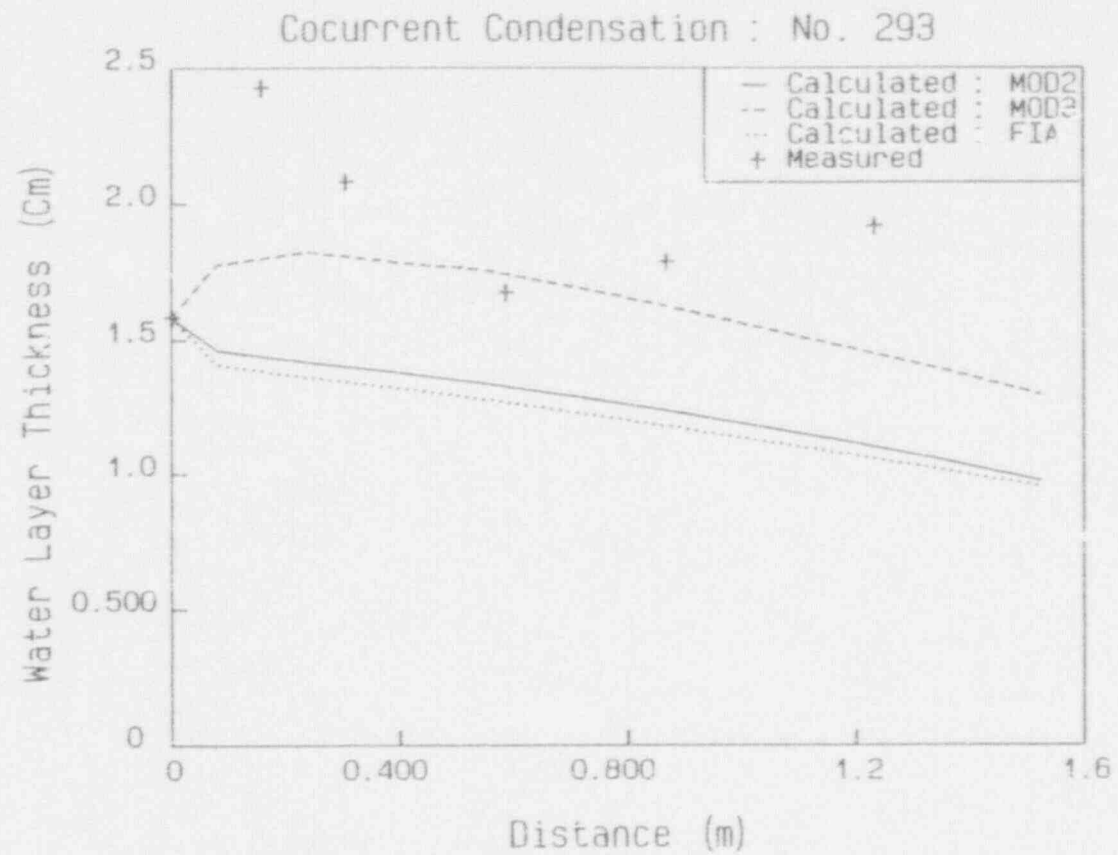


Fig. 32 Water Layer Thickness (No. 293)

Cocurrent Condensation : No. 293

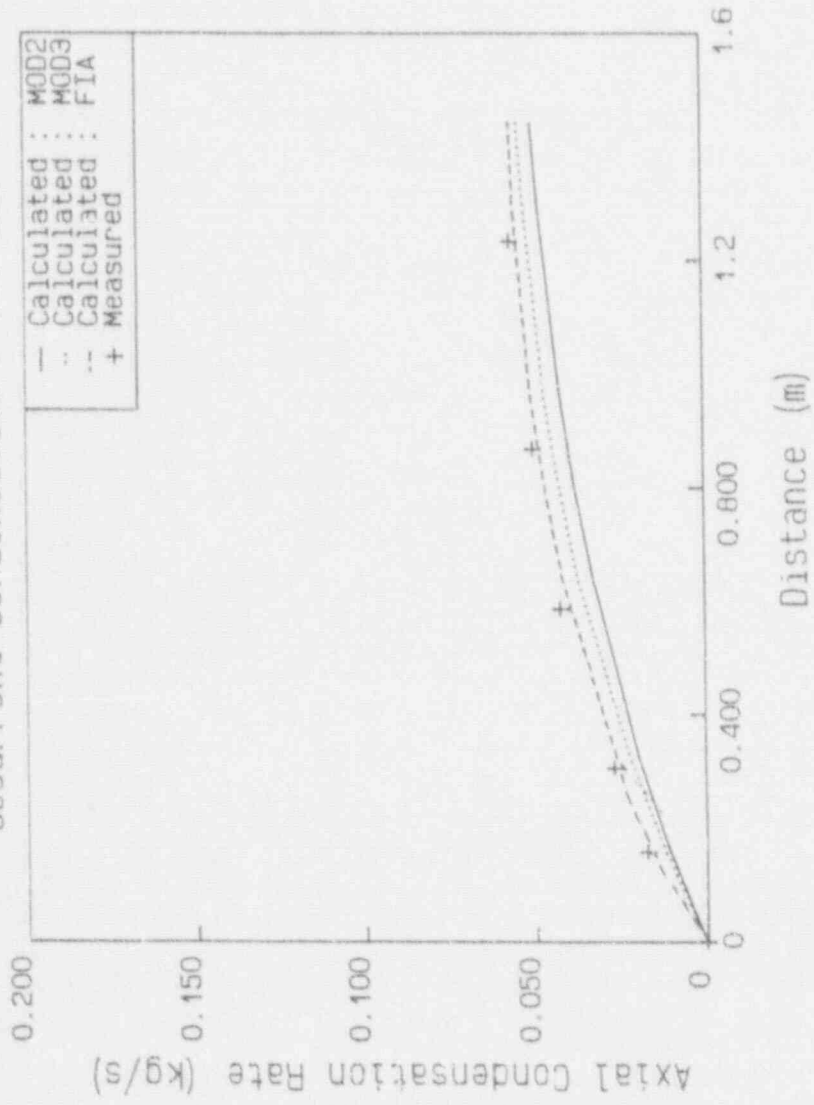


Fig. 33 Axial Condensation Rate (No. 293)

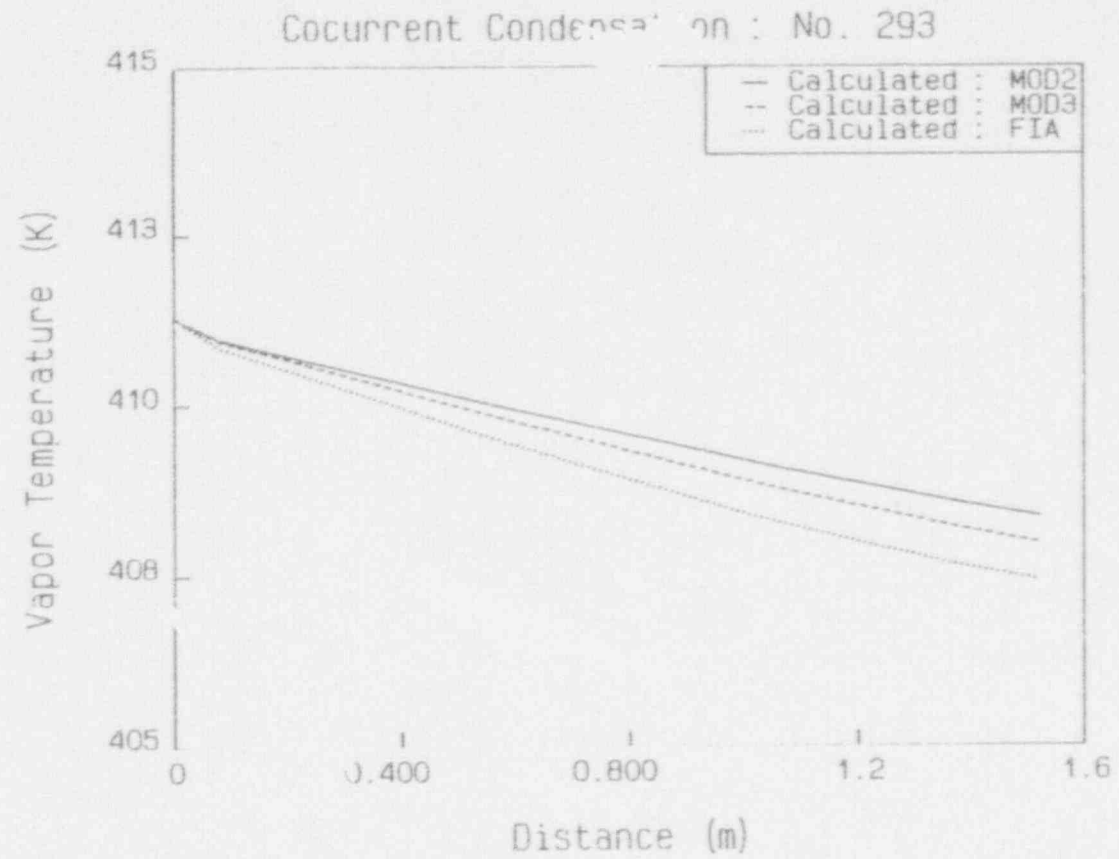
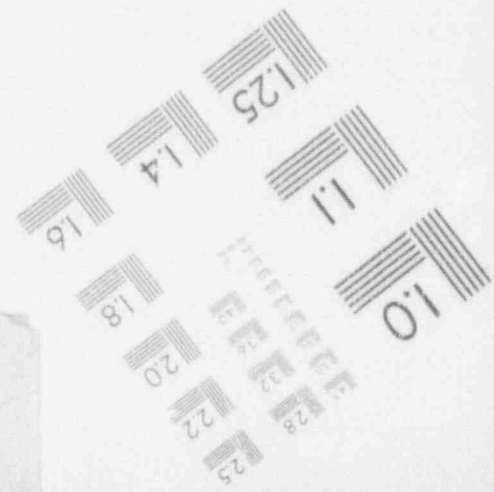
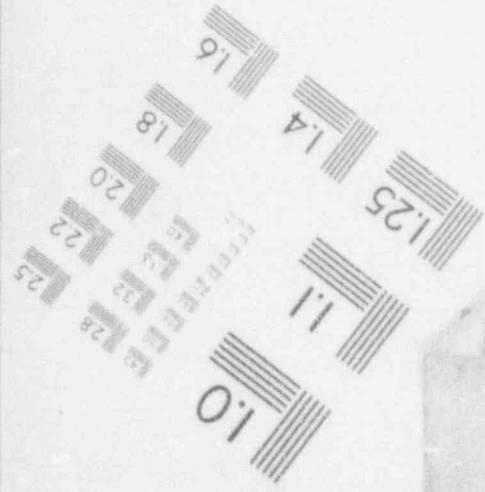
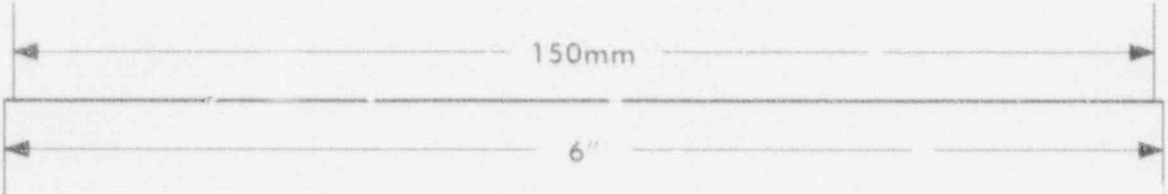
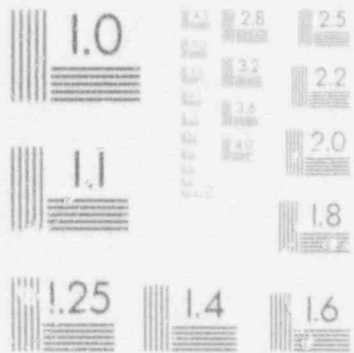
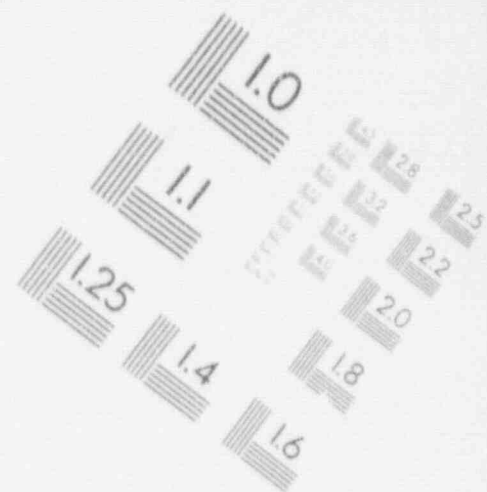
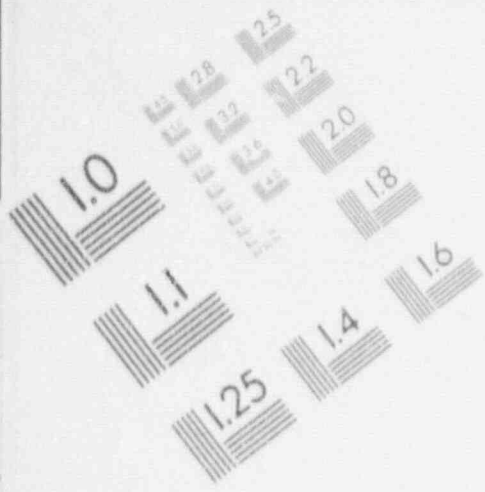


Fig 34 Vapor Temperature (No. 293)

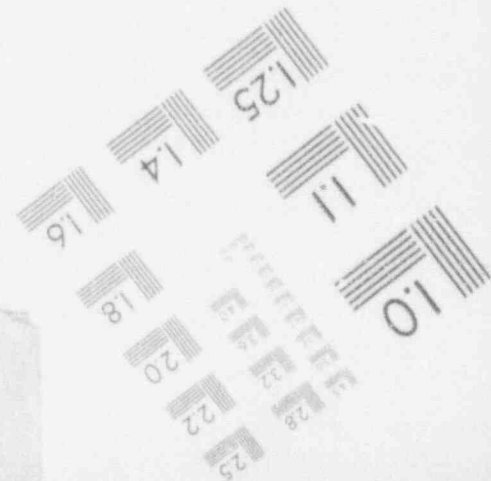
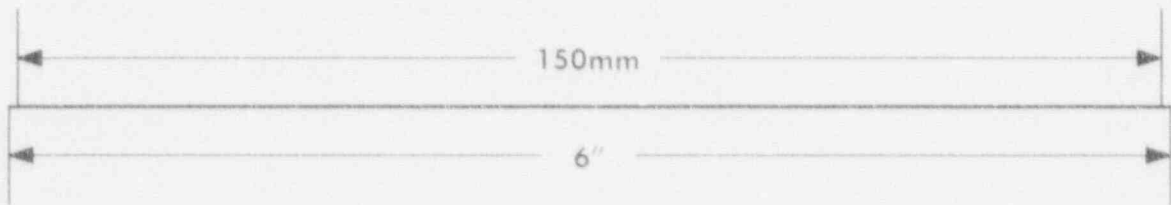
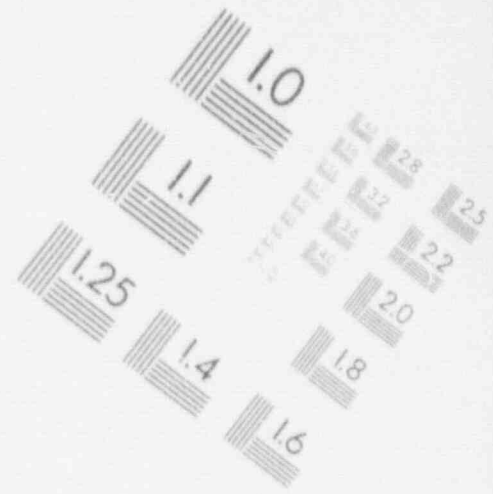
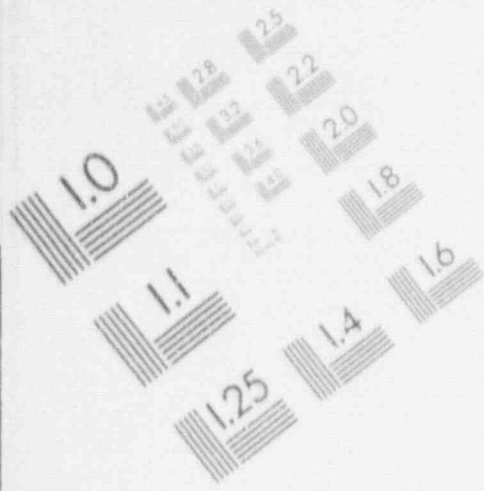
1

IMAGE EVALUATION TEST TARGET (MT-3)



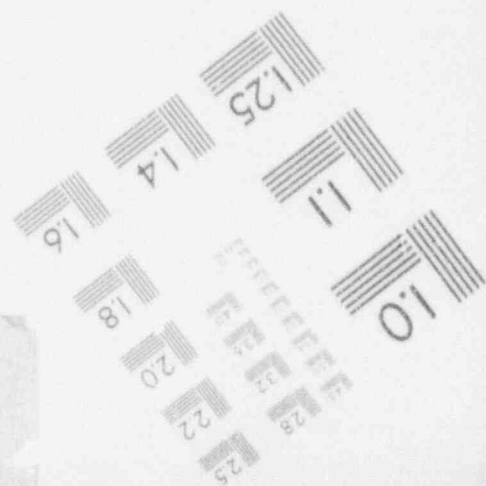
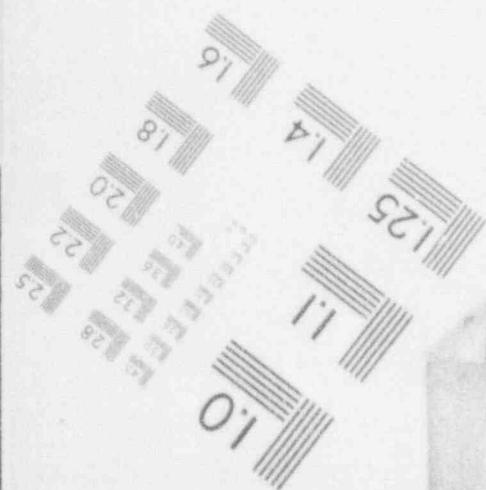
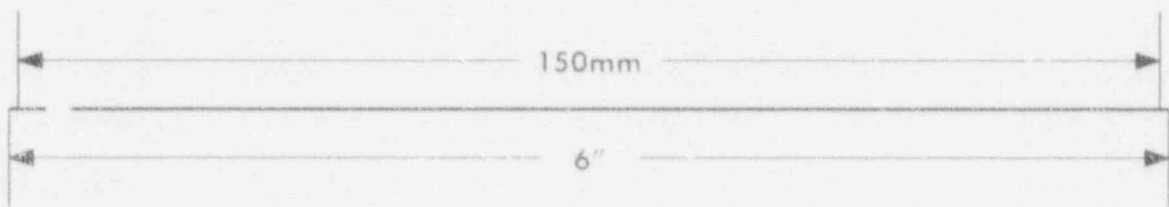
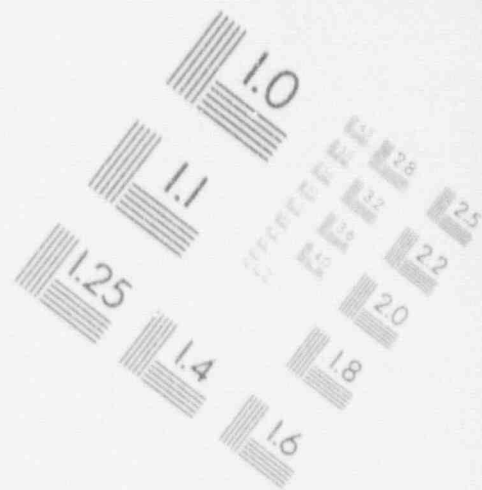
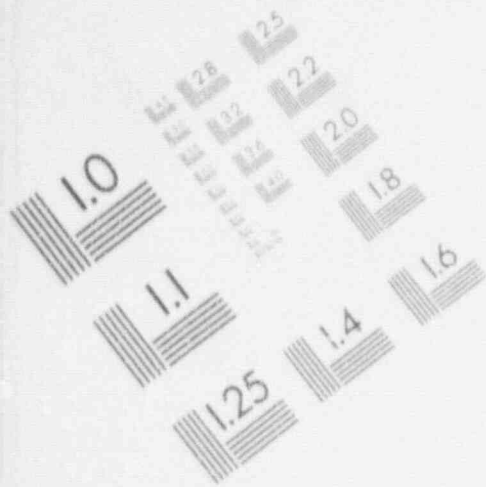
1

IMAGE EVALUATION TEST TARGET (MT-3)



1

IMAGE EVALUATION TEST TARGET (MT-3)



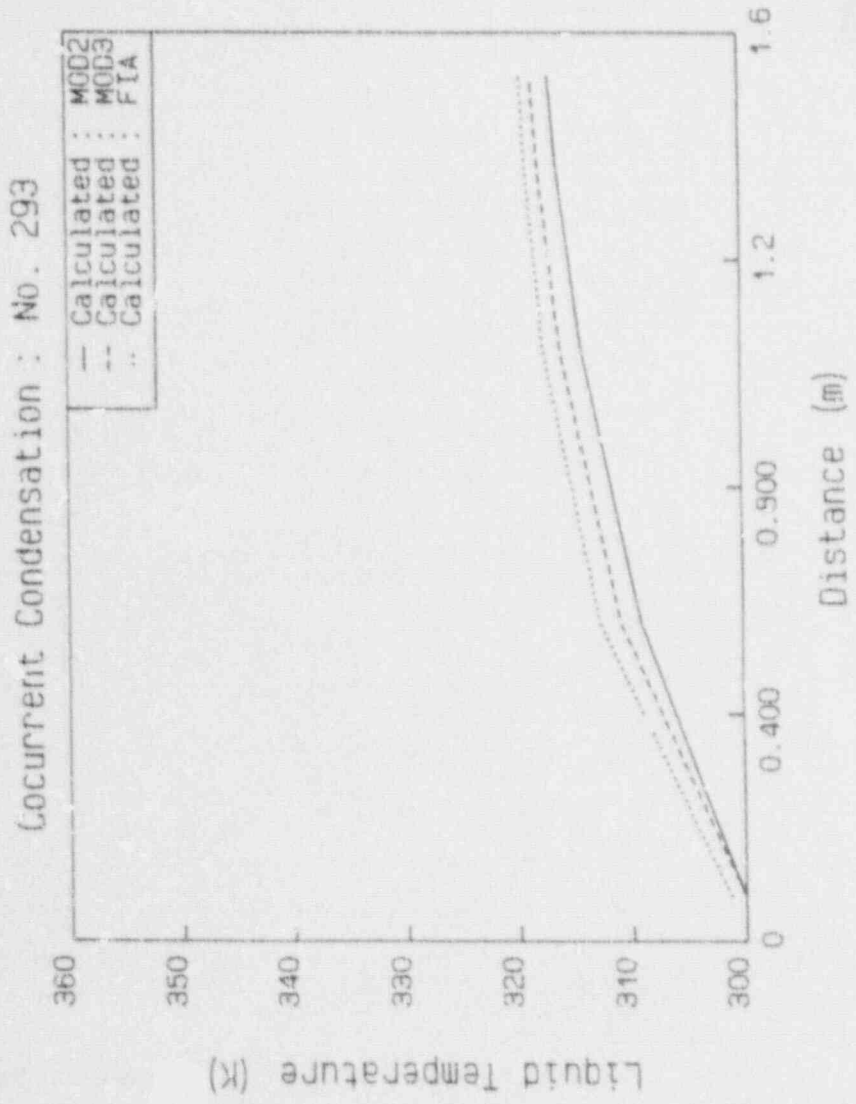


Fig. 35 Liquid Temperature (No. 293)

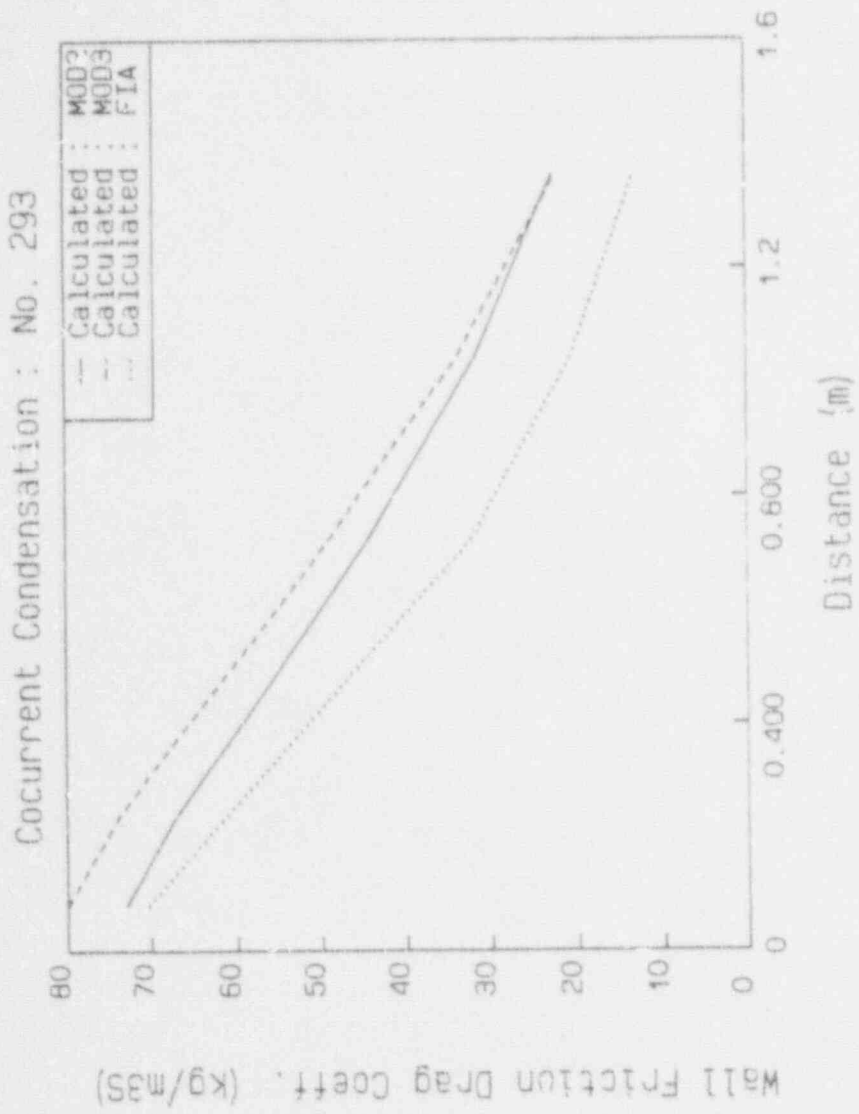


Fig. 36 Liquid Wall Friction Drag Coefficient (No. 293)

Cocurrent Condensation : No. 293

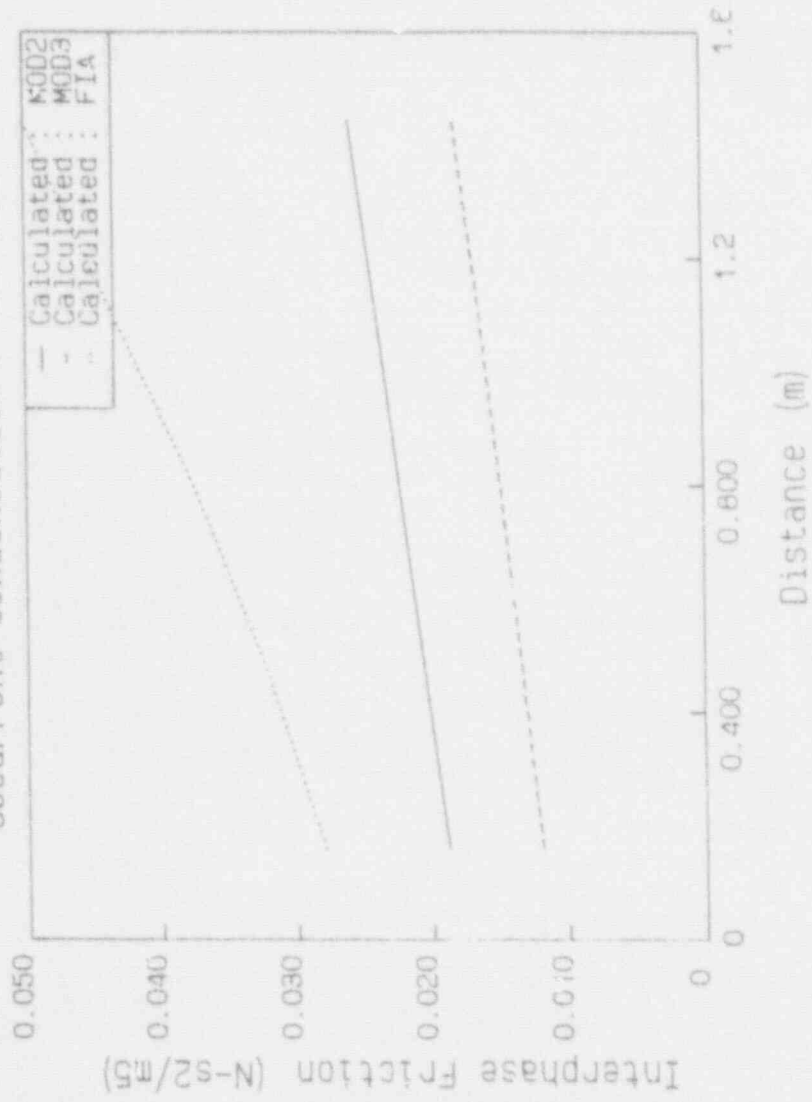


Fig. 37 Interphase Friction (No. 293)

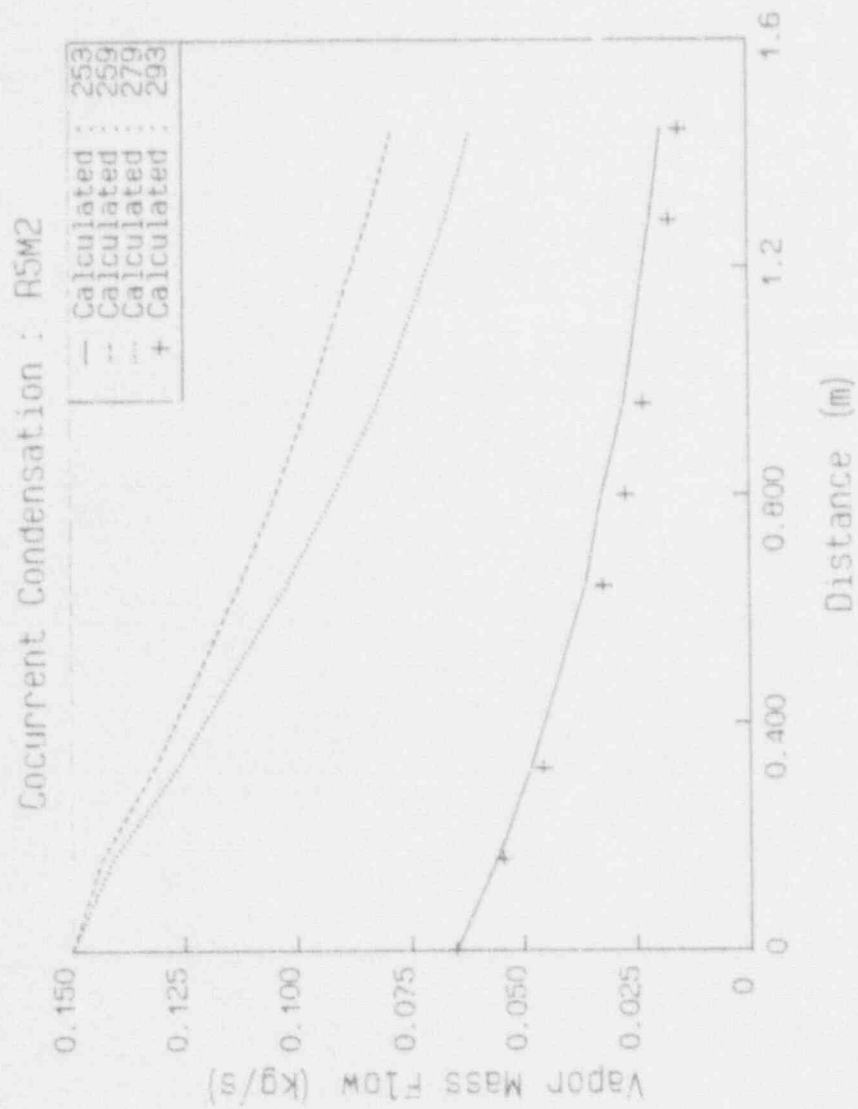


Fig. 38 Vapor Mass Flow (RELAP5/MOD2)

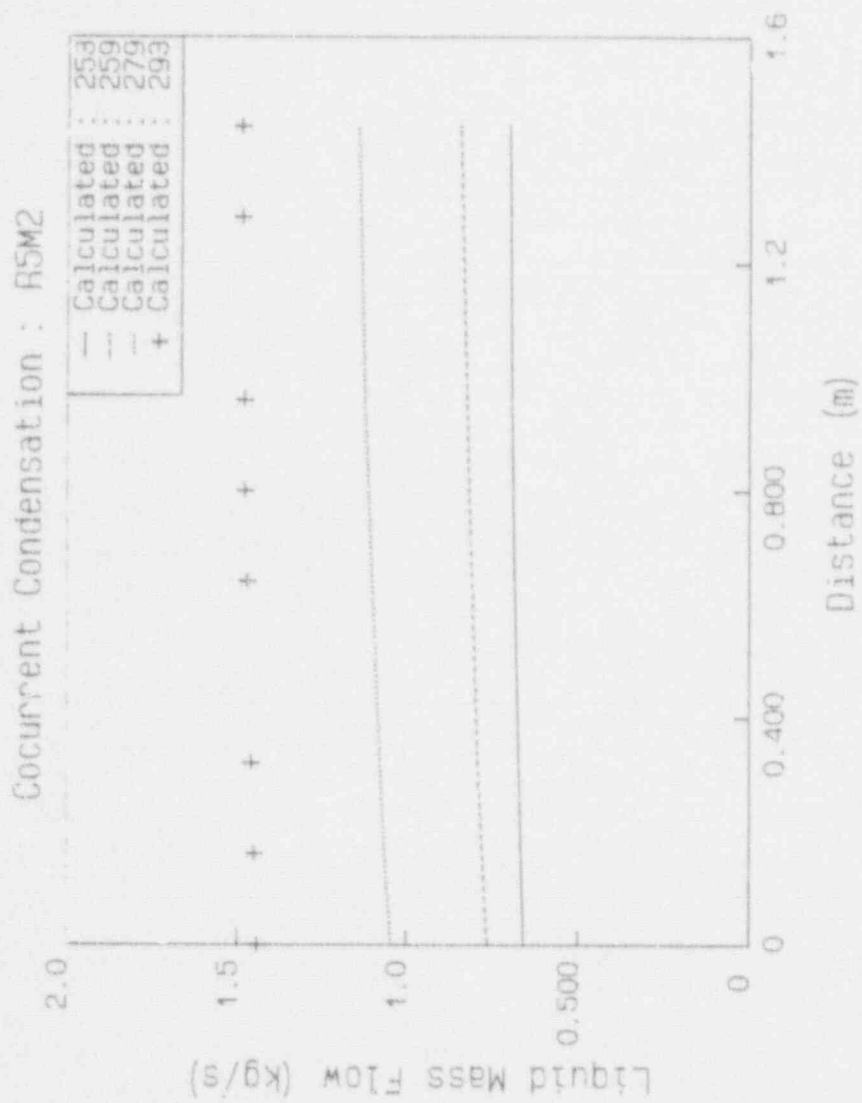


Fig. 39 Liquid Mass Flow (RELAP5/MOD2)

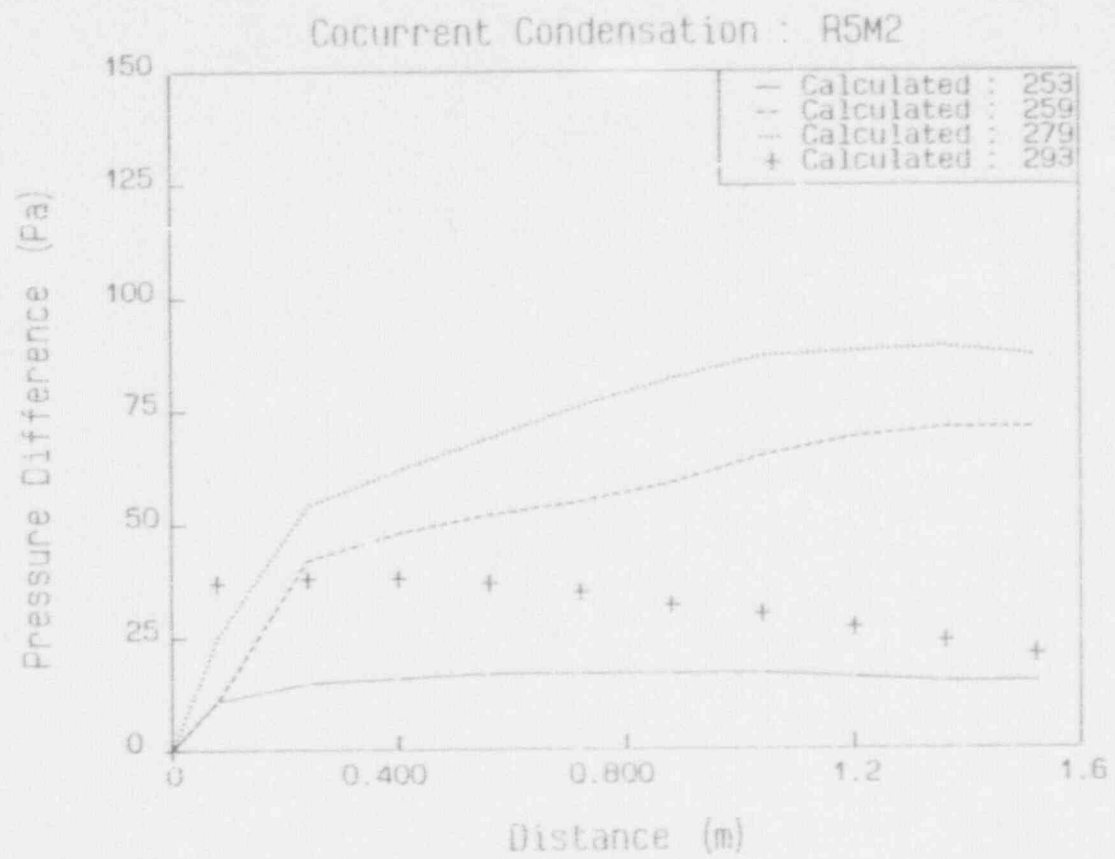


Fig. 40 Pressure Difference (RELAP5/MOD2)

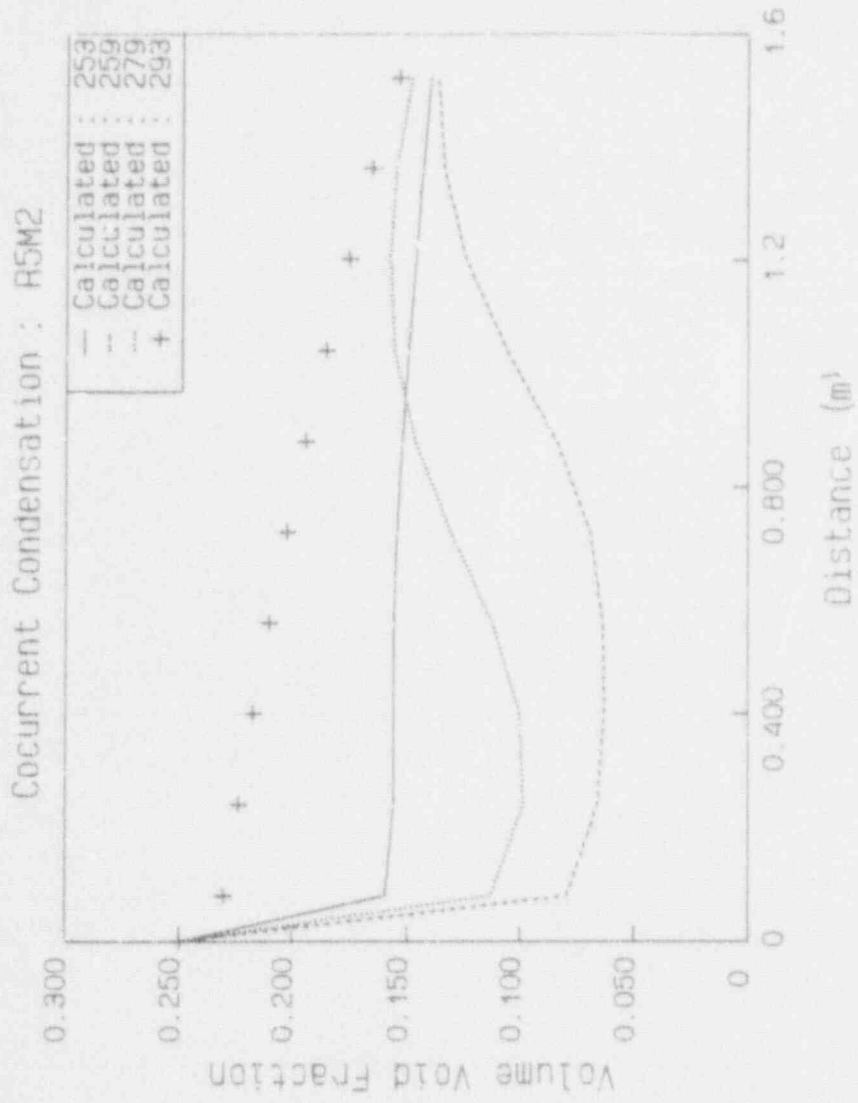


Fig. 41 Water Layer Thickness (RELAP5/MOD2)

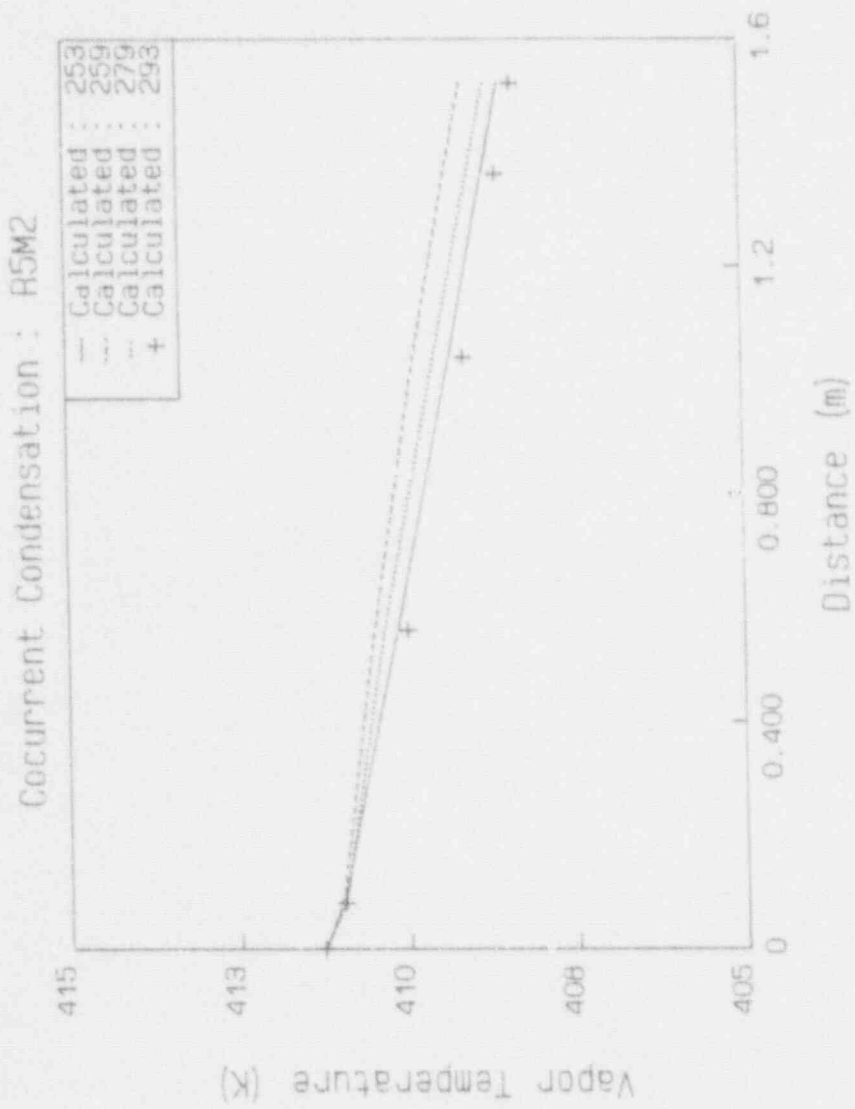


Fig. 42 Vapor Temperature (RELAP5/MOD2)

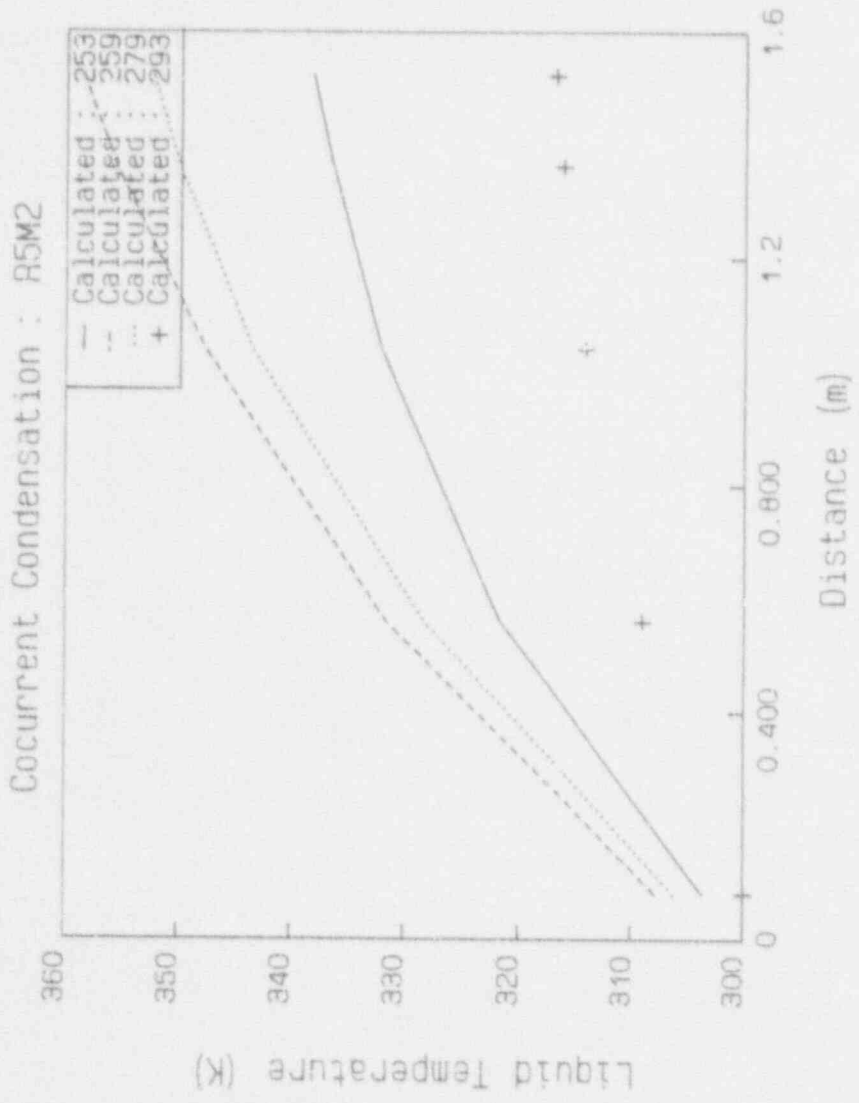


Fig. 43 Liquid Temperature (RELAP5/MOD2)

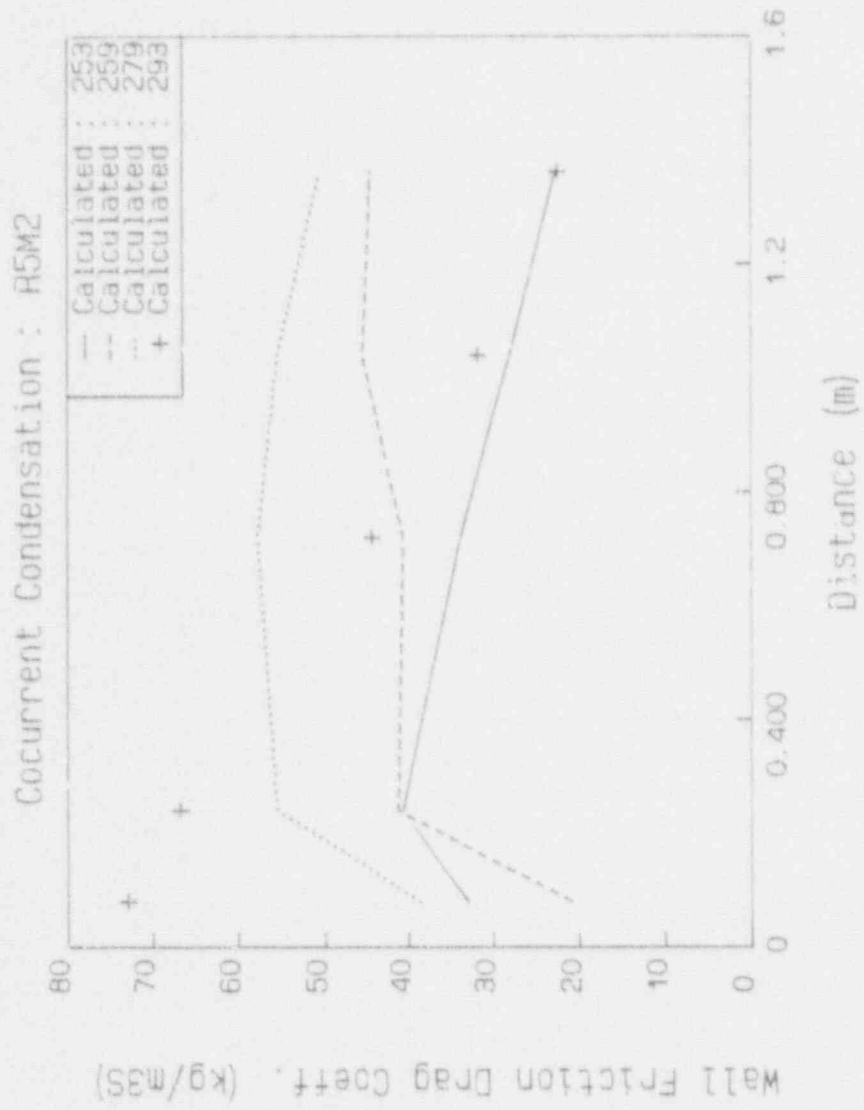


Fig. 44 Liquid Wall Friction Drag Coefficient. (RELAP5/MOD2)

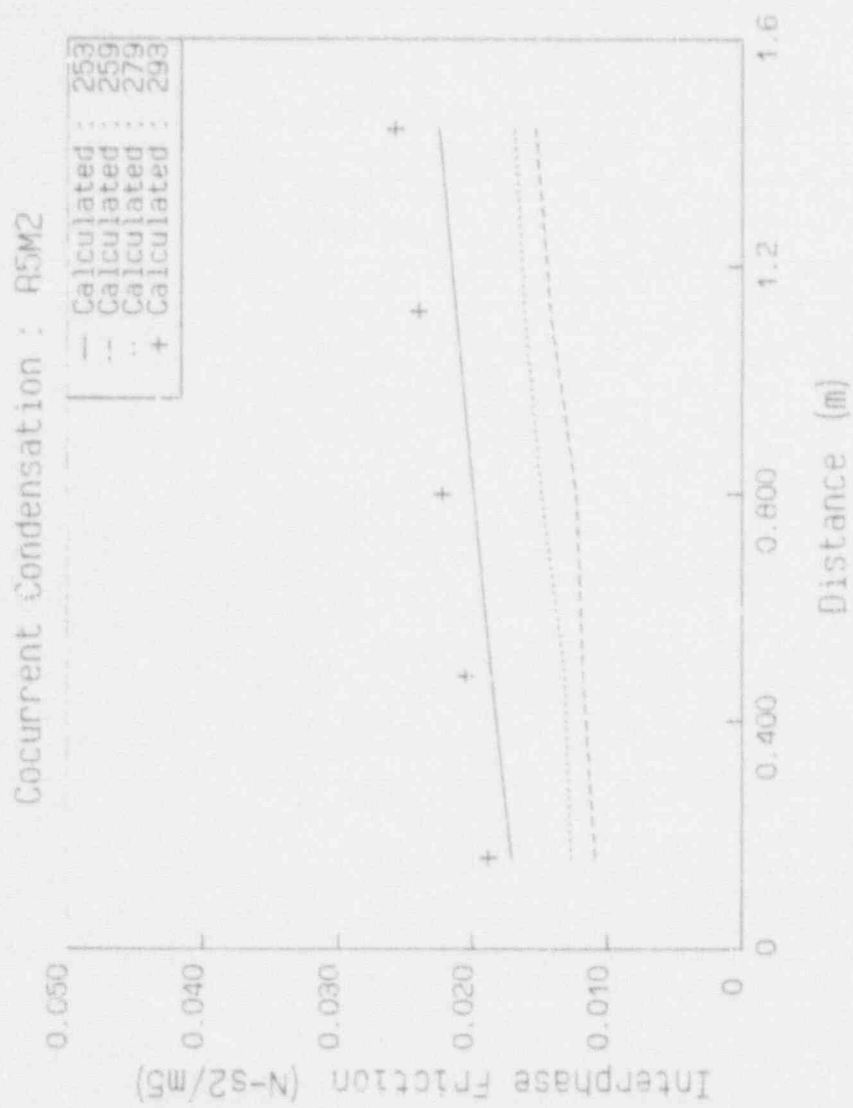


Fig. 45 Interphase Friction (RELAP5/MOD2)

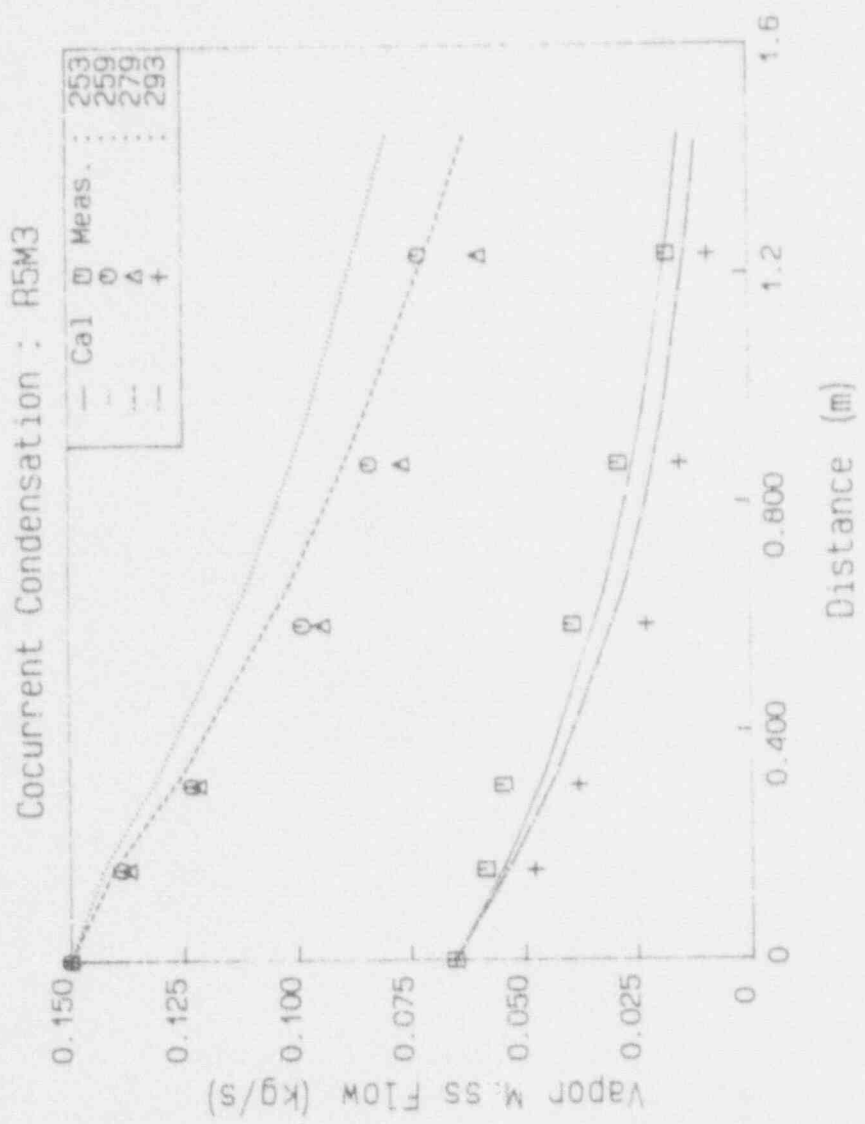


Fig. 46 Vapor Mass Flow (RELAP5/MOD3)

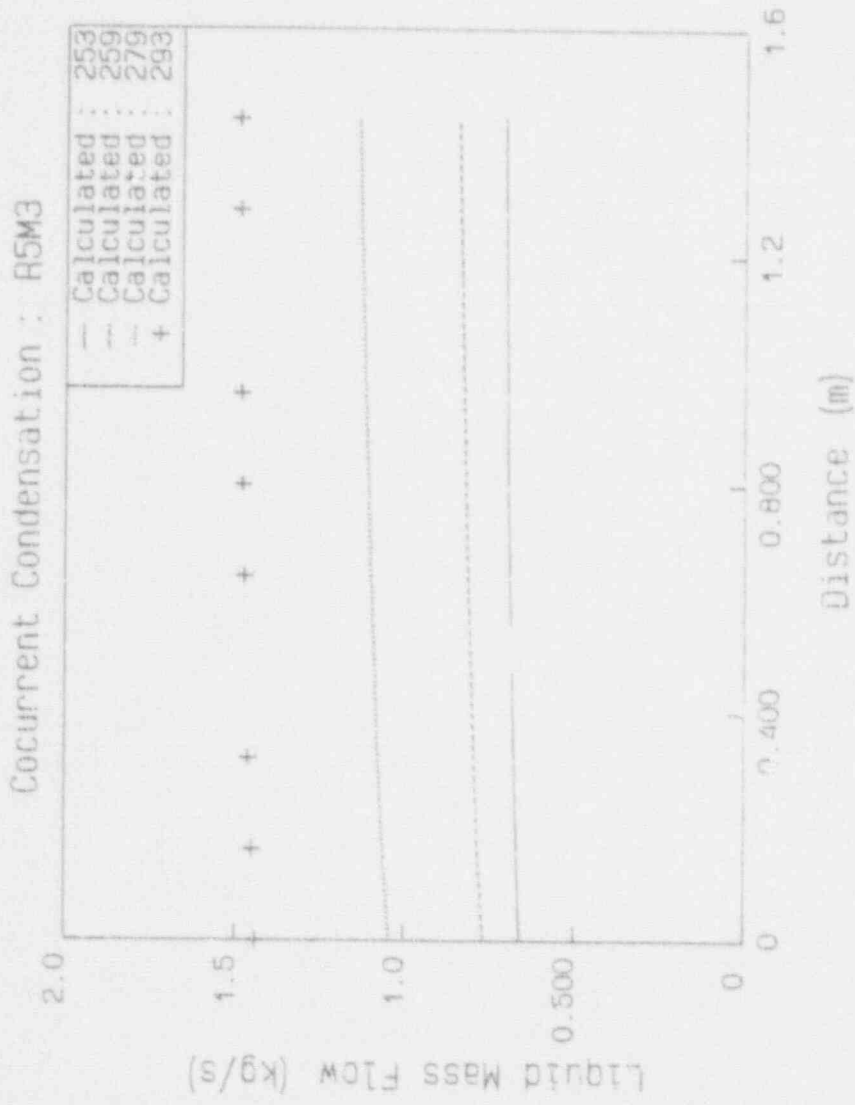


Fig. 47 Liquid Mass Flow (RELAP5/MOD3)

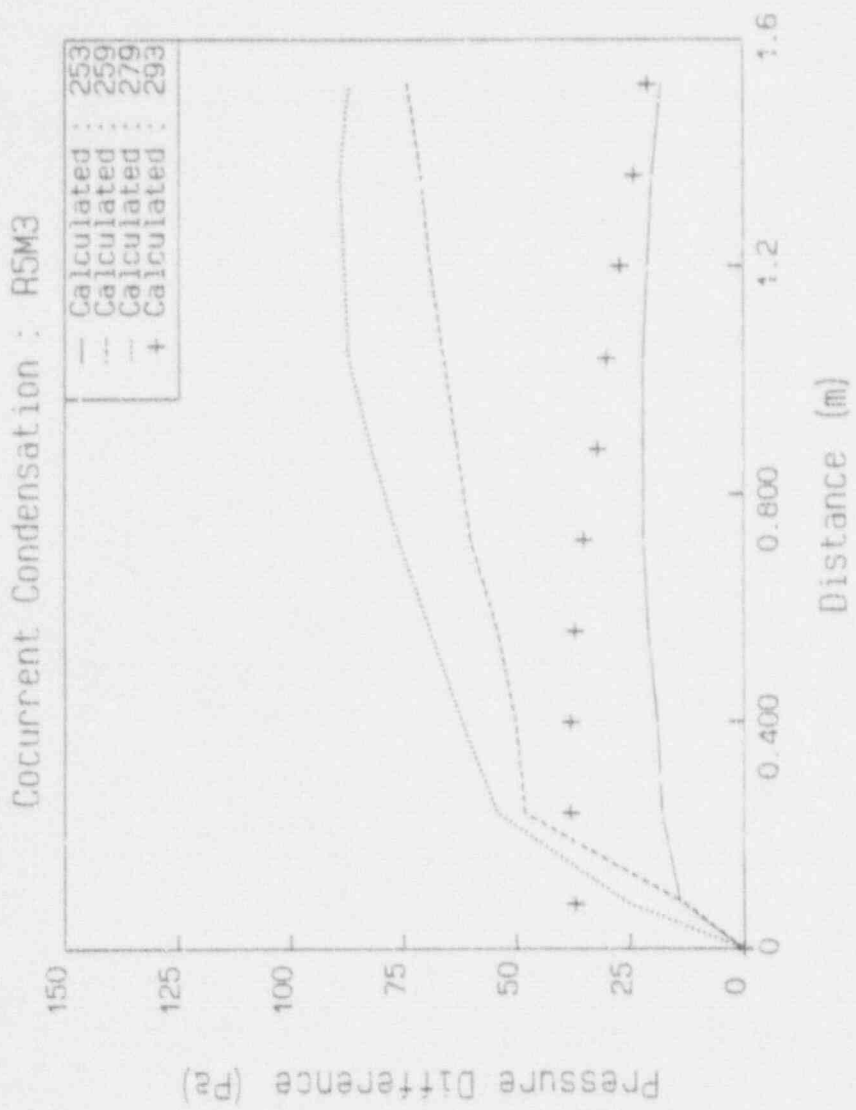


Fig. 48 Pressure Difference (RELAP5/MOD3)

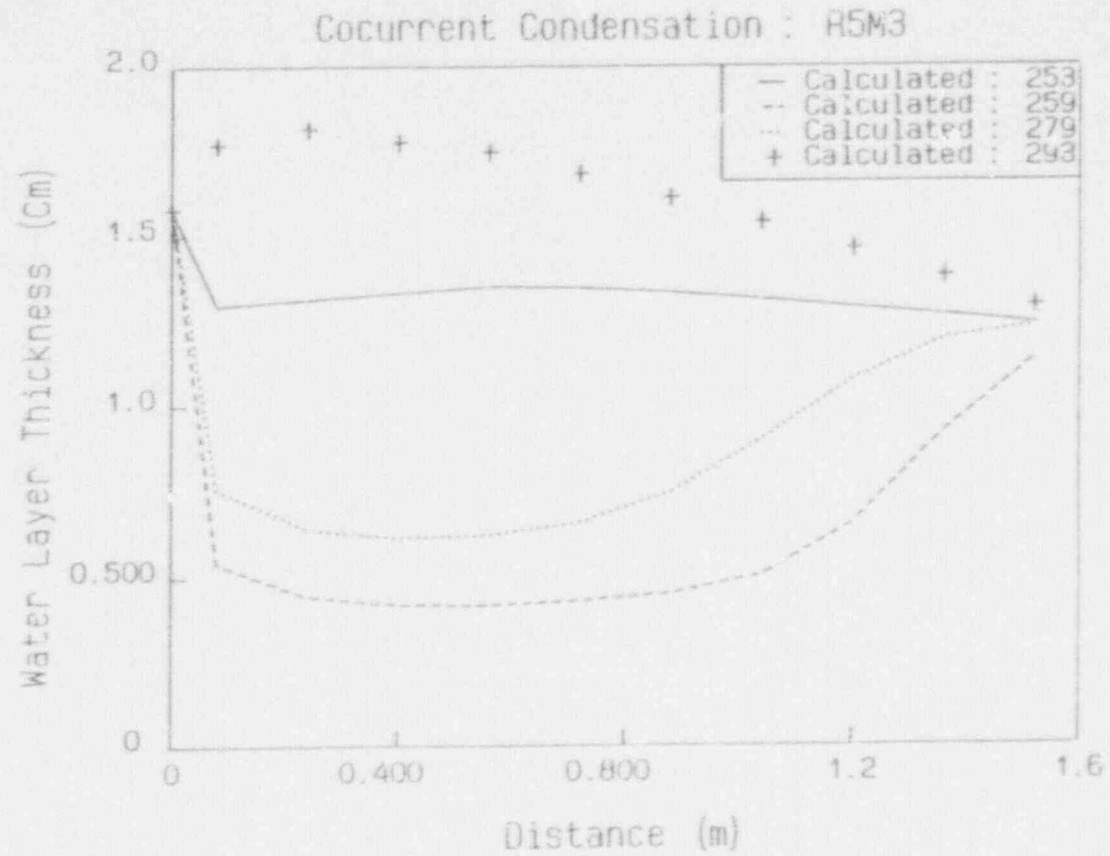


Fig. 49 Water Layer Thickness (RELAP5/MOD3)

Cocurrent Condensation : R5M3

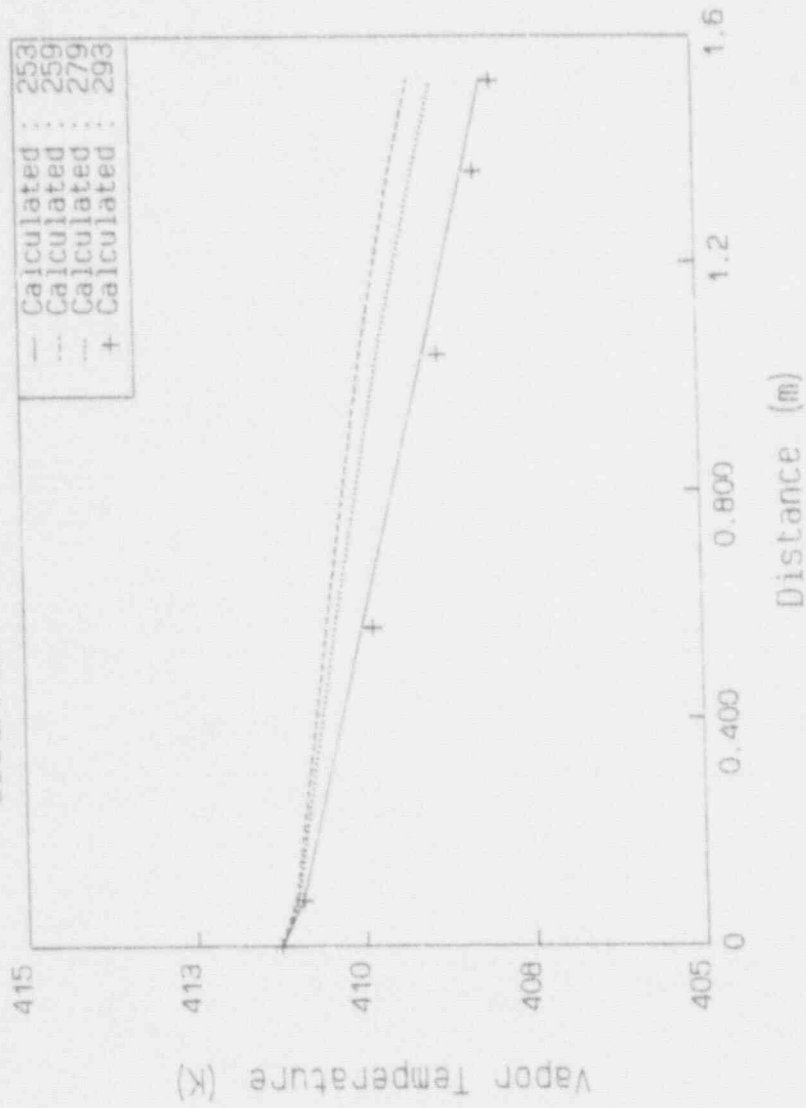


Fig. 50 Vapor Temperature (RELAP5/MOD3)

11

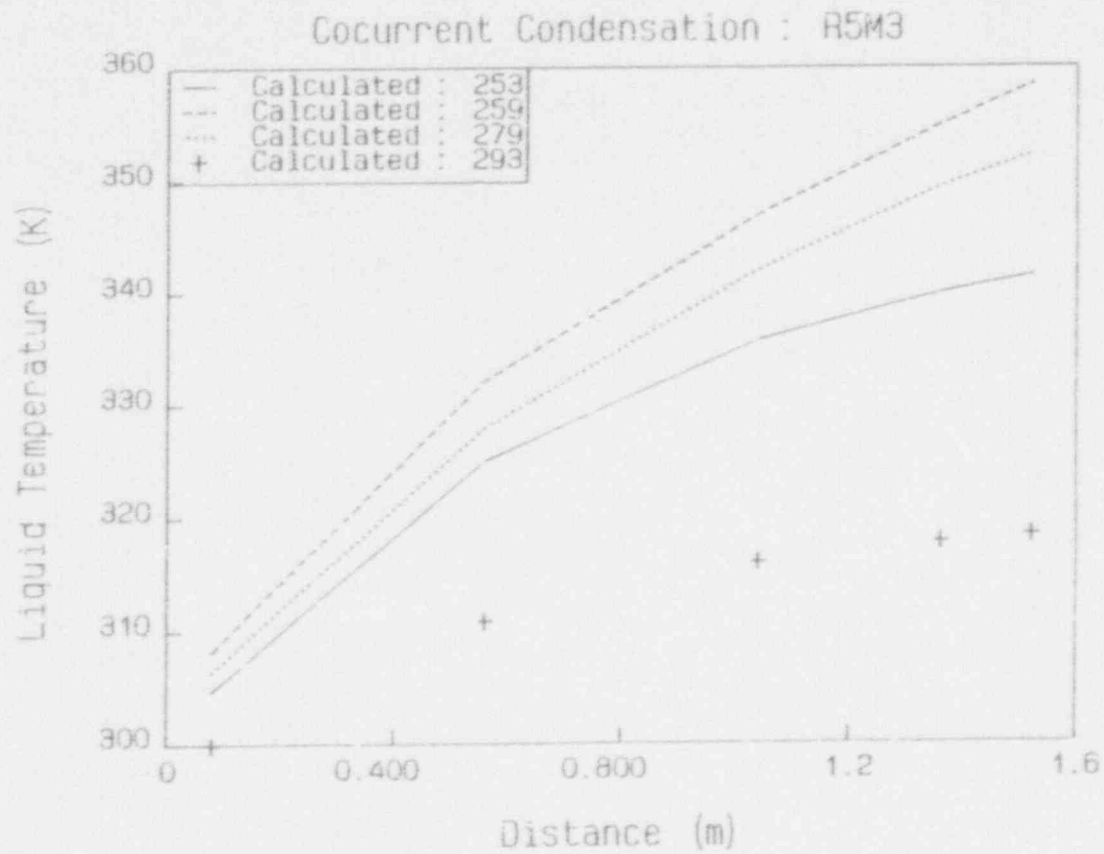
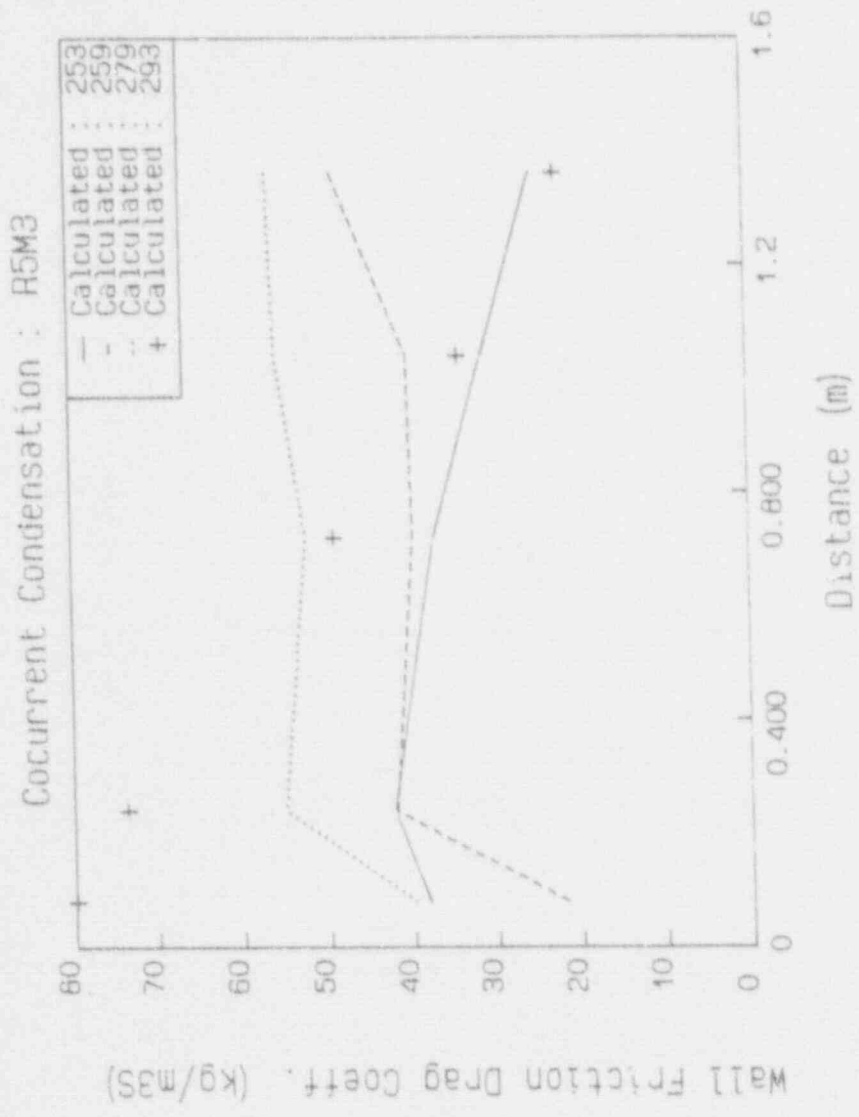


Fig. 51 Liquid Temperature (RELAP5/MOD3)



Wall Friction Drag Coeff. (kg/m³s)

Fig. 52 Liquid Wall Friction Drag Coefficient (RELAP5/MOD3)

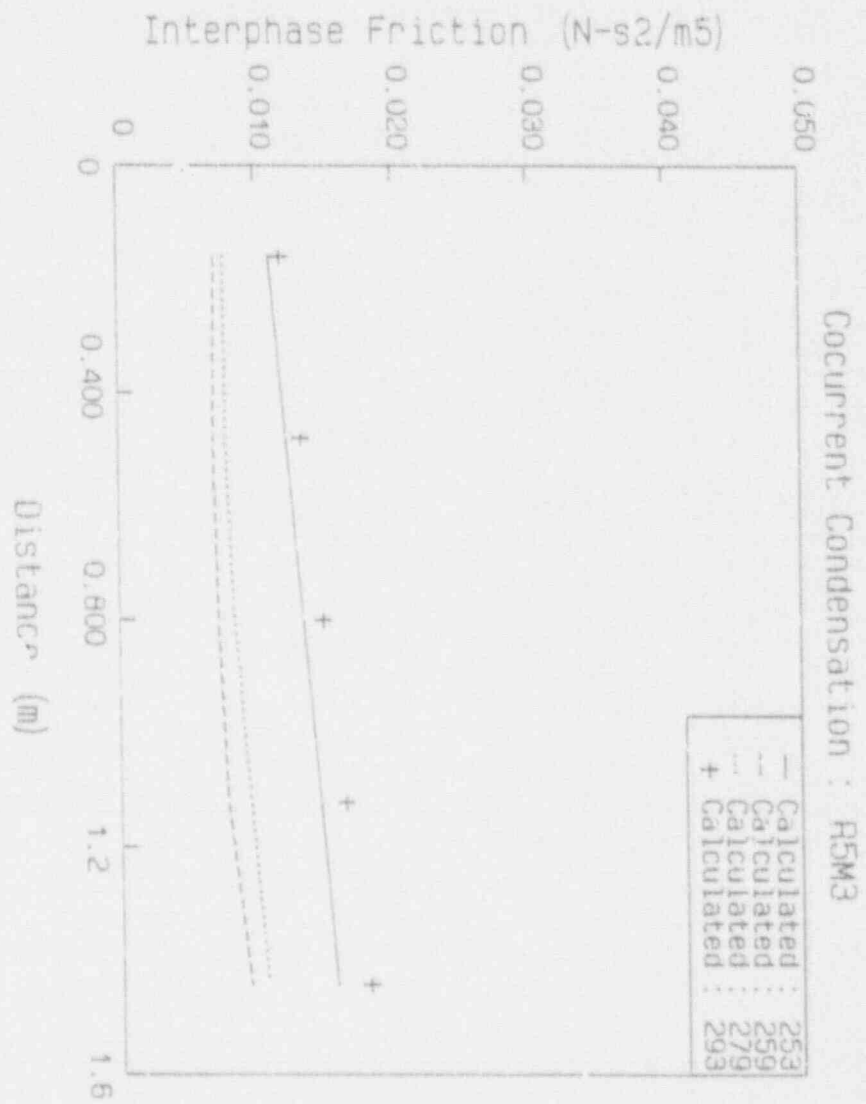


Fig. 53 Interphase Friction (RELAP5/MOD3)

Axial Local Heat Transfer Coeff. (k_x/m^2K)

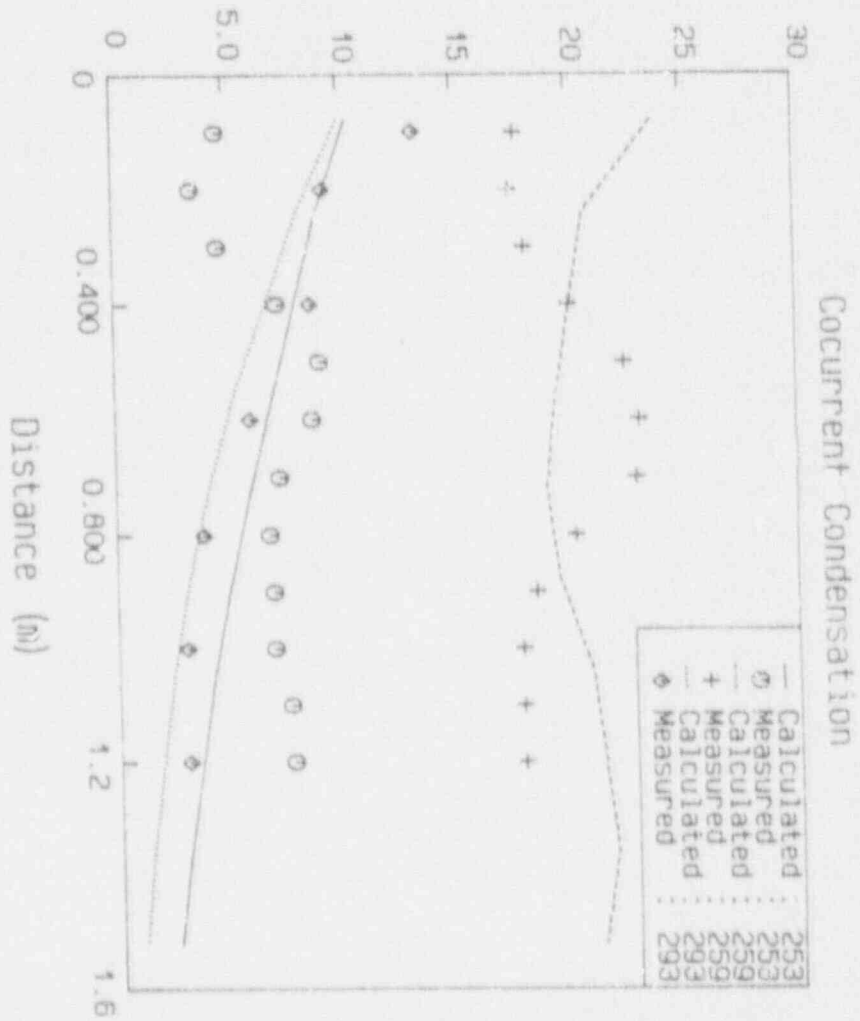


Fig. 54 Axial Local Heat Transfer Coefficient (RELAP5/MOD3)

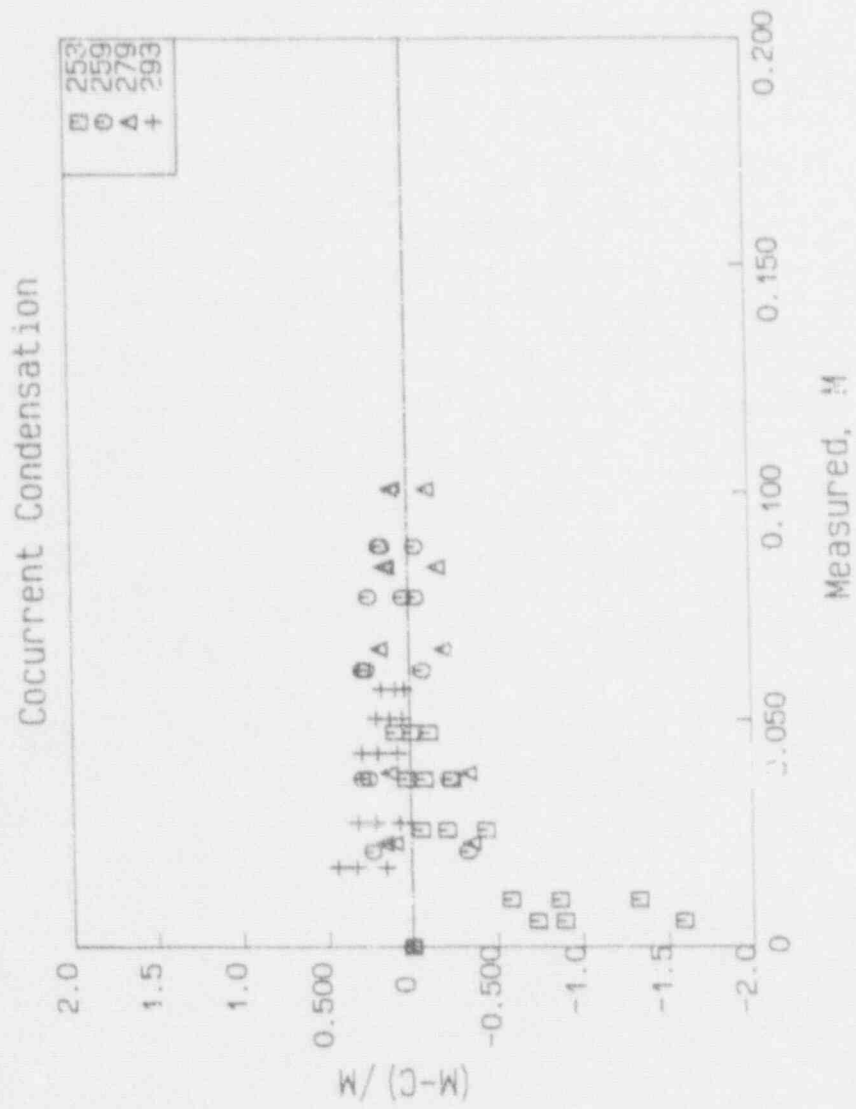


Fig. 55 Prediction of Local Condensation Rate

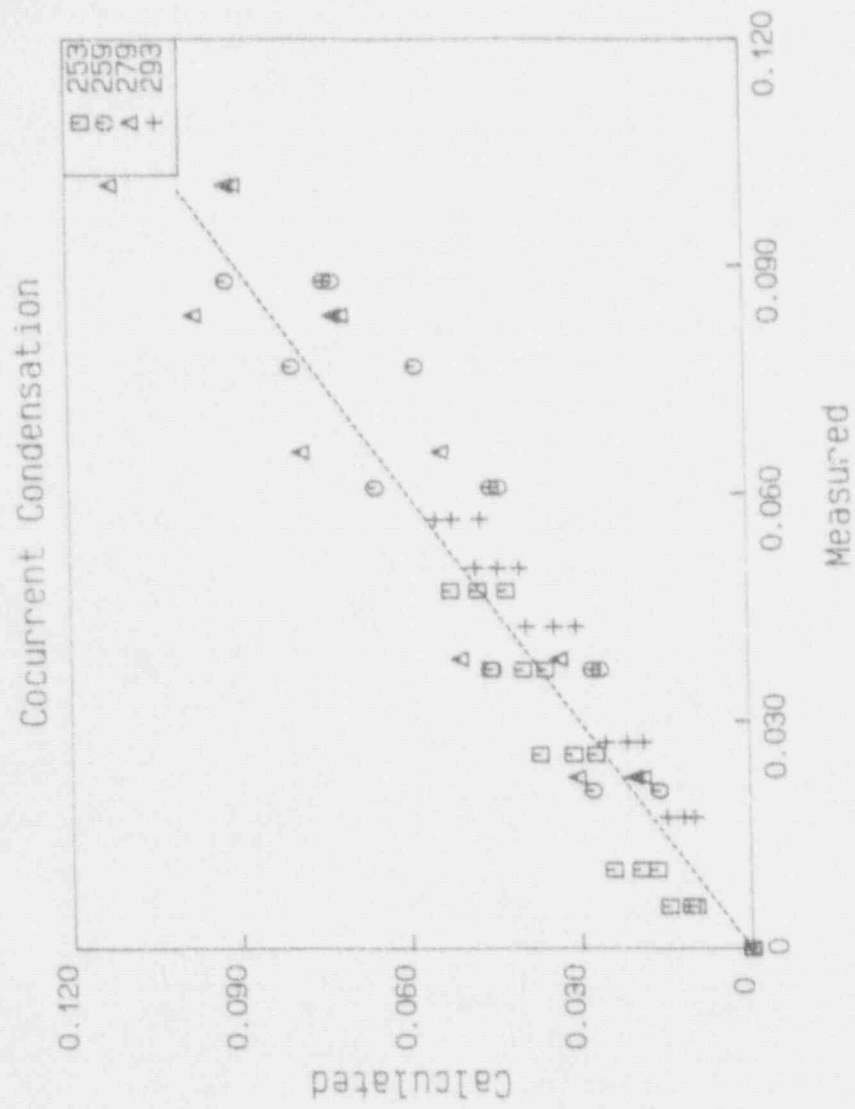


Fig. 56 Comparison of Local Condensation Rates

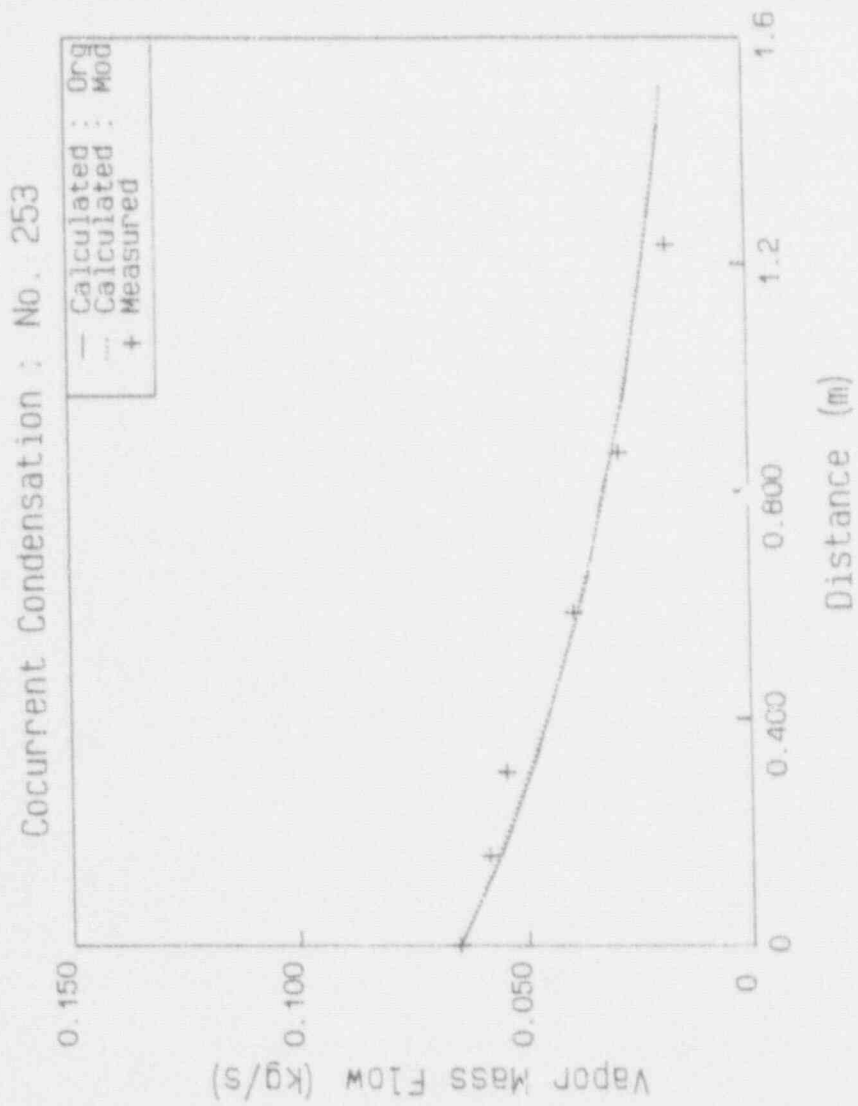


Fig. 57 Vapor Mass Flow (No. 253 : Mod)

Cocurrent Condensation : No. 253

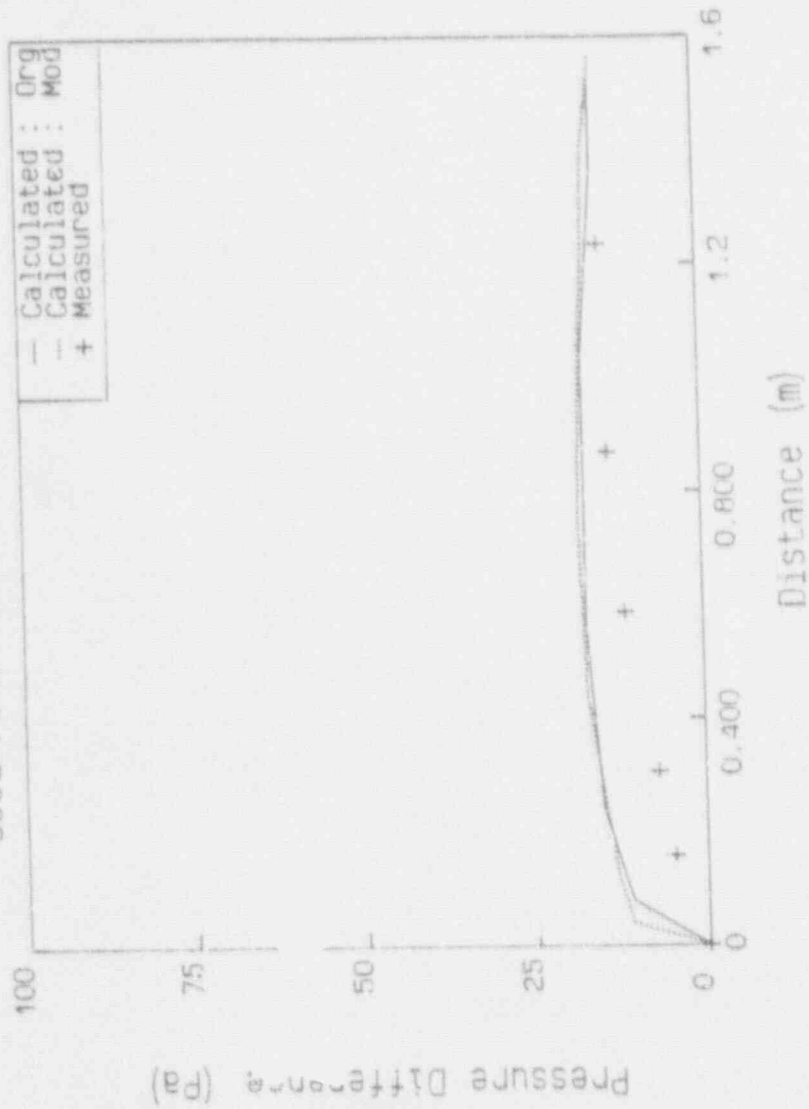


Fig. 58 Pressure Difference (No. 253 : Mod)

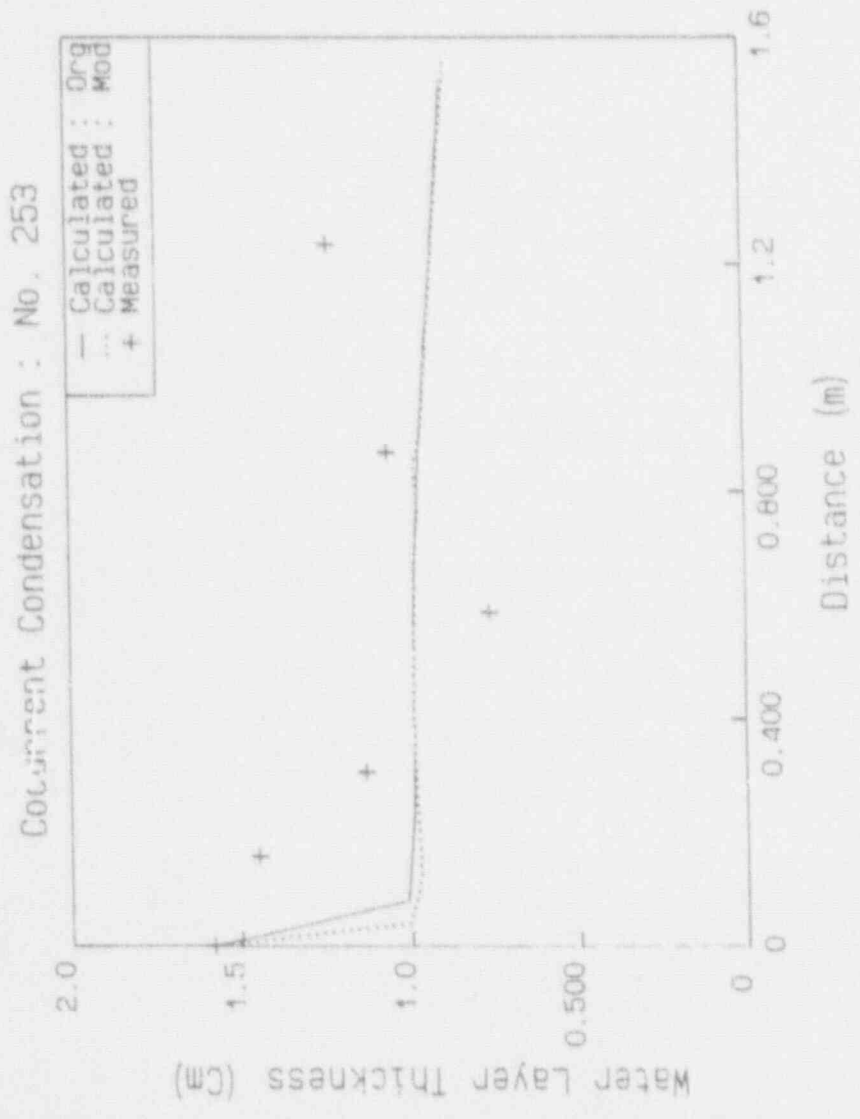


Fig. 59 Water Layer Thickness (No. 253 : Mod)

Cocurrent Condensation : No. 253

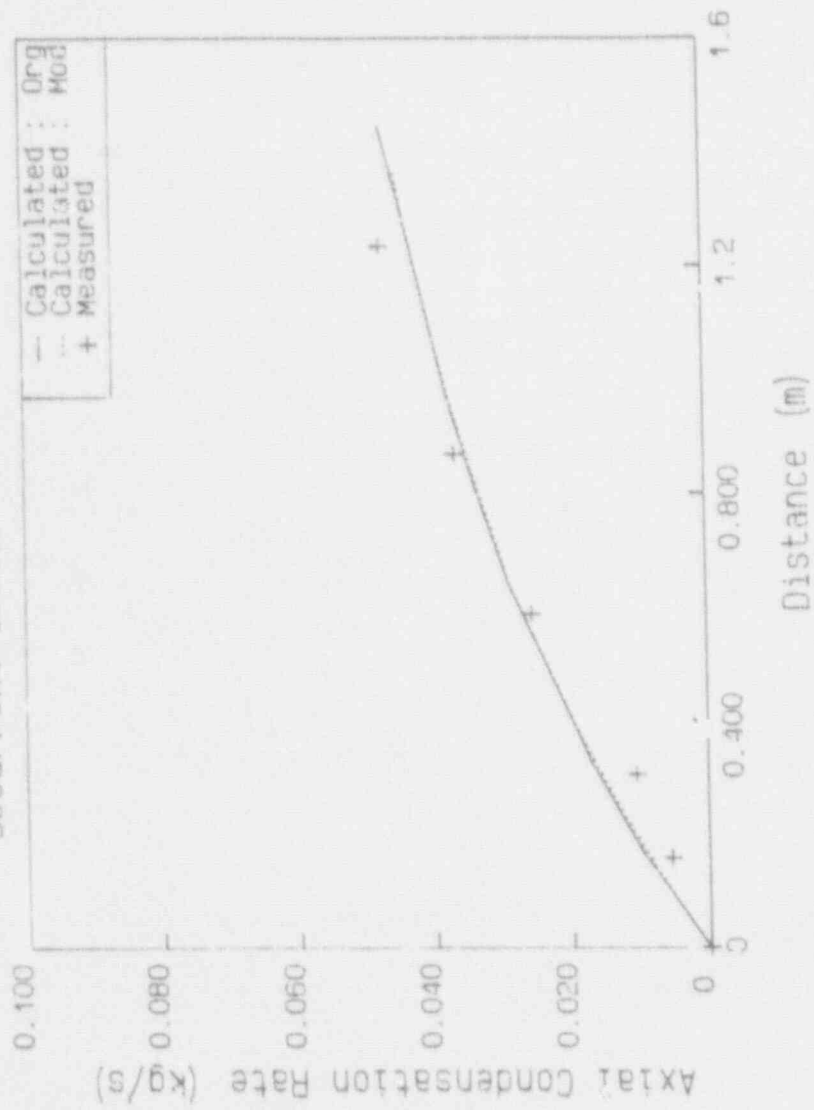


Fig. 60 Axial Condensation Rate (No. 253 : Mod)

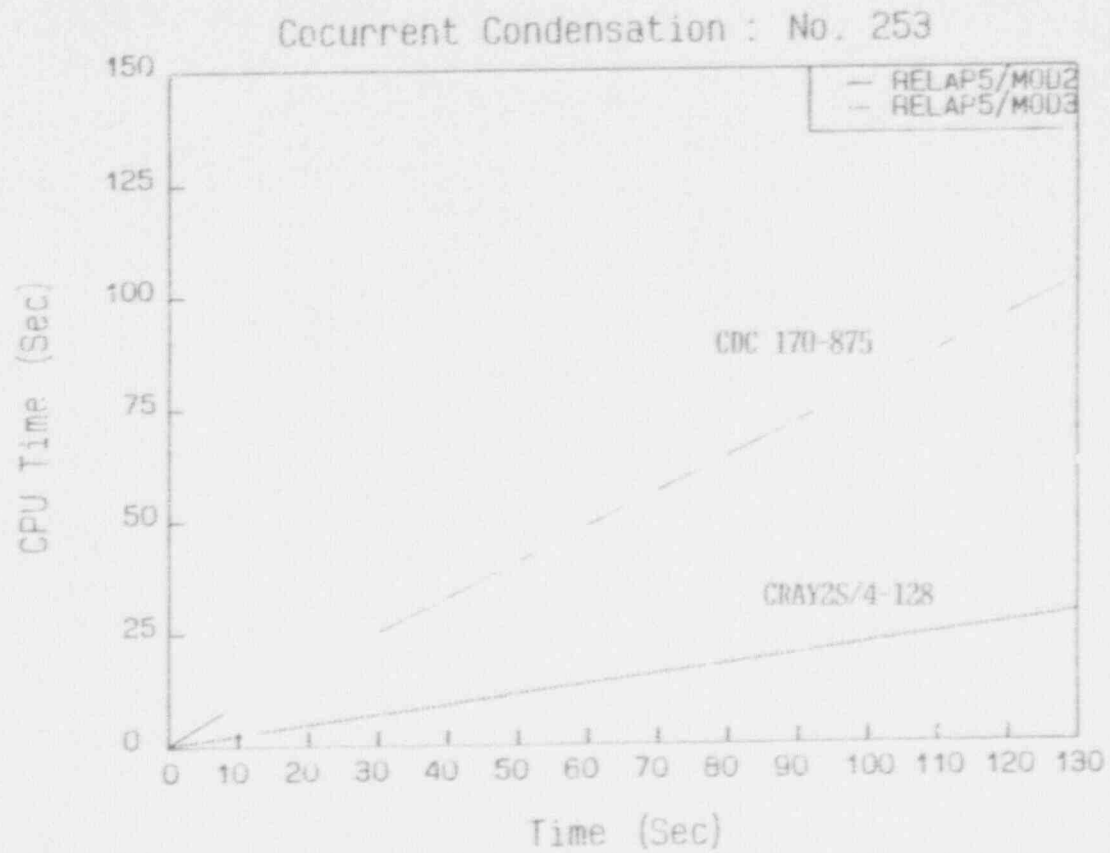


Fig. 61 CPU Time in Base Calculations (No. 253)

Appendix

```

/JOB
BANK253,T1000.
/USER
/NCSEQ
ATTACH,STH2XT,RE364BX.
PURGE,BANKRS1/NA.
*PURGE,BANKPF1/NA.
DEFINE,RSTPLT=BANKRS1.
*DEFINE,PLOTFI=BANKPF1.
FILE,RSTIN,SBF=NO.
FILE,RSTPLT,SBF=NO.
RFL,CM=300000,EC=100.
REDUCE(-)
RE364BX,*PL=10000.
/EOR

```

```
*****
```

```

*
= COCURRENT CONDENSATION TEST NO. 253 WITH REGALIZATION A *
*

```

```
*****
```

```
* PROBLEM TYPE
```

```

*
0000100 NEW STDY-ST
0000104 NONE
0000201 200. 1.E-6 0.1 00003 10 100 1000
*

```

```
*****
* MINOR EDIT VARIABLES *
*****
```

```

*
301 CNTRLVAR 1
302 CNTRLVAR 2
303 CNTRLVAR 3
304 CNTRLVAR 4
305 CNTRLVAR 5
306 CNTRLVAR 6
307 CNTRLVAR 7
308 CNTRLVAR 8
309 CNTRLVAR 9
310 CNTRLVAR 10
311 CNTRLVAR 11
312 CNTRLVAR 12
313 CNTRLVAR 13
314 CNTRLVAR 14
315 CNTRLVAR 15
316 CNTRLVAR 16
317 CNTRLVAR 17
318 CNTRLVAR 18
319 TEMPF 3010000
320 TEMPF 3020000
321 TEMPF 3030000

```

322 TEMPF 3050000
323 TEMPF 3070000
324 TEMPF 3090000
325 TEMPF 3100000
326 TEMPG 3010000
327 TEMPG 3020000
328 TEMPG 3030000
329 TEMPG 3050000
330 TEMPG 3070000
331 TEMPG 3090000
332 TEMPG 3100000
333 VOIDG 3010000
334 VOIDG 3020000
335 VOIDG 3030000
336 VOIDG 3040000
337 VOIDG 3050000
338 VOIDG 3060000
339 VOIDG 3070000
340 VOIDG 3080000
341 VOIDG 3090000
342 VOIDG 3100000
343 HIF 3010000
344 HIF 3020000
345 HIF 3030000
346 HIF 3040000
347 HIF 3050000
348 HIF 3060000
349 HIF 3070000
350 HIF 3080000
351 HIF 3090000
352 HIF 3100000
353 HIG 3010000
354 HIG 3020000
355 HIG 3030000
356 HIG 3040000
357 HIG 3050000
358 HIG 3060000
359 HIG 3070000
360 HIG 3080000
361 HIG 3090000
362 HIG 3100000
363 P 02010000
364 P 04010000
365 P 5010000
366 P 3010000
367 P 3020000
368 P 3030000
369 P 3050000
370 P 3050000
371 P 3060000
372 P 3070000

373 P 3080000
374 P 3090000
375 P 3100000
376 VAPGEN 3010000
377 VAPGEN 3020000
378 VAPGEN 3030000
379 VAPGEN 3040000
380 VAPGEN 3050000
381 VAPGEN 3060000
382 VAPGEN 3070000
383 VAPGEN 3080000
384 VAPGEN 3090000
385 VAPGEN 3100000
386 VAPGEN 5010000
387 SATTEMP 5010000
388 TEMPF 5010000
389 TEMPG 5010000
390 FWALF 3010000
391 FWALF 3020000
392 FWALF 3050000
393 FWALF 3070000
394 FWALF 3090000
395 FIJ 3010000
396 FIJ 3030000
397 FIJ 3050000
398 FIJ 3070000
399 FIJ 3090000

*

* NODALIZATION

*

0020000 INLETP SINGLVOL
0020101 0.0193548 0.50 0. 0. 0. 0.
0020102 3.333E-5 0.1051 10
0020200 2 101325. 1.0

*

0030000 TESTS PIPE
0030001 10
0030101 0.0193548 10
0030301 0.1601 10
0030601 0.0 10
0030801 3.333E-5 0.1051 10
0031001 0 10
0031101 1000 9
0031201 2 101325. 0.12 0. 0. 0.0 10
0031301 0 0. 0. 9

*

0040000 ACCINJ SINGLVOL
0040101 1.96-3 0.0 0. 0. -90. -0.2
0040102 3.333E-5 0.05 10

```

0040200 2 103285. 0.0
*
0060000 WTEXT SINGLVOL
0060101 1.96-3 2.0 0. 0. -90. -0.2
0060102 3.333E-5 0.05 0
0060200 2 1.0E5 0.0
*
0050000 EXITVOL SINGLVOL
0050101 0.08 1.0 0.0 0. 0. 0.
0050102 3.333E-5 0.22 0
0050200 2 101325. 0.12
-
0080000 STMEXIT TMDPVOL
0080101 0.5 1.0 0.0 0. 0. 0.
0080102 0. 0. 0.
0080200 2
0080201 0. 101325. 1.0
*
0090000 WATER TMDPVOL
0090101 0.2 1.0 0.0 0. 0. 0.
0090102 0. 0. 0.
0090200 2
0090201 0. 101325. 0.0
*
0100000 TESTIN TMDPJUN
0100101 100000000 002000000 0.0
0100200 1
0100201 200. 0.0 0.0651 0.0
*
0200000 ACCINJJ TMDPJUN
0200101 200000000 004010000 0.0
0200200 1
0200201 200. 0.657 0.0 0.0
*
0300000 ACCJUN SINGLJUN
0300101 004000000 003000000 0.0 0.0 100. 1100
0300201 0 0.0 0.0 0.0
*
0560000 WTEXT SINGLJUN
0560101 005010000 006000000 4.0-4 1.0 100. 21100
0560201 0 0.0 0.0 0.0
*
0500000 TEST2IN SINGLJUN
0500101 002010000 003000000 0.0 0.0 100. 1000
0500201 0 0.0 0.0 0.0
*
0690000 WATER SINGLJUN
0690101 006010000 009000000 0.0 0.0 0.0 1100
0690201 0 0.0 0.0 0.0
*
0600000 TESTZEX SINGLJUN

```

0600101 003010000 005000000 0.05 1.0 0.0 1000
0600201 0 0.0 0.0 0.0

*
0580000 STMEXIT SNGLJUN
0580101 005010000 008000000 2.0-4 0.0 0.0 10100
0580201 0 0.0 0.0 0.0

*
1000000 STMGEN TMDPVOL
1000101 0.2 100. 0. 0. 0. 0.
1000102 0. 0. 0.
1000200 3
1000201 0. 101325. 411.25

*
2000000 ACC TMDPVOL
2000101 0.2 100. 0. 0. 0. 0.
2000102 0. 0. 0.
2000200 3
2000201 0. 103285. 294.75

* CONTROL VARIABLES *

20500100 GMFLWJ1 MULT 1.93548-2 0.0 1
20500101 VOIDGJ 3010000 VELGJ 3010000 RHOGJ 3010000
20500200 GMFLWJ2 MULT 1.93548-2 0.0 1
20500201 VOIDGJ 3020000 VELGJ 3020000 RHOGJ 3020000
20500300 GMFLWJ3 MULT 1.93548-2 0.0 1
20500301 VOIDGJ 3030000 VELGJ 3030000 RHOGJ 3030000
20500400 GMFLWJ4 MULT 1.93548-2 0.0 1
20500401 VOIDGJ 3040000 VELGJ 3040000 RHOGJ 3040000
20500500 GMFLWJ5 MULT 1.93548-2 0.0 1
20500501 VOIDGJ 3050000 VELGJ 3050000 RHOGJ 3050000
20500600 GMFLWJ6 MULT 1.93548-2 0.0 1
20500601 VOIDGJ 3060000 VELGJ 3060000 RHOGJ 3060000
20500700 GMFLWJ7 MULT 1.93548-2 0.0 1
20500701 VOIDGJ 3070000 VELGJ 3070000 RHOGJ 3070000
20500800 GMFLWJ8 MULT 1.93548-2 0.0 1
20500801 VOIDGJ 3080000 VELGJ 3080000 RHOGJ 3080000
20500900 GMFLWJ9 MULT 1.93548-2 0.0 1
20500901 VOIDGJ 3090000 VELGJ 3090000 RHOGJ 3090000
20501000 GMFLW10 MULT 1.93548-2 0.0 1
20501001 VOIDFJ 3010000 VELFJ 3010000 RHOFJ 3010000
20501100 GMFLW11 MULT 1.93548-2 0.0 1
20501101 VOIDFJ 3020000 VELFJ 3020000 RHOFJ 3020000
20501200 GMFLW12 MULT 1.93548-2 0.0 1
20501201 VOIDFJ 3030000 VELFJ 3030000 RHOFJ 3030000
20501300 GMFLW13 MULT 1.93548-2 0.0 1
20501301 VOIDFJ 3040000 VELFJ 3040000 RHOFJ 3040000
20501400 GMFLW14 MULT 1.93548-2 0.0 1
20501401 VOIDFJ 3050000 VELFJ 3050000 RHOFJ 3050000
20501500 GMFLW15 MULT 1.93548-2 0.0 1
20501501 VOIDFJ 3060000 VELFJ 3060000 RHOFJ 3060000

20501600 GMFLW16 MULT 1.93548-2 0.0 1
20501601 VOIDFJ 3070000 VELFJ 3070000 RHOFJ 3070000
20501700 GMFLW17 MULT 1.93548-2 0.0 1
20501701 VOIDFJ 3080000 VELFJ 3080000 RHOFJ 3080000
20501800 GMFLW18 MULT 1.93548-2 0.0 1
20501801 VOIDFJ 3090000 VELFJ 3090000 RHOFJ 3090000

*

```

/JOB
BAN1253,T1000.
/USER
/NOSEQ
ATTACH,STH2KT,RE364BX.
PURGE,BANKR:S1/NA.
*PURGE,BANKPF1/NA.
DEFINE,RSTPLT=BANKRS1.
*DEFINE,PLOTPL=BANKPF1.
FILE,RSTIN,SPF=NO.
FILE,RSTPLT,SBF=NO.
RFL,CN=300000,EC=100.
REDUCE(-)
RE364BX,*PL=10000.
/EOR
*****
*
= COCURRENT CONDENSATION TEST NO. 253 WITH NODALIZATION B *
*
*****
* PROBLEM TYPE
*
0000100 NEW STDY-ST
0000104 NONE
0000201 300. 1.E-6 0.1 00003 10 100 1000
*
*****
* MINOR EDIT VARIABLES *
*****
*
301 CNTRLVAR 1
302 CNTRLVAR 2
303 CNTRLVAR 3
304 CNTRLVAR 4
305 CNTRLVAR 5
306 CNTRLVAR 6
307 CNTRLVAR 7
308 CNTRLVAR 8
309 CNTRLVAR 9
310 CNTRLVAR 10
311 CNTRLVAR 11
312 CNTRLVAR 12
313 CNTRLVAR 13
314 CNTRLVAR 14
315 CNTRLVAR 15
316 CNTRLVAR 16
317 CNTRLVAR 17
318 CNTRLVAR 18
319 TEMPF 1010000
320 TEMPF 2010000
321 TEMPF 2040000

```


322 TEMPF 2070000
323 TEMPF 2090000
324 TEMPF 2100000
325 TEMPF 3010000
326 TEMPG 1010000
327 TEMPG 2010000
328 TEMPG 2040000
329 TEMPG 2070000
330 TEMPG 2090000
331 TEMPG 2100000
332 TEMPG 3010000
333 VOIDF 1010000
334 VOIDF 2010000
335 VOIDF 2020000
336 VOIDF 2040000
337 VOIDF 2050000
338 VOIDF 2060000
339 VOIDF 2070000
340 VOIDF 2090000
341 VOIDF 2100000
342 VOIDF 3010000
343 HIF 1010000
344 HIF 2010000
345 HIF 2020000
346 HIF 2040000
347 HIF 2050000
348 HIF 2060000
349 HIF 2070000
350 HIF 2090000
351 HIF 2100000
352 HIF 3010000
353 HIG 1010000
354 HIG 2010000
355 HIG 2020000
356 HIG 2040000
357 HIG 2050000
358 HIG 2060000
359 HIG 2070000
360 HIG 2090000
361 HIG 2100000
362 HIG 3010000
363 P 1010000
364 P 2010000
365 P 2020000
366 P 2030000
367 P 2040000
368 P 2050000
369 P 2060000
370 P 2070000
371 P 2080000
372 P 2090000

373 P 2100000
 374 P 3010000
 376 VAPGEN 1010000
 377 VAPGEN 2010000
 378 VAPGEN 2020000
 379 VAPGEN 2040000
 380 VAPGEN 2050000
 381 VAPGEN 2060000
 382 VAPGEN 2070000
 383 VAPGEN 2080000
 384 VAPGEN 2090000
 385 VAPGEN 2100000
 386 VAPGEN 3010000
 387 SATTEMP 3010000
 388 TEMPF 3010000
 389 TEMPG 3010000
 390 FWALF 2010000
 391 FWALF 2020000
 392 FWALF 2050000
 393 FWALF 2070000
 394 FWALF 2090000
 395 FIJ 2010000
 396 FIJ 2030000
 397 FIJ 2050000
 398 FIJ 2070000
 399 FIJ 2090000

*

* NODALIZATION

*

0010000 INLET TMDPVOL
 0010101 0.0193548 0.1601 0. 0. 0. 0. 0. 0.10510 10
 0010200 100
 0010201 0. 1.01E5 0.905371E5 0.256459E7 0.75

*

0020000 TESTS PIPE
 0020001 10
 0020101 0.0193548 10
 0020301 0.1601 10
 0020401 0. 10
 0020601 0.0 10
 0020801 3.333E-5 0.1051 10
 0021001 0 10
 0021101 1000 9
 0021201 100 1.01007E5 0.189417E6 0.256466E7 0.7779 0. 10
 0021300 1
 0021301 0.7 0.04 0. 9

*

0030000 OUTLET TMDPVOL
 0030101 0.0193548 0.1601 0. 0. 0. 0. 0. 0.10510 10

0030200 100
0030201 0. 1.01014234E5 0.288323E6 0.256459E7 0.80630

*

0110000 INLET TMDPJUN
0110101 001000000 002000000 0.0193548
0110200 1
0110201 0. 0.657 0.0651 0.0

*

0120000 OUTLETJ SNGLJUN
0120101 002010000 003000000 0.0193548
0120102 0. 0. 01000 1.0 1.0
0120201 1 0.7398 0.0177 0.

*

* CONTROL VARIABLES *

*

20500000 999
20500100 GMFLWJ1 MULT 1.93548-2 0.0 1
20500101 VOIDGJ 11000000 VELGJ 11000000 RHOGJ 11000000
20500200 GMFLWJ2 MULT 1.93548-2 0.0 1
20500201 VOIDGJ 2010000 VELGJ 2010000 RHOGJ 2010000
20500300 GMFLWJ3 MULT 1.93548-2 0.0 1
20500301 VOIDGJ 2020000 VELGJ 2020000 RHOGJ 2020000
20500400 GMFLWJ4 MULT 1.93548-2 0.0 1
20500401 VOIDGJ 2040000 VELGJ 2040000 RHOGJ 2040000
20500500 GMFLWJ5 MULT 1.93548-2 0.0 1
20500501 VOIDGJ 2050000 VELGJ 2050000 RHOGJ 2050000
20500600 GMFLWJ6 MULT 1.93548-2 0.0 1
20500601 VOIDGJ 2060000 VELGJ 2060000 RHOGJ 2060000
20500700 GMFLWJ7 MULT 1.93548-2 0.0 1
20500701 VOIDGJ 2080000 VELGJ 2080000 RHOGJ 2080000
20500800 GMFLWJ8 MULT 1.93548-2 0.0 1
20500801 VOIDGJ 2090000 VELGJ 2090000 RHOGJ 2090000
20500900 GMFLWJ9 MULT 1.93548-2 0.0 1
20500901 VOIDGJ 12000000 VELGJ 12000000 RHOGJ 12000000
20501000 GMFLW10 MULT 1.93548-2 0.0 1
20501001 VOIDFJ 11000000 VELFJ 11000000 RHOFJ 11000000
20501100 GMFLW11 MULT 1.93548-2 0.0 1
20501101 VOIDFJ 2010000 VELFJ 2010000 RHOFJ 2010000
20501200 GMFLW12 MULT 1.93548-2 0.0 1
20501201 VOIDFJ 2020000 VELFJ 2020000 RHOFJ 2020000
20501300 GMFLW13 MULT 1.93548-2 0.0 1
20501301 VOIDFJ 2040000 VELFJ 2040000 RHOFJ 2040000
20501400 GMFLW14 MULT 1.93548-2 0.0 1
20501401 VOIDFJ 2050000 VELFJ 2050000 RHOFJ 2050000
20501500 GMFLW15 MULT 1.93548-2 0.0 1
20501501 VOIDFJ 2060000 VELFJ 2060000 RHOFJ 2060000
20501600 GMFLW16 MULT 1.93548-2 0.0 1
20501601 VOIDFJ 2080000 VELFJ 2080000 RHOFJ 2080000
20501700 GMFLW17 MULT 1.93548-2 0.0 1

20501701 VOIDFJ 2090000 VELFJ 2090000 RHOFJ 2090000
20501800 GMFLW18 MULT 1.93548-2 0.0 1
20501801 VOIDFJ 12000000 VELFJ 12000000 RHOFJ 12000000

*

BIBLIOGRAPHIC DATA SHEET

(See instructions on the reverse.)

1. REPORT NUMBER
*(Assigned by NRC. Add Vol., Supp., Rev.,
and Addendum Numbers, if any.)*

NUREG/IA-0077

2. TITLE AND SUBTITLE

RELAP5 Assessment on Direct-Contact Condensation
in Horizontal Cocurrent Stratified Flow

3. DATE REPORT PUBLISHED

MONTH YEAR

April 1992

4. FUND OR GRANT NUMBER

A4682

5. AUTHOR(S)

S. Lee, H. J. Kim

6. TYPE OF REPORT

Technical

7. PERIOD COVERED *(Inclusive Dates)*

8. PERFORMING ORGANIZATION -- NAME AND ADDRESS *(If NRC, provide Division, Office or Region, U.S. Nuclear Regulatory Commission, and mailing address; if contractor, provide name and mailing address.)*

Korea Institute of Nuclear Safety
P.O. Box 16, Daeduk-Danji
Taejon, Korea

9. SPONSORING ORGANIZATION -- NAME AND ADDRESS *(If NRC, type "Same as above". If contractor, provide NRC Division, Office or Region, U.S. Nuclear Regulatory Commission, and mailing address.)*

Office of Nuclear Regulatory Research
U.S. Nuclear Regulatory Commission
Washington, DC 20555

10. SUPPLEMENTARY NOTES

11. ABSTRACT *(200 words or less)*

Assessment on the direct-contact condensation model was carried out using RELAP5/MOD2 Cycle 36.04 and the RELAP5/MOD3 Version 5m5 codes. The test data was obtained from the experiments at Northwestern University, which involved the horizontal cocurrent stratified steam/water flow in a rectangular channel. A nodal location sensitivity study and a simulation with a fixed interfacial area, same as test section, were also carried out to examine the effect of the interfacial heat and mass transfer. The results showed that the RELAP5 code model under the horizontal stratified flow regime predicted the condensation rate well, though the interfacial heat transfer area was underpredicted. However, some discrepancies with experimental results were found in water layer thickness and local heat transfer coefficient especially when there was a wavy interface. The interfacial wave structure was found to play an important role in describing the interfacial heat and mass transfer, as obtained in the experiment.

12. KEY WORDS/DESCRIPTORS *(List words or phrases that will assist researchers in locating the report.)*

RELAP5, Assessment on Direct-Contact Condensation, Horizontal
Concurrent, Stratified Flow

13. AVAILABILITY STATEMENT

Unlimited

14. SECURITY CLASSIFICATION

(This Page)

Unclassified

(This Report)

Unclassified

15. NUMBER OF PAGES

16. PRICE

THIS DOCUMENT WAS PRINTED USING RECYCLED PAPER

UNITED STATES
NUCLEAR REGULATORY COMMISSION
WASHINGTON, D.C. 20555

SPECIAL FOURTH-CLASS RATE
POSTAGE AND FEES PAID
USNFC
PERMIT NO. G-67

OFFICIAL BUSINESS
PENALTY FOR PRIVATE USE, \$300

120555139531 1 1AN1CI
US NRC-OADM
DIV FOIA & PUBLICATIONS SVCS
TPC-PDR-NUREG
P-211
WASHINGTON DC 20553